LBNL-61798

Mobility of Tritium in Engineered and Earth Materials at the NuMI Facility, Fermilab

Progress Report

Investigators:

Stefan Finsterle, Mark Conrad, Mack Kennedy,
Timothy Kneafsey, Karsten Pruess, Rohit Salve, Grace Su, and Quanlin Zhou

Earth Sciences Division
Lawrence Berkeley National Laboratory (LBNL)
Berkeley, California

March, 2007

This work was supported by the Fermi National Accelerator Laboratory (Fermilab). The support is provided to Berkeley Lab through the U.S. Department of Energy Contract No. DE-AC02-05CH11231.

TABLE OF CONTENTS

LIST OF FIGURES

LIST OF TABLES

ACRONYMS

D	deuterium
DS	downstream
EAV	exhaust air vent
EOS	equation of state
FNAL	Fermi National Accelerator Laboratory (Fermilab)
HDO	deuterium oxide
HERL	Heavy Element Research Laboratory
HTO	tritium oxide
iTOUGH2	inverse TOUGH2
LBNL	Lawrence Berkeley National Laboratory
MINC	multiple interacting continua
MINOS	Main Injector Neutrino Oscillation Search
NuMI	Neutrino at the Main Injector
POT	protons on target
T	tritium
TOUGH2	transport of unsaturated groundwater and heat, release 2
US	upstream

EXECUTIVE SUMMARY

Background

This report details the work mainly done between June 13 and September 30, 2006 by Lawrence Berkeley National Laboratory (LBNL) scientists to assist Fermi National Accelerator Laboratory (Fermilab) staff in understanding tritium transport at the Neutrino at the Main Injector (NuMI) facility. The report has been modified between October 1, 2006 and February 28, 2007 to address comments by Fermilab staff.

As a byproduct of beamline operation, the facility produces (among other radionuclides) tritium in engineered materials and the surrounding rock formation. Once the tritium is generated, it may be contained at the source location, migrate to other regions within the facility, or be released to the surrounding environment.

The main issue that prompted Fermilab to seek LBNL's assistance in understanding tritium transport at the NuMI facility was the observation that tritium levels in collected drainage water showed only a modest decline after the beam was turned off in February 2006. This behavior was unexpected and raised the question of where the tritium was coming from, and how it made its way into air and water collected along the facility. An understanding of tritium behavior in engineered and earth materials as well as through underground openings is needed to address key environmental concerns about possible tritium levels when the beamline is operated for longer durations and/or at higher intensities.

The report has been revised to include comments by Fermilab staff made between September 30 and February 28, 2007.

Project Objective

The overall purpose of the studies described in this progress report is to better understand the fate and transport of tritium in the NuMI facility in order to be able to (1) evaluate potential environmental impacts, (2) determine tritium sources after the beam is shut off, and (3) estimate the effects of the planned increase in beam intensity on tritium production and tritium releases. The information provided will help design and optimize mitigation measures.

Conceptual Model of Tritium Migration at the NuMI Facility

A conceptual understanding of tritium production and transport in the NuMI facility is being developed based on a systematic analysis of Fermilab's tritium data, our preliminary laboratory and modeling work, and a review of various NuMI facility reports, site visits, and discussions with Fermilab staff. The main tritium transport mechanisms are (1) advective transport with airflow and mass transfer between gaseous and aqueous phases in the passageway (also referred to as walkway) and other underground openings, (2) advective and diffusive transport in concrete and fractured rock, and (3) mass transfer between tritium vapor in the underground openings and concrete or rock walls. The transport processes occurring along various sections of the NuMI facility are summarized below:

- Pre-Target Tunnel: Tritium enters this section of the NuMI either in the water collected as seepage, or as water vapor leaking from the Target Hall.
- Target Pile and Target Hall: Tritium produced around the target is transported within the Target Hall as water vapor; it either condenses, is absorbed, or is transported in vapor or liquid form to other locations in the facility.
- Decay Pipe and Passageway: Tritium vapor ventilated along the passageway transfers into water seeping along the walls; the tritiated collectable seepage water discharges through grates into the main drain, or diffuses into the walls. Tritium produced in the fractured rock diffuses from the matrix to the fractures, where it is carried by water to the drainage system (dimple mat and main drain). Tritium produced in the Decay Pipe concrete may diffuse into the dimple mat.
- Absorber Hall: Tritium produced by the absorbers is transported in vapor form along the passageway and in liquid form to the main drain.

Approach

A systematic approach consisting of the following components was developed to assist Fermilab in understanding tritium transport in various earth and engineered materials at the NuMI facility:

- A detailed analysis of the tritium data collected by Fermilab was performed to understand the observed total system behavior of tritium production and transport.
- Laboratory diffusion tests were conducted to measure transport properties and to understand small-scale tritium transport.
- Isotopic analyses were performed to measure tritium concentration in concrete cores extracted from the tritium source zones to confirm the tritium production pattern.
- A plan for field experiments and monitoring was developed to understand airflow and water pathways for tritium movement at NuMI.
- A numerical modeling analysis was initiated to reproduce the observed system behavior. A refined version of the model incorporating our understanding of the geology and the profiles of tritium production will be developed in the future to predict the system response to different operational scenarios.

Summary of Work Conducted between June 13 and September 30, 2006

Analysis of Fermilab Tritium Data Sets

Purpose: Develop a conceptual understanding of tritium production and transport in various underground openings, concrete shielding, and surrounding rock.

- High tritium vapor concentrations were observed within condensate in the Target Hall and in dehumidifiers in the Target and Absorber Halls, with a gradual decline of the vapor concentration away from these two halls.
- Significant changes in the tritium concentration within the holding tank in response to operation of five engineering controls (recirculation fan, EAVs 2 and 3, chase, chiller, and dehumidifier) were observed, with a strong correlation between tritium levels

observed in the main drain and the tritium vapor transport pattern through the ventilation system.

- Tritium concentrations in the grates of the Decay Pipe were higher than those observed in the holding tank, indicating that the seepage water collected in the passageway is diluted by the collectable water entering the main drain from the dimple mat.
- Time series of tritium concentrations observed in the upstream and downstream regions of the Decay Pipe show different temporal patterns in response to the operation of the beamline and the five engineered facility controls.
- Tritium vapor concentrations (measured by equilibrating with water collected in open pails and trays) along the Decay Pipe passageway were higher than those observed in grates, with a concentration gradient from the Target Hall and Absorber Hall to EAVs 2 and 3.
- Tritium concentrations measured along concrete core samples collected in the Target Hall and Decay Pipe passageway showed a U-shaped profile, indicating two overlapping phenomena: (1) the increase in concentration towards the central beamline indicates in-situ tritium production., and (2) the increase in concentration towards the surfaces of the concrete that are exposed to ambient air indicates secondary tritium accumulation as a result of condensation of tritium vapor on concrete surfaces and subsequent diffusion into the concrete.

Diffusion Tests in Concrete and Host Rock

Purpose: Diffusion cell tests were conducted to estimate tritium mobility through concrete and rock using deuterium as an analogue for tritium.

- Two through-diffusion experiments were conducted on fabricated Decay Pipe concrete exposed to deuterated water vapor. The concrete was fully water saturated in Experiment 1 and had a water saturation of 0.6 in Experiment 2.
- The deuterium concentration in the downstream cell of Experiment 2 increased with time at about half the rate of Experiment 1, indicating that the diffusion rate decreases as the liquid saturation of the concrete decreases.
- The semianalytical solution developed by Moridis (1999) was used to analyze the results from Experiment 1, giving an effective diffusion coefficient of 3.4×10^{-10} m^2/s. This estimated diffusion coefficient was used in the numerical model.
- Back-diffusion experiments were performed on powdered concrete from the Target Hall. An increase in deuterium concentration over time in the air was measured, indicating that back-diffusion could be contributing to the tritium concentrations observed after the beamline is shut down.

Identification of Tritium Location in Concrete and Rock, and Evaluation of Tritium Mobility

Purpose: Tritium concentrations in the concrete shielding and the surrounding rock in the NuMI facility were measured to determine whether or not the concrete and/or rock walls contain sufficient tritium to act as a long-term source.

- Tritium concentrations were measured in pore water extracted from three Target Hall concrete samples. In all three cases, the tritium concentration in the extracted pore water was significantly less (5 to 30 times) than the concentration of the leached concrete sample measured by Fermilab.
- The discrepancy needs to be investigated further. There are several potential possibilities: the concrete samples may have experienced drying out and exchange with non-tritiated water vapor during storage, the pore water sample may have been diluted (contaminated) by nontritium-bearing drilling fluid during the coring process, or the two measurement techniques are measuring tritium from different reservoirs in the concrete.

Numerical Modeling and Systematic Flow and Transport Analysis

Purpose: A simplified numerical model was developed to integrate hypothesized processes and features as well as geometry elements into a tritium fate and transport model of the NuMI facility. The aim was to reproduce the observed system behavior and to simulate tritium transport from three different sources (fractured rock, concrete, and passageway) after the beam was turned off.

- This first-order modeling effort was focused on water flow and tritium transport in a vertical cross section of the Decay Pipe. Transient tritium transport simulations were performed assuming that water flow is at steady state.
- The simulated breakthrough curves from the three source zones were compared to determine their relative contributions to tritium in collected drainage water:
  - The dominant tritium contribution to drainage water appeared to be from the airflow through the passageway, which contained high tritium concentrations (assuming equilibrium with the measured aqueous-phase concentrations). The preliminary simulations indicate that contributions from tritium sources in the fractured rock and concrete were not significant.
  - Tritium continued to be released to the main drain from the fractured rock, the concrete, from vapor flow through the passageway (during ventilation), and back-diffusion from the concrete to the passageway (when ventilation was off).

Plan to Develop Field Investigations of Tritium at the NuMI Facility

A field investigation plan with the following components was developed:

- *Tracing air flow along the NuMI facility*

  Purpose: Determine airflow pathways through the facility from the two primary tritium source zones (Target Pile and Absorber Hall) and the residence times in each facility element.

- *Monitoring liquid-vapor exchange and water movement in the vicinity of and within the NuMI facility*

  Purpose: Differentiate the tritium exchange between liquid pore-water and water vapor in the NuMI facility from water transport in the vicinity of and within the facility.

- *Determine dynamic depth profiles of tritium concentration in component materials of the NuMI facility*

  Purpose: Determine the dynamic tritium-concentration depth profiles in engineered and natural materials along the NuMI facility during and between the periods when the beam is running.

- *Set up a long-term monitoring program*

  Purpose: Provide details of moisture dynamics in the immediate vicinity of the facility.

Recommendations

Based on the results from the investigations conducted between June 13 and September 30, 2006, five key questions have been identified that must be addressed to understand the movement of tritium at the NuMI facility:

1. What are the main sources and mechanisms for tritium release when the beamline is off?
2. What is the total tritium inventory (from production, diffusion, and sorption) and what are the tritium exchange and release rates between different elements in the Target Pile and Target Hall?
3. What are the main pathways for tritium movement through the air and water at the NuMI facility?
4. What are potential long-term environmental impacts of tritium and other radionuclides of concern to Fermilab?
5. What are the projected absolute tritium concentrations expected for future beamline operation scenarios, and what mitigation measures for tritium release could be developed?

To address these questions, we recommend a systematic and integrated approach, consisting of the following laboratory, field, and modeling investigations:

- Resolve differences in tritium concentration as measured at Fermilab and LBNL by (1) performing a cross calibration of the Fermilab and LBNL analytical laboratories using a documented tritium standard, (2) reproducing the leach technique for measuring tritium concentrations used at Fermilab by powdering aliquots of dehydrated concrete and leaching with de-ionized water; and (3) analyzing extracted pore water and water from the leaching experiments at both laboratories.
- Further measurements (using the leach and vacuum de-hydration technique) of tritium concentrations in concrete pore-water and pore-water saturation for accurate determination of the tritium inventory in the two primary source zones,
- Initiate investigation of tritium concentrations and mobility in steel shielding in the Target Hall,
- Further laboratory experiments quantifying transport properties under varying liquid/vapor conditions for tritium and other radionuclides of potential interest,
- Multiple gas tracer tests to track the major airflow pathways,

- Sample boxes containing multiple blocks of engineered and natural materials placed throughout the facility to capture the dynamic depth profiles of tritium concentrations into these materials,
- A monitoring program of groundwater, collected water, and water vapor that will provide details of moisture dynamics in the immediate vicinity of the facility, and
- Development of a three-dimensional fluid flow and tritium transport model to integrate various observations from the laboratory and field, reproducing the observed behavior and predicting responses to future operational scenarios (e.g., longer-term beam operation, increase in beam intensity, and implementation of mitigation measures).

1. INTRODUCTION

Fermi National Accelerator Laboratory (Fermilab) operates the Neutrino at the Main Injector (NuMI) beamline for experimental studies in physics. NuMI is an approximately 1,300 m long underground facility, consisting of a Pre-Target Tunnel, the Target Pile within the Target Hall, the Decay Pipe, a passageway running parallel to the Decay Pipe, the Absorber Hall, the MINOS Hall, several ventilation shafts, and various surface facilities (Figure 1-1). The slope of the Decay Pipe is approximately 5.8%; the depth of the sump is approximately 100 m below land surface. The facility has been excavated in Silurian dolomite, siltstone and shale overlain by glacial till. Airflow through NuMI is controlled by two engineered ventilation systems, and the exhaust air is discharged to the atmosphere at four locations. Water entering the facility is collected in a drainage system and pumped to surface holding tanks.

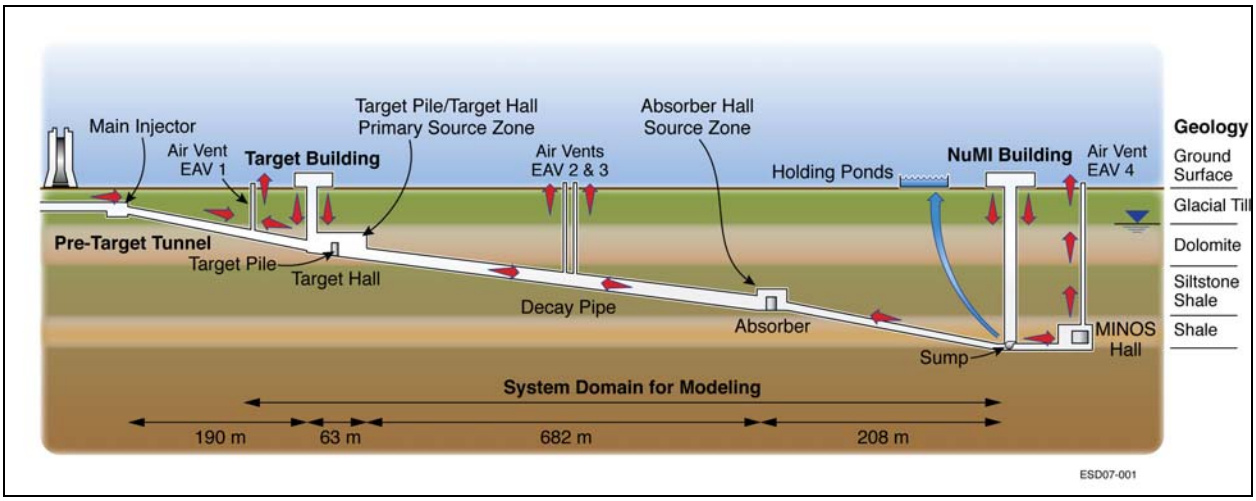

Figure 1-1. Schematic of the NuMI facility (not to scale; modified from Hylen, 2006a, Slide 1)

The NuMI beamline produces (among other radionuclides) tritium as a byproduct. This tritium production occurs predominantly in the Target Pile within the Target Hall, but also in the Absorber Hall, in the concrete along the Decay Pipe, and in the surrounding rock formation. Tritium may be generated in the gas phase, in pore-water, and in the solid components of the surrounding engineered and earth materials. Once the tritium is generated, it may be contained at the source location or migrate to other parts of the facility, with the possibility of being released to the surrounding environment. To monitor the fate of tritium, samples of water, concrete, and rock have been collected at multiple locations within the facility to infer tritium concentrations in the vapor phase, pore-water, drainage water, condensate, and solid materials. Preliminary analyses of the data show that tritium concentrations in drainage water pumped from the facility (while meeting environmental standards) remain on the order of 10 pCi/mL when the NuMI beamline is turned off, which is about a factor of two lower than the concentrations observed during beam operation. This suggests that the tritium generated in engineered and earth materials during beam operation is slowly released from the source zones and transported to the Decay Pipe region through relatively mobile phases (e.g., ventilation air, collected water, and groundwater).

The overall purpose of the studies described in this progress report is to better understand the fate of tritium in the NuMI facility, in order to (1) evaluate potential environmental impacts, (2) determine tritium sources after the beam is shut off, (3) estimate the effects of the planned increase in beam intensity on tritium production and tritium releases, and (4) help design and optimize mitigation measures. Achieving these goals requires the analysis of (1) tritium production mechanisms and the current tritium inventory at NuMI, (2) water flow and air circulation patterns, (3) tritium transport mechanisms through engineered and earth materials (e.g., diffusion and advection), (4) tritium transport through other engineered elements of the facility (e.g., passageways, drainage system), and (5) the effects of NuMI operating conditions (i.e., beam intensity, ventilation regime, dehumidifier and chiller operation, chase sealing, drainage system) on tritium fate and transport.

This report summarizes the work that LBNL has conducted between June 13 and September 30, 2006 on the tasks described in LBNL's proposal to Fermilab of May 2006. The report has been revised to include comments by Fermilab staff made between September 30 and February 28, 2007. It includes a brief background description on the tritium issue at NuMI (Section 2), the development of a preliminary conceptual model of tritium transport through the NuMI facility (Section 3), the development of an approach to evaluate the fate of tritium at the NuMI facility (Section 4), a review of the data collected by Fermilab (Section 5.1), a literature review of tritium transport through concrete and steel (Section 5.2), results from diffusion cell experiments to estimate tritium mobility through engineered and earth materials (Section 5.3), measurements of where the tritium resides within the concrete and rock and evaluation of the corresponding tritium mobility (Section 5.4), the development of a field plan to investigate tritium at the NuMI facility (Section 5.5), and initial results from a numerical modeling study of collectable groundwater flow and tritium transport through the NuMI facility (Section 5.6). Preliminary conclusions are presented in Section 6, followed by recommendations for further investigations (Section 7).

2. BACKGROUND

Tritium concentrations at the NuMI facility have been monitored since June 2005. The tritium concentrations in the holding tank water were typically around 13 pCi/mL from June 2005 to February 2006. After the beam was shut off in late February 2006 for routine maintenance, the average tritium concentrations in the holding tank remained around 10 pCi/mL (see discussion of Figure 5.1-1 below), indicating that tritium accumulates in the NuMI facility during beam operation and is slowly released from the source zones even after the beam is turned off. This issue prompted Fermilab to ask LBNL to provide insight into tritium transport through various earth and engineered materials at the NuMI facility. An understanding of tritium behavior in these materials is needed to address key environmental concerns about possible future tritium levels after prolonged beamline operation at potentially higher beam intensity.

A detailed analysis of the tritium data collected by Fermilab will be presented in Section 5.1. The main findings are summarized here to provide context for the conceptual understanding of tritium production and migration in the NuMI facility presented in the next section:

- High tritium vapor concentrations are observed in condensate in the Target Hall and in dehumidifiers in the Target and Absorber Halls, with a gradual decline of the tritium vapor concentration away from these two halls to other parts of the NuMI facility.
- Sharp and significant changes in the tritium concentration were observed in the holding tank in response to the operation status of five engineering controls (recirculation fan, EAVs 2 and 3, chase, chiller, and dehumidifier), with tritium levels measured in the main drain showing a strong correlation to the tritium vapor transport patterns affected by the ventilation regime.
- Tritium concentrations in the grates of the Decay Pipe are higher than those observed in the holding tank, indicating that the seepage water collected in the passageway is diluted by the collected water entering the main drain from the dimple mat (a building material used to create air space for water drainage).
- Different temporal patterns of tritium concentration are observed in the upstream and downstream regions of the Decay Pipe in response to the operation of the beamline and the five engineered facility controls.
- Tritium vapor concentrations inferred from water concentrations measured in open pails and trays along the passageway in the Decay Pipe are higher than those observed in grates, with a global concentration gradient from the Target and Absorber Halls to EAVs 2 and 3, and a local gradient from the tritium vapor in the passageway to the seepage water.
- Tritium concentrations measured along concrete core samples collected in the Target Hall and Decay Pipe passageway showed a U-shaped profile, indicating two overlapping phenomena: (1) the increase in concentration towards the central beamline indicates in-situ tritium production., and (2) an increase in concentration towards the surfaces of the concrete that are exposed to ambient air indicates secondary tritium accumulation as a result of condensation of tritium vapor on concrete surfaces and subsequent diffusion into the concrete.

Based on these observations, a conceptual model of tritium production and migration in the NuMI facility was developed (see Section 3).

3. CURRENT CONCEPTUAL MODEL OF TRITIUM MIGRATION AT THE NuMI FACILITY

Based on the systematic data analysis, a review of various NuMI facility reports and presentation material, site visits, discussions with Fermilab staff, and the preliminary work presented in Section 5, a conceptual understanding of tritium production and transport in the NuMI facility was developed, as discussed in this section.

There are three primary source zones for tritium production: the Target Pile and Absorber Hall, and the Decay Pipe. When the high-energy proton beam hits the target, located in the Target Pile, radiation and energy loss directly produce tritium in the air, steel piles, and concrete of the Target Pile. The hadron flux passes along the beampipe, with a significant fraction scraping off on the Decay Pipe steel and surrounding concrete, and the rest hitting the absorber pile in the Absorber Hall, resulting in high radiation and energy loss, again producing tritium. These zones are associated with the highest star density values (Grossman, 2006, Slides 15–17) calculated by the MARS model[1]. Direct evidence of primary tritium production in the target and absorber zones is the high tritium vapor concentrations measured in condensate and dehumidifiers located in these zones (see Section 5.1). The tritium produced in the third zone, the Decay Pipe, has not significantly diffused out through the concrete shield yet. The two primary source zones appear to have a different impact on the surrounding environment with respect to (1) the tritium inventory of each source zone (see Section 5.1.4), and (2) the tritium release rates. The understanding gained from the concentration data should be compared to tritium production estimates from the MARS model as calculated for the Target Hall and Absorber Hall.

Tritium that is directly produced in the Target Pile is most likely released in the form of tritium vapor into the Target Hall, facilitated by a fan that recirculates air within the chase, the occasional opening of the chase, and leaking through the chase cover. The tritium vapor (defined as air humidity containing HTO molecules) in the Target Hall is transported advectively and mixed by airflow to the passageway along the Decay Pipe, where it either partitions into the collectable water or is carried to the vents and released to the atmosphere. The tritium vapor released from the Absorber Hall is transported to the atmosphere via the downstream section of

[1] The MARS model has been developed to (1) estimate particle generation by simulating the discrete interactions that occur when a particle collides with a nucleus, and (2) track the passage (or continuous interactions) of generated particles through various engineered materials (e.g., concrete and steel) and natural soil and rock (Mokhov and James, 2006). The particle generation and reaction is reproduced using a variety of cross-section probability and production models, depending on the incoming particles and their energy. Particles are followed till their kinetic energy falls below a threshold (e.g., 30 MeV) specified in the model. One of the model output is the three-dimensional distribution of star density for an incident proton. The standard definition of a star is a nuclear interaction that produces a hadron with kinetic energy greater than the threshold.

The star-density distribution from the MARS model can be used to predict the production rate of tritium and other radionuclides, with the beam intensity (number of incident protons per second) available at the Main Injector (Grossman, 2001). The MARS model was used for the NuMI Shielding Assessment in assisting the construction of the NuMI facility (Wehmann et al., 1997; Grossman, 2001). During NuMI operation with known beam intensity and energy, the neutron levels have been measured using the thermoluminescent dosimetry (TLD) equipment located in the decay enclosure walkway, and depth profiles of tritium concentration in the concrete of the Decay Pipe has been obtained. These data are used by Fermilab to calibrate the MARS model (Lundberg, 2006).

the passageway. Airflow in the facility is primarily controlled by four engineered ventilation systems. The pathways for airflow are also influenced by the configuration of various ventilation control elements.

When tritium vapor is transported along airflow pathways from the production zones to the air vents, part of the tritium mass is transferred from the gaseous phase to the aqueous phase by phase equilibration. In portions of the Pre-Target Tunnel, Target Hall, passageway (walkway), Absorber Hall, and MINOS tunnel, water flows as films along the rock/concrete walls or drips from the ceiling as seepage. The water accumulates on the floor and discharges through grates to the main drain. The relatively long transport distance and large contact area between ventilated air and the walls of the underground openings provide an opportunity for mass transfer between tritium vapor and collectable water, leading to elevated tritium concentrations in the drainage system. Strong mass transfer from the high-concentration tritium vapor to low-concentration liquid water is evidenced (1) by the sharp and significant change in tritium water concentrations in the drainage system in response to changes in the ventilation system, and (2) by tritium concentration gradients along the airflow pathways, measured by equilibration with water collected in open trays and pails along the passageway and in dehumidifiers at different locations.

The tritium in the gaseous phase also diffuses into the surrounding fractured rock and concrete. This is supported by the elevated tritium concentrations measured in the diffusion-affected zone near concrete/rock walls and the diffusion-like concentration profiles into the concrete. Back-diffusion from engineered and natural materials could also be a mechanism for the release of tritium when the tritium vapor concentrations in the underground openings are lowered. This back-diffusion transport mechanism may be important when the tritium source from the Target Pile and Absorber Hall is diminished.

In addition to the production and transport of the tritium generated in the two primary source zones, tritium is also produced in the Decay Pipe concrete and fractured rock. Production of tritium in these zones is also predicted by the spatial star-density distribution (Grossman, 2006, Slides15–17) calculated by the MARS model, and is evidenced by the tritium concentration profiles measured in concrete (excluding the diffusion effects from tritium vapor near the passageway walls). Tritium produced in Decay Pipe concrete is transported advectively and diffusively into the collectable water flowing in the dimple mat around the concrete and into the underground openings through diffusion. The tritium produced in the matrix of the fractured rock slowly diffuses to the fractures, from where it is transported relatively quickly with collectable water to the dimple mat, and from there to the main drain. Based on the mass-balance analysis performed by Fermilab and the systematic data analysis described in Section 5.1, the contribution from the tritium produced in the Decay Pipe concrete and fractured rock to the total tritium collected in the sump may be secondary compared to the tritium originating in the Target and Absorber Halls, which is transported by ventilation along the passageway, partitioned into the liquid phase, and discharged through the grates to the main drain. However, should the migration of tritium through the passageway be significantly reduced or eliminated by mitigation measures, the long-term release of tritium from the Decay Pipe concrete and fractured rock may become the predominant source of tritium in the sump, although at much lower overall concentrations.

The total tritium inventory of the possibly large tritium reservoir in the Target Pile is uncertain. As indicated by the analysis of the condensate collected from air flowing through the Target Pile,

tritium concentrations remain elevated even after the beam has been shut off (tritium concentrations in the condensate are reduced only by a factor of approximately two after three months).

The conceptual model is sketched in Figure 3-1, which shows the main components of the NuMI facility as well as the key processes contributing to tritium production, fate, and transport through underground openings as well as engineered and earth materials.

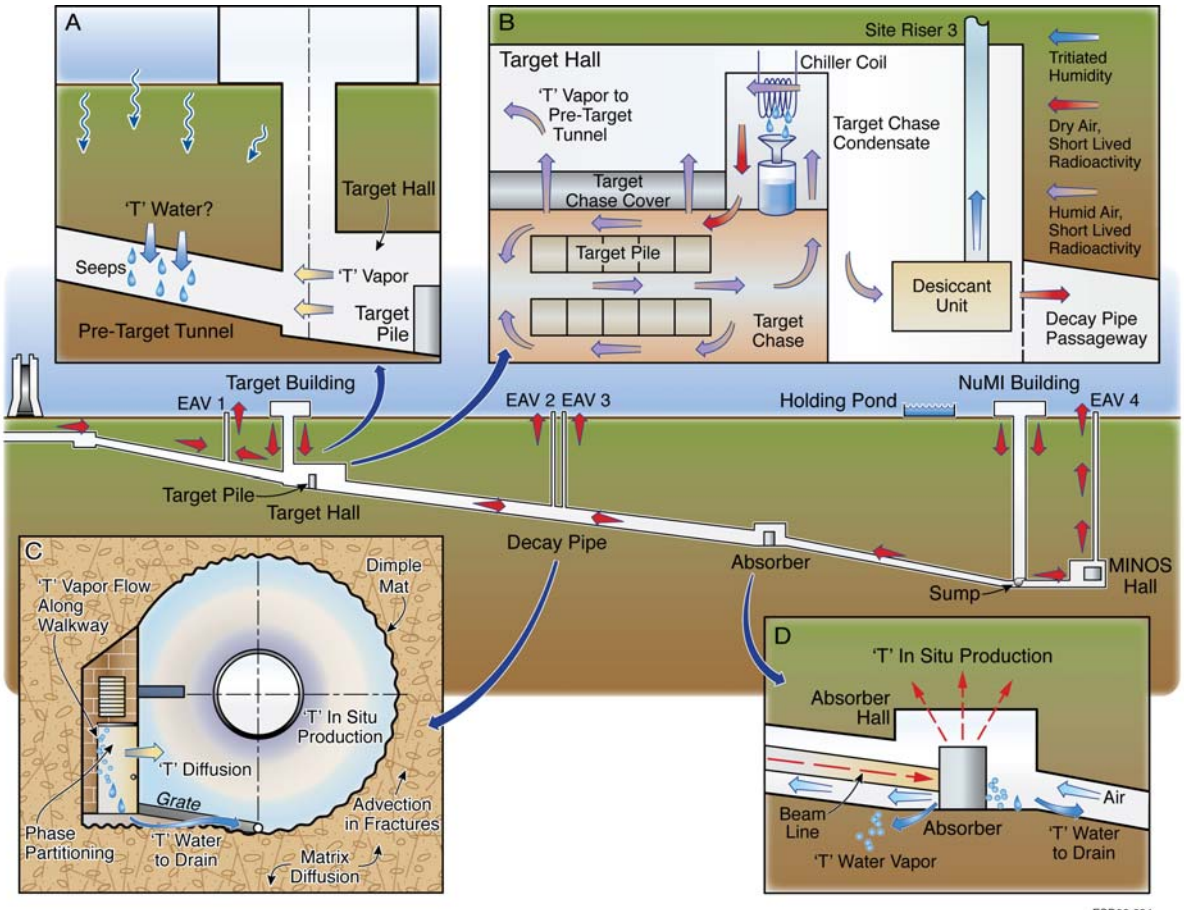

Figure 3-1. Schematic of the general layout of the NuMI facility, and key processes affecting transport of tritium ('T' indicates "tritiated"; red thick arrows indicate ventilation direction; red thin arrows indicate particle beam and radiation). (A) Pre-Target Tunnel: Tritium enters this section of the NuMI either in the water collected as seepage, or as water vapor leaking from the Target Hall. (B) Target Pile and Target Hall: Tritium produced around the target is transported within the Target Hall as water vapor; it condenses, is absorbed, or is transported in vapor or liquid form to other locations in the facility. (C) Decay Pipe and passageway: Tritium vapor ventilated along the passageway partitions into water seeping along the walls, which is collected through grates by the main drain. Tritium produced in the fractured rock diffuses from the matrix to the fractures, where it is carried by water to the drainage system (dimple mat and main drain). Tritium produced in the Decay Pipe concrete may diffuse to the dimple mat. (D) Absorber Hall: Tritium produced by the absorbers is transported in vapor form along the passageway, and in liquid form to the main drain.

4. APPROACH

LBNL developed a systematic approach to assist Fermilab in addressing the key issues arising from the operation of the NuMI facility. Specifically, the approach aims at (1) understanding the migration of tritium within and near the NuMI facility, (2) determining the sources of tritium when the beam is shut off, and (3) predicting the potential environmental impact of the proposed increase in beam intensity. Addressing these issues provides information in support of the design and optimization of mitigation measures to contain tritium or reduce its release to the surrounding environment. Our work thus far has focused on addressing the first two issues by analyzing the tritium data collected by Fermilab, conducting diffusion tests on concrete, performing isotopic analyses of extracted concrete pore-water, developing a field monitoring plan to investigate movement of tritium at NuMI, and conducting numerical modeling for reproducing observed system behavior.

A systematic analysis of the data collected by Fermilab provides the basis to develop a conceptual understanding of tritium production and transport in various underground openings, concrete shielding, and surrounding rock. These data include tritium concentrations in the concrete, the drainage system, and the ventilation system at multiple locations.

To understand tritium transport in concrete, and to address interactions (i.e., vapor deposition and back-diffusion) between the concrete shielding and underground openings, diffusion and sorption coefficients were determined to estimate diffusive transport processes and adsorptive retardation processes, respectively. Batch sorption tests and through-diffusion tests were conducted on replicated Decay Pipe concrete samples, concrete samples from the Target Hall, and rock from the Decay Pipe passageway. Diffusion tests were conducted in cells using both water-saturated and unsaturated samples exposed to the vapor to mimic the ambient interaction between tritium vapor and tritiated water in concrete. The derived diffusion coefficients are used for modeling and analyzing diffusive transport through concrete shielding. Back-diffusion tests are also conducted to investigate whether back-diffusion from concrete to the underground openings provides sufficient tritium to support the relatively constant tritium concentrations observed throughout the facility after the beam is turned off.

Accurate quantification of the tritium production rate, inventory, and spatial distribution in the source zones is important to the fate and transport of tritium in the NuMI facility. To determine whether or not the concrete and/or rock walls could act as a significant long-term source to eventually be released to the groundwater, pore-water samples were extracted from core samples using a vacuum dehydration technique. Tritium concentration was measured using the scintillation technique at LBNL's Heavy Element Research Laboratory (HERL), yielding concentrations that are different from those measured at Fermilab (see Section 5.4 for a discussion).

To integrate the results from laboratory experiments and field monitoring as well as the data collected by Fermilab, numerical modeling was used to simulate the transport of tritium and other radionuclides in the NuMI facility. The numerical model was developed to account for the different transport processes discussed in Section 3. LBNL's multiphase, multicomponent simulator TOUGH2 (Pruess, 2004) with the EOS7R module was used for simulation and

prediction of tritium transport in the NuMI facility. In future studies, this model will be calibrated using the observed system responses (e.g., tritium concentrations at different locations in both gaseous and aqueous phases). The calibrated model will have predictive power to investigate the system responses to the proposed increase in beam intensity and to identify potential mitigation measures to reduce tritium concentrations in the surrounding environment.

As shown in the conceptual model and data analysis sections (Sections 3 and 5.1), ventilation-driven airflow through the NuMI facility plays a critical role in transporting tritium from the two primary source zones to the drainage system and the atmosphere. We propose to design a field monitoring program to quantify the flow rates, directions, and residence times of air in each of the four ventilation systems. Multiple gas tracers could be used to track airflow, with a focus on the airflow in the Target Pile, Target Hall, and Pre-Target Tunnel. In addition to monitoring airflow patterns, we propose to place boxes containing multiple specimens of typical materials (i.e., concrete, rock, steel) at various locations in the underground openings to capture tritium production within and transient penetration into these materials during beam operation. Finally, we propose to extend Fermilab's current long-term environmental monitoring program as appropriate to obtain additional information relevant to the analysis and prediction of the tritium system.

This report focuses on our investigation of the production, fate, and transport of tritium, the most abundant radionuclide found in the NuMI facility. Our analysis may be extended to Na-22 and other radionuclides of potential interest.

5. ANALYSIS OF TRITIUM DATA SETS, LITERATURE REVIEW, AND RESULTS OF LABORATORY, FIELD, AND MODELING STUDIES

This section presents the results of the tasks conducted by LBNL between June and September 2006. The tritium data collected by Fermilab is compiled and analyzed in Section 5.1. A literature review of tritium transport through concrete and steel, two main materials used in the NuMI facility as shielding from radiation, is presented in Section 5.2 to provide background for our laboratory studies. The results of diffusion-cell experiments to estimate tritium mobility through concrete are described in Section 5.3. In Section 5.4, the liquid saturation and the tritium concentration of pore-water from NuMI concrete samples were measured to investigate where the tritium resides. In Section 5.5, a brief field plan to investigate the movement of air and flow of water collectable in the NuMI facility was developed based on site visits and discussions between Fermilab and LBNL staff. Section 5.6 presents the transport modeling results of tritium from multiple sources in a representative vertical cross section of the upstream section of the Decay Pipe.

5.1 Analysis of Fermilab Tritium Data Sets

A systematic analysis of the data collected by Fermilab was conducted to develop a conceptual understanding of tritium production and transport in underground openings, concrete shielding, and surrounding rock. These data include tritium concentrations in the concrete, the drainage system, and the ventilation system at multiple locations (Hylen, 2006c). The time-dependent behavior of the system is reflected by periodic measurements collected between June 2005 and November 2005, and by more frequent measurements after November 2005. These data help reveal the system behavior in response to beamline operation and intentional changes to five engineering controls (i.e., recirculation fan in the Target Pile, chiller, the sealed/open status of chase, air vents EAVs 2 and 3, and dehumidifiers). In addition to the tritium concentration measurements, there are also data on water collected in the facility, and airflow through the system. Since the flow rate data are straightforward, the data analysis presented in this section focuses on the tritium concentration dataset.

Concentrations exceeding background levels of tritium have been observed in the air and collectable water within the NuMI facility. In particular, the system responses to varying operating conditions of five engineering controls have been monitored to develop mitigation measures. The impacts are reflected in observed changes of (1) tritium transport in concrete and fractured rock (affecting the inventory and release rates), (2) tritium vapor concentrations in condensate and dehumidifiers (containing information about the tritium source zones and tritium vapor transport paths), (3) tritium concentrations in the drainage system (i.e., grates and main drain) at different locations (revealing spatial variability within the facility), and (4) tritium concentrations in water collected in the sump and tritium vapor concentrations in air vents (reflecting the response of the entire facility).

5.1.1 Data on Total System Behavior

Water containing tritium that is collected in the NuMI facility sump and then pumped into the holding tank on the ground surface is an environmental concern for Fermilab. To address this concern, Fermilab has collected data on tritium concentrations in the sump water and correlated the data with the records of facility operation (Hylen, 2006c).

Figure 5.1-1 shows the tritium concentration in the holding tank and daily beam intensity as a function of time. In spite of the fluctuations in the tritium concentration caused by the changes in the operation of the five engineering controls, the tritium concentration is generally correlated to the beam operation and beam intensity, particularly for the later time when the engineering controls are kept relatively stable. Note that while the beam intensity (or the cumulative count of protons on target) directly determines the amount of tritium mass produced in the Target Pile, Absorber Hall, Decay Pipe concrete, and surrounding rock mass, the tritium concentration or the measured tritium mass flux (flow rate of collected water times tritium concentration) at the sump holding tank is affected by the tritium transport mechanisms from the tritium source zones to the drainage system. Tritium transport from the source zones to the drainage system depends on several factors, as shown by the preliminary results of tritium transport modeling discussed in Section 5.6. It is apparent that tritium mass is continuously transported to the drainage system even after the beam is turned off. This is because a sufficient amount of tritium mass is accumulated in the source zones during the beamline operation, from where it is continuously released to the ventilated air and collectable water. As shown in Figure 5.1-1, additional tritium mass produced by continuous beamline operation at later times does increase the measured tritium concentrations. The additional mass generated and temporarily stored in the system is likely to affect the long-term tritium concentrations.

As shown in Figure 5.1-1, tritium concentrations in the holding tank vary significantly, reflecting the system response to varying operational conditions of the NuMI facility. To search for mitigation measures, operation conditions of the recirculation fan, EAV 2 and 3 fans, chase sealing, chiller, and dehumidifiers were systematically changed, and the corresponding response in tritium concentrations was monitored. Figure 5.1-2 shows the sensitivity of the tritium concentration in the holding tanks to the varying operation conditions of the recirculation fan, chiller, chase, EAVs 2 and 3, and dehumidifiers. As shown in Time Window 1 (TW1) in Figure 5.1-2a, the tritium concentration in the holding tank increases sharply immediately after the recirculation fan is turned on, and it decreases dramatically after the fan is turned off; the change, by a factor of two, is caused by the change in the recirculation-fan operation only. Figure 5.1-2b shows that the tritium concentration also quickly changes by a factor of two when EAVs 2 and 3 are shut down in TW2. As shown in TW3 in Figure 5.1-2c, the tritium concentration increases (or decreases) by approximately a factor of two immediately after the chase is opened (or sealed); the concentration is relatively stable when the chase remains open (except the change shown in TW2). Figure 5.1-2d (TW4) shows that tritium concentration increases (decreases) when the chiller is off (on), but the changes are not as quick and as large as for the other three controls (i.e., recirculation fan, EAVs 2 and 3 fans, and chase). Figure 5.1-2e shows the reduction in the tritium concentration in the holding tank after dehumidifiers are introduced. The sharp changes in each of the five time windows (WT1 to WT5) show the strong sensitivity of the tritium concentration in the holding tank to the change in the corresponding control. There are also some significant concentration changes caused by the combined effects of more than one of

the five controls involved, indicating that the tritium transport through the entire system is sensitive to the operation of the recirculation fan, chase, chiller, EAVs 2 and 3, and dehumidifiers, which affect the transport of tritiated vapor.

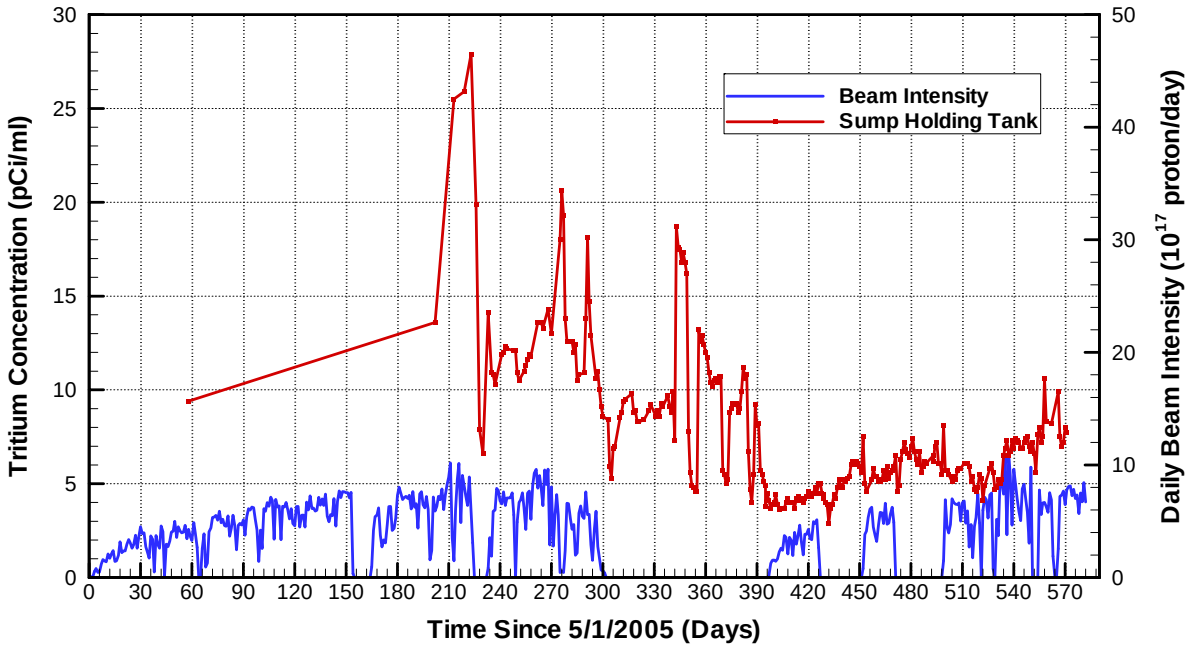

Figure 5.1-1. Tritium concentrations measured in the holding tank and beam intensity as a function of time

The sensitivities observed in Figure 5.1-2 indicate that the operation of the recirculation fan and the opening of the chase enhance the tritium mass exchange between the Target Pile (one of the major source zones for direct tritium production) and the Target Hall. The tritium vapor in the Target Hall is carried in the airflow from the Target Hall down to the passageway along the Decay Pipe. This allows some tritium to be transported from the source zone in the Target Pile to the atmosphere via EAV2 in the vapor phase. The relatively long transport distance and large contact area between ventilated air and the walls of the passageway also provide an opportunity for mass transfer between tritium vapor of relatively higher concentration and seepage water of low concentration collected in the passageway, leading to higher tritium concentrations in the sump. With this understanding, the addition of a dehumidifier in the Target Hall to capture tritium vapor resulted in lower tritium concentrations in the holding tank by a factor of two after Day 397

Unlike the extensive monitoring of tritium concentration of water collected in the sump, there are only six measurements in EAVs 1–3, through which the tritium vapor is released to the atmosphere (Hylen, 2006c). For example, there are two concentration measurements for the vapor through EAV 2 (284 pCi/mL on 1/31/2006, and 362 pCi/mL on 4/4/2006). More frequent sampling and monitoring of tritium concentration in the vents may be important to improve the understanding of the mass balance of the entire system.

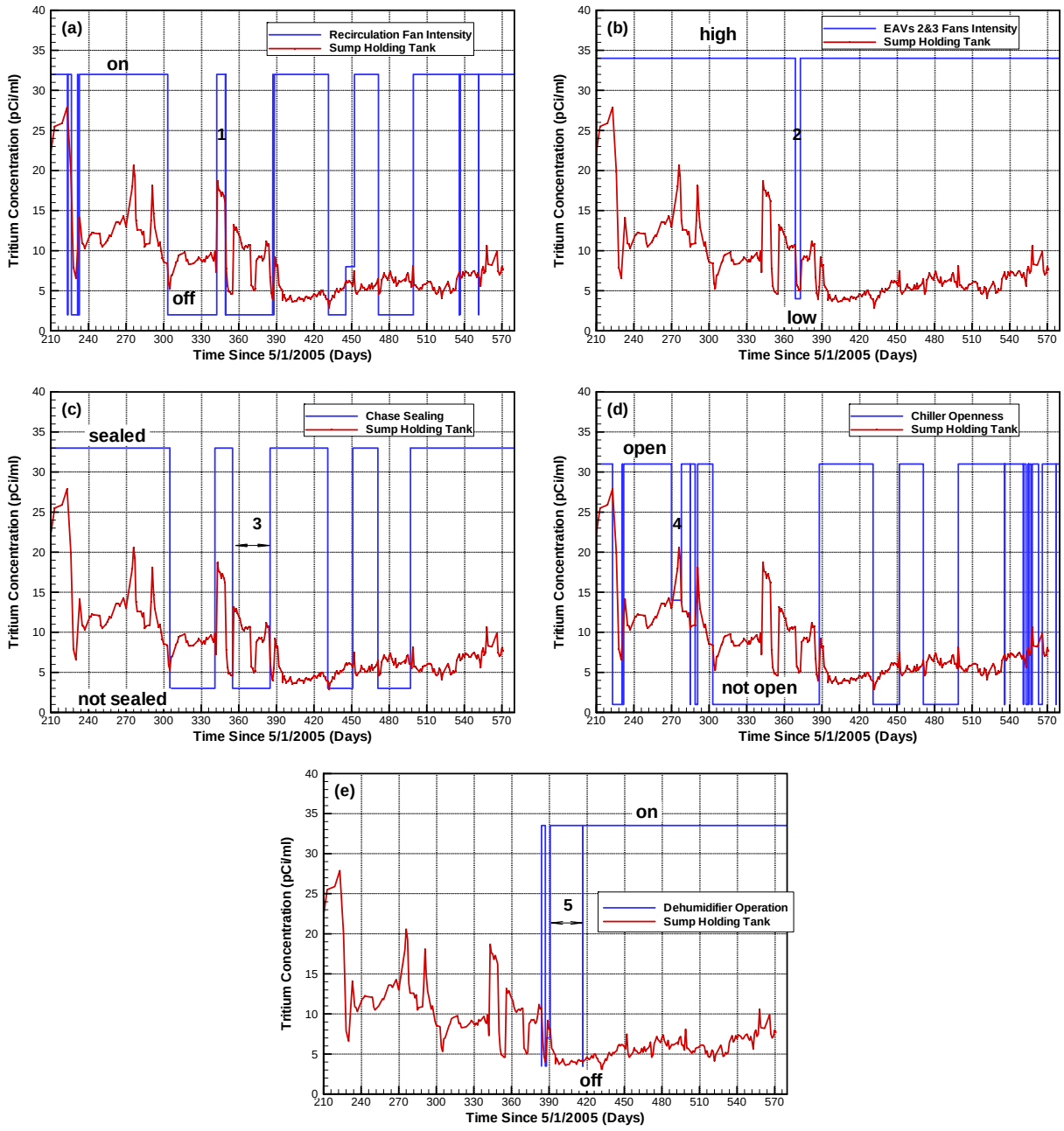

Figure 5.1-2. The response of the tritium concentration in the holding tank to changes in the operation of (a) the recirculation fan, (b) EAVs 2 and 3, (c) chase, (d) chiller, and (e) dehumidifiers. The numbers (1-5) indicate the selected time windows for which the change in operation status of one of the five components is discussed in the text.

5.1.2 Data from Drainage System

The water and tritium observed at the sump (i.e., the outlet of the drainage system) originates from seepage water and condensate collected by (1) Pre-Grate 1, which is located in the upstream section of the Decay Pipe near the Target Hall, (2) various grates in the passageway along the Decay Pipe, and (3) water collected from the fractured rock by the Dimple Mat. Figure 5.1-3 shows the tritium concentrations measured in the drainage system as a function of time (Hylen, 2006c). As shown in Figure 5.1-3a, the tritium concentrations in the upstream grates (Grates 1–5) of the Decay Pipe are higher than those in the holding tank, indicating that the seepage water with higher concentration in grates from the passageway is diluted by the collected water entering the main drain from the dimple mat. The concentrations in the upstream grates respond to the operation of the five engineering controls, similar to the holding-tank concentrations. In particular, the concentrations in the upstream grates significantly decrease when EAV2 is turned off; the concentrations measured on May 8, 2006 (Day 373 in Figure 5.1-3), when EAV2 was off, are approximately 25% of those just before the vent is turned off (except for Grate 1). This and the mitigation achieved by the dehumidifier installed to capture tritium water vapor in the Target Hall indicate that the majority of tritium collected in the grates originates from the Target Hall and is transported through the passageway by ventilation.

The pattern of time-dependent tritium concentrations measured in the downstream grates is very different from that for the upstream grates of the Decay Pipe. The only sharp change in the concentrations of the downstream grates occurs when EAVs 2 and 3 are turned off; the concentrations measured on May 8, 2006, are two thirds of those before the vents were turned off (except for Grates 7 and 8, which are close to the fire door between EAV2 and EAV3). This indicates that the changes in the operation of the recirculation fan, chase, and chiller do not affect the concentrations in the downstream grates. This is because the two ventilation systems (the one from the Target-Hall Shaft to EAV 2, and the one from the MINOS Shaft to EAV3) are separated by the fire door.

A notable difference between the data from the upstream and downstream grates is the observed transient behavior of the tritium concentrations in the upstream and downstream grates. It is, however, difficult to evaluate the response in the concentration of the upstream grates to beamline operation for two reasons. In the period up to Day 400 (particularly after Day 300, when the beamline temporarily stopped operating), the Target Chase was opened and the operating conditions of the ventilation and chiller systems were continually changing; these all affect the transport of tritium water vapor from the Target Chase via the Target Hall, the major route for tritium, into the upstream grates. In the period after Day 400, when the beamline started operating again, there are only three data points. The downstream grates are somewhat easier to analyze since their air system is isolated from the ventilation system of the Target Chase, Target Hall, etc. The concentrations of the downstream grates show a steady decrease after the beam is turned off on Day 300 (February 25, 2006; see Figure 5.1-3b), decreasing to a minimum of 20% (on average 25% for all downstream grates) just before EAVs 2 and 3 are turned off. After the beam is turned on again on June 1, 2006, the concentrations in the downstream grates increase to what they were before the beamline is turned off, as shown by the concentrations measured on June 21, 2006. The correlation between the concentration in the downstream grates and beam intensity is also evident from the response of grate concentrations to beam intensity after Day 400. This correlation may imply that the tritium inventory of the Absorber Hall (i.e., open space,

steel, concrete shielding) is smaller and/or released more slowly than the tritium inventory in the Target Pile/Hall.

Finally, we mention that the period of relatively stable operation since Day 400 has allowed a parameterization of the holding tank tritium concentration to be developed. The parametrization has the form

$$\text{Concentration} = A \times \textit{Total Integrated Exposure} + B \times \textit{Daily Exposure} \times \exp(-\textit{Time} / C).$$

This parameterization includes both a long-term build-up and a daily intensity dependency.

Figure 5.1-3c shows the transient patterns of the tritium concentrations in the Pre-Target drains and in the main drain before seepage water collected in Grates 1 and 2 enters into the main drain. The transient patterns for the Pre-Target drains are similar to the pattern for the holding tank, with the exception of the Pre-Target drain response to the closure of EAVs 2 and 3. The significant concentration drop in the Pre-Target drains at later time may indicate the effect of sealing the connection between the Pre-Target Tunnel and the Target Hall.

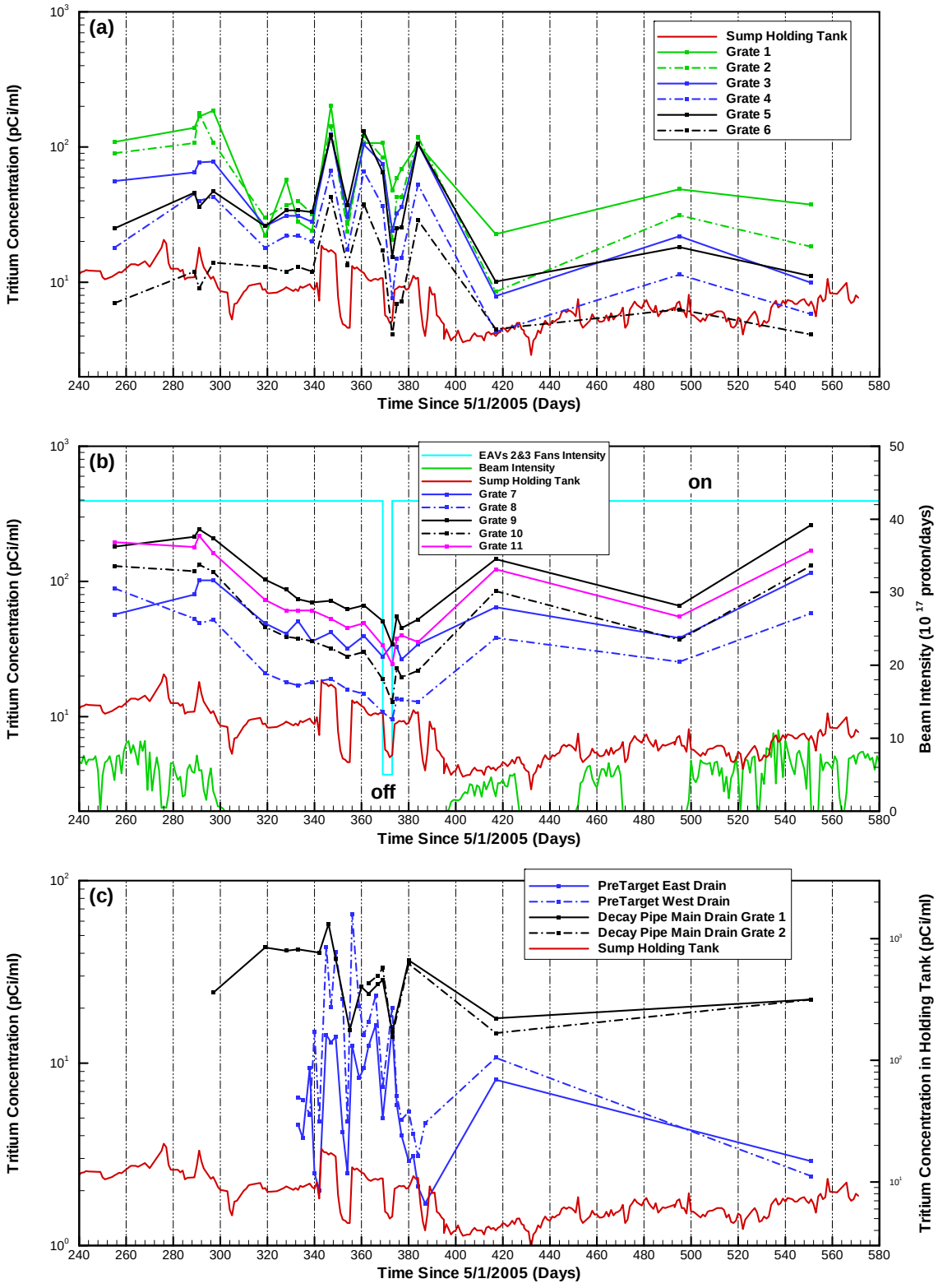

Figure 5.1-3. Tritium concentrations measured in the drainage system in (a) the upstream grates of the Decay Pipe, (b) the downstream grates of the Decay Pipe, (c) the main drain of the Decay Pipe and drains in the Pre-Target Tunnel.

5.1.3 Data from the Target Pile Source Area

Figure 5.1-4 shows the transient behavior of tritium concentrations within condensate collected in the Target Pile area as a function of time. The concentration varies with time by a factor of two. Such variations correspond well to the changes in beam intensity. Increases in beam intensity result in an increase in tritium concentration, as seen from the steady increase in extensively measured concentrations after the beam was turned on again on June 1, 2006 (Day 397). This trend can also be seen in the correspondence between the highest concentration of 831,000 pCi/mL on January 23, 2006 (Day 268 in Figure 5.1-4), with the highest value of beam intensity (approximately 9.0×10^{17} POT/day) for the continuous 9-day period from January 15 to January 23, 2006. The unusual data points before the beamline was turned on again may reflect the effect of the recirculation fan operation. The recirculation fan may facilitate mass transfer in the Target Pile between the vapor (whose concentration is measured from condensate) and the tritium in the pore-water in concrete/steel.

The change (by a factor of two) in the tritium vapor concentration in condensate and its correlation with beam intensity may indicate that the vapor concentration has not reached its saturation limit. The proposed increase in beam intensity may significantly increase the tritium concentration in condensate; water vapor of higher tritium concentrations may be transported through the Target Hall from which it will further migrate with airflow to the passageway and eventually to the surrounding environment. As a result, the higher tritium vapor concentrations may result in higher concentrations in the holding tank.

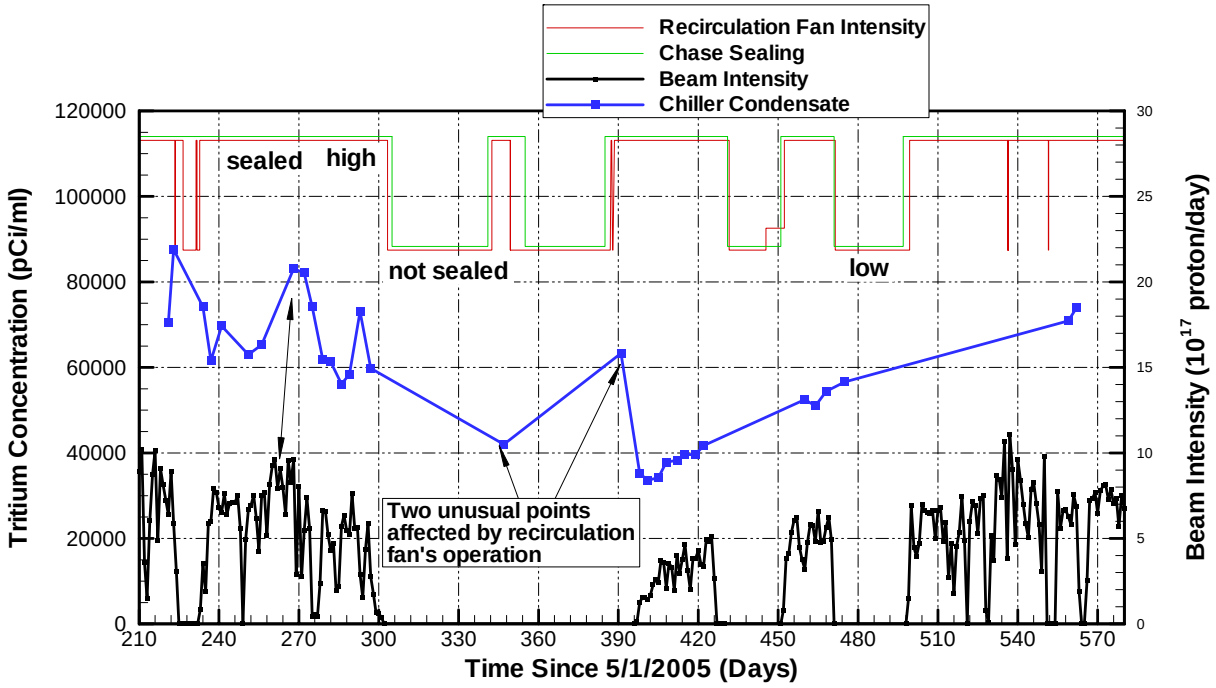

Figure 5.1-4. Tritium concentration in condensate in the Target Pile, beam intensity, and operation status of the recirculation fan and chase as a function of time

5.1.4 Data on Tritium Vapor

In addition to the concentration data of condensate, the concentrations measured in dehumidifiers at different locations also show the concentration of tritium vapor, assuming equilibrium between the gaseous and aqueous phases. (Note that the time constants needed to reach equilibrium between tritiated vapor and liquid water—either free or in pore space—is unknown and should be investigated.) As shown in Figure 5.1-5, the transient pattern of concentration in the dehumidifiers located in the Target Hall and Decay Pipe is similar to that of the concentration in the holding tank. The only difference is that the concentration in the holding tank is lower when EAVs 2 and 3 are turned off, while the concentrations in the dehumidifiers in the Target Hall and Absorber Hall become higher at that time. This is caused by the tritium mass accumulating in the Target Hall and Absorber Hall, resulting from the closure of the passageway doors to the Decay Pipe. Such an increase in concentrations is particularly apparent for the dehumidifier in the Absorber Hall.

The other important feature revealed by Figure 5.1-5 is the spatial variability of the concentrations in the dehumidifiers, which show a higher concentration in the Target Hall than that in the Decay Pipe and the Pre-Target Tunnel. The vapor concentration gradient is along the airflow pathway, carrying tritium vapor from the Target Hall to other areas. The continuous decrease in the dehumidifier concentration in the Pre-Target Tunnel indicates the effects of ongoing mitigation measures.

The vapor concentrations were also measured in the vicinity of the grates in the Decay Pipe using open pails in wet areas and open trays in relatively dry areas (Hylen, 2006b). The pails and trays were left in the passageway for three to seven days, with tents over them, to measure the tritium concentration in the vapor phase (assuming quasi-equilibrium between the gaseous and aqueous phases). These data are particularly useful, because they show the spatial trend of the vapor concentration from the inlet to the passageway (from the Target Hall) to EAV2 and from the Absorber Hall to EAV3 (see Figure 5.1-6). There is strong mass transfer between the gaseous phase and seepage water in the areas from the passageway near the Target Hall to Grate 3, where the passageway is wet because of strong water seepage from the dolomite wall and the ceiling. From Grate 3 to EAV2, where the Decay Pipe is located in siltstone and shale, the reduction in vapor concentration is small, and the tritium mass loss into the drainage system from the airflow is reduced correspondingly.

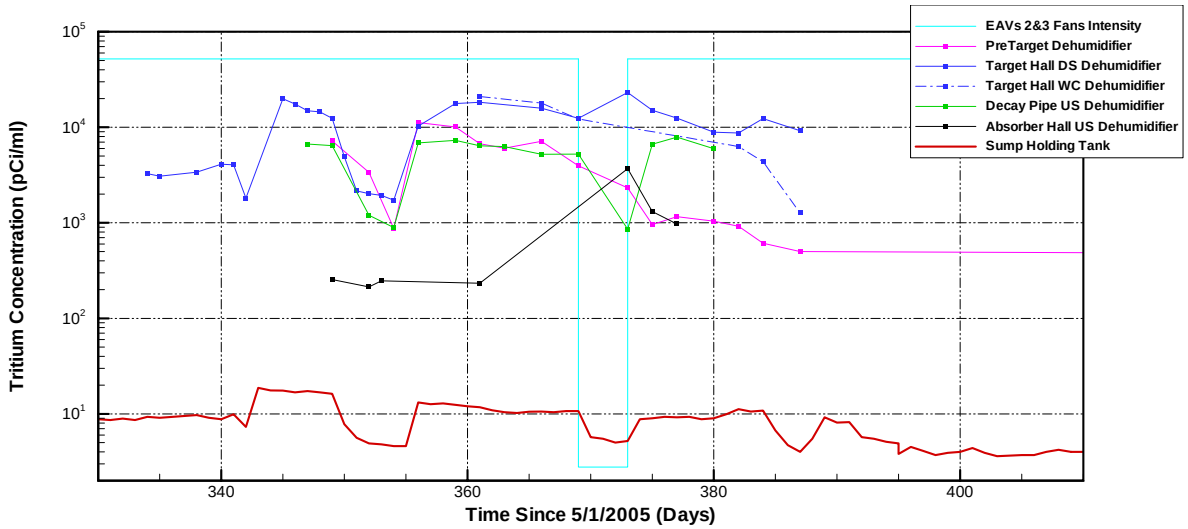

Figure 5.1-5. Tritium concentration in the holding tank and in dehumidifiers at different locations as a function of time

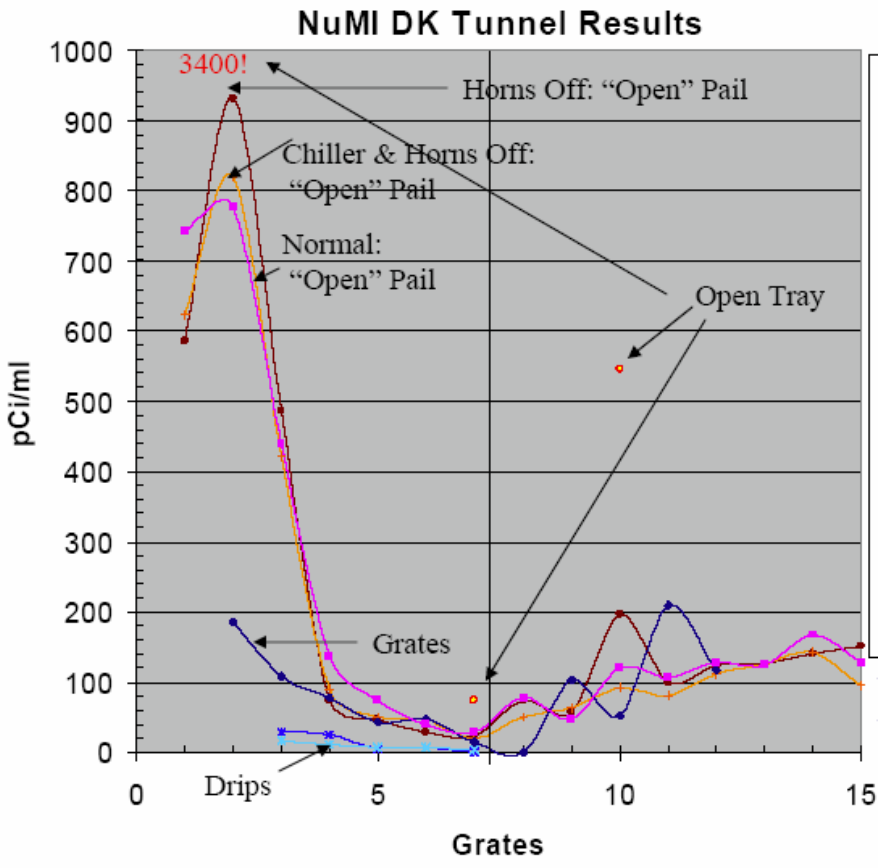

Figure 5.1-6. Tritium concentrations measured in open pails, open trays, drips, and grates in the Decay Pipe, showing the spatial variability along the passageway (Grossman, 2006a, Slide 8)

The decrease in the tritium vapor concentration measured in the open pails between the Absorber Hall and EAV3 is not as pronounced as that from the Target Hall to EAV2. The concentrations in open pails and grates are very similar, indicating that there is sufficient time for the gas and aqueous phases to equilibrate. This is consistent with the fact that seepage rates and flow rates to the main drain are much smaller in the lower section of the passageway, which is situated in the low-permeability shale and siltstone.

It is interesting to compare (1) the tritium concentrations of the dehumidifiers in the Target Hall with that in the Absorber Hall (see Figure 5.1-5) and (2) the tritium-vapor concentrations in the passageway near the Target Hall and near the Absorber Hall (see Figure 5.1-6). The tritium concentration in the dehumidifier in the Target Hall is up to two orders of magnitude higher than that in the Absorber Hall. The tritium-vapor concentration near the Target Hall is one order of magnitude higher than that near the Absorber Hall. These significant differences may indicate that the Target Pile in the Target Hall is the major source zone for tritium vapor, while the Absorber Hall is the secondary source zone. This understanding should be compared to tritium production estimated by the MARS model for the Target Hall and Absorber Hall, and the conceptualization and estimation of transport mechanisms from these source zones to the observation points.

5.1.5 Data on Direct Production in Concrete and Interaction between Tunnels and Concrete

Figure 5.1-7 shows the tritium concentration measured in the core samples to a depth of 0.8 m into the concrete. The increase in concentration towards the outer (tunnel) wall shows tritium being transferred from ambient air into the concrete, while the increase towards the central vacuum pipe results from increased tritium production close to the beamline. Direct production of tritium in the concrete results in a smaller concentration at greater depths within the concrete (in comparison with the vapor-diffusion affected zone). The concentrations of tritium directly produced in the concrete increase as the samples get closer to the beam.

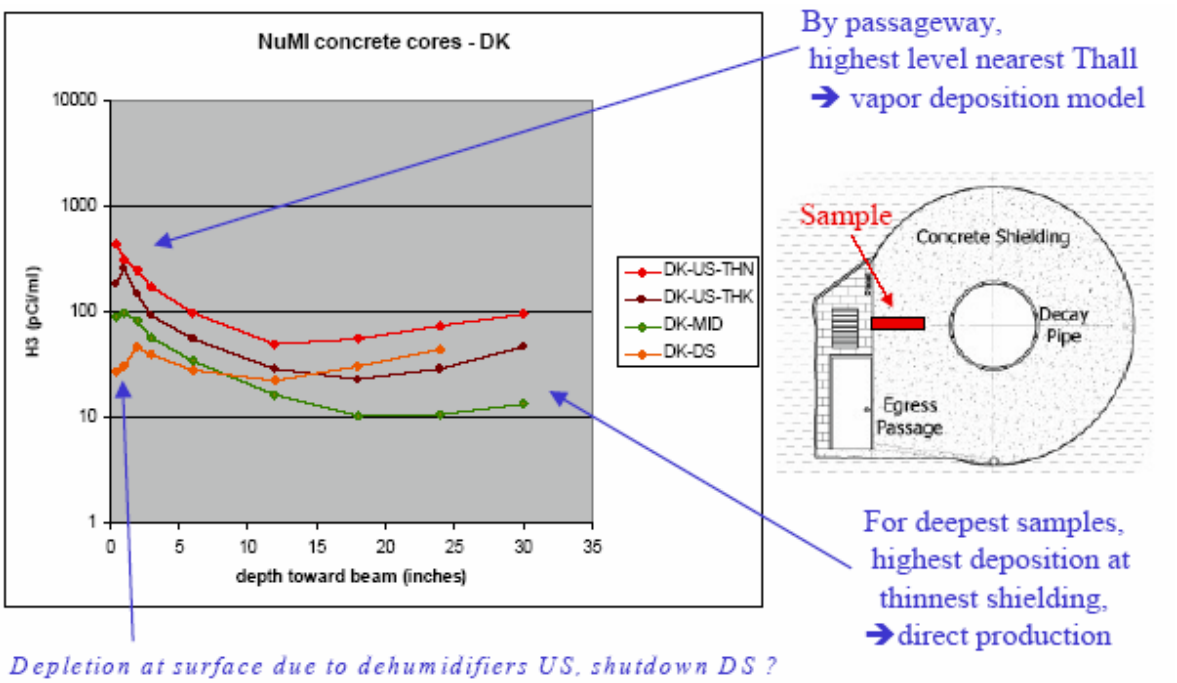

Figure 5.1-7. Tritium concentration profiles measured in concrete, showing diffusive transport from the passageway wall into the concrete, and direct tritium production in concrete (Hylen, 2006d, Slide 6)

5.2 Literature Review of Tritium Transport through Concrete and Steel

Water in concrete and rock ranges in mobility, from the relatively mobile water contained in cracks and the connected pore space, to cement and mineral hydration water, which is relatively fixed. Thus, tritium in pore-water may be relatively mobile, whereas tritium in hydration water may be much less mobile, but potentially available as a long-term source as it may exchange with more mobile water. Five pathways for tritium migration in concrete have been identified, and these can also be generalized to rock (Hochel and Clark, 1999):

1. Advection of tritium in pore-water through the connected pore space within the concrete or rock
2. Tritium exchange with hydrogen in hydrated cement components or hydrogen in minerals composing the rock
3. Advection of gaseous tritium or tritiated water vapor through available gas-filled pore space
4. Diffusion of T+, OT- ions and HT molecules
5. A combination of pore movement and HTO diffusion through pore-boundary materials under barometric or hydrostatic pressures

Numata et al. (1990a) performed thermogravimetric analyses of four different cement materials to determine the temperature range over which major water releases occurred. They found that the water released from cement can be distributed into four groups:

1. Liquid water, which desorbed below 200°C
2. Water of crystallization, which desorbed between 200-450°C
3. Decomposition of calcium hydroxide between 450-550°C
4. Dissociation of OH^- base in calcium silicate hydrates between 550-850°C

Numata et al. (1990a) also exposed the four different cement materials to tritiated water vapor. The exposed samples were then heated to remove the water to determine the tritium concentration in each of the four water groups. Approximately 77% of the tritium was present in the liquid water, 15% in water of crystallization, 7% in $Ca(OH)_2$, and 1% in the OH^- base of calcium silicate hydrates.

Several studies have examined tritiated water vapor interaction with concrete (Numata et al., 1990a, 1990b; Furuichi et al., 2006). Tritiated water vapor will exchange with water in the pores that directly contact the atmosphere, or condense in the pores if the concrete is not saturated with water. Tritiated water will also eventually reach the pores that do not contact the atmosphere by diffusing through the concrete (Dickson, 1990). Numata et al. (1990b) measured the tritium concentration in cement plugs exposed to tritiated water vapor at different times, as well as the depth profile of tritium in cement plugs. They obtained apparent diffusion coefficients by fitting the experimental data with the theoretical solution (numerically solving the one-dimensional diffusion equation). Furuichi et al. (2006) conducted experiments in a packed bed of cement

particles to obtain the overall mass transfer coefficients representing adsorption of water vapor onto the concrete and the isotope exchange reaction. They obtained an isotope exchange capacity about 20% of the reported value in Numata et al. (1990b). Furuichi et al. (2006) noted that a smaller value may have been obtained because preferential paths for the vapor existed along the walls of the cement paste tube.

Diffusion of tritated water through saturated cement samples has also been investigated in the laboratory. Numata (1990b) conducted through-diffusion experiments on the different saturated-cement materials to examine the relationship between the diffusion coefficient of tritiated water and porosity. They found that the diffusion coefficient increased proportionally to the increase in porosity. Tits et al. (2003) also set up through-diffusion cells to investigate diffusion of tritiated water and Na-22 through saturated cement. A pure diffusion model and a diffusion/sorption model were used to describe the breakthrough curves, and they fit the data equally well. However, when the best-fit parameters from these two models were used to fit the curves from out-diffusion tests, the pure diffusion model was not able to describe the measured data, whereas the model with sorption had good agreement with the data. The diffusion coefficients obtained by Tits et al. (2003) were about two orders of magnitude larger than the ones estimated by Numata (1990b). The differences in the diffusion coefficients from these two studies could be explained by the fact that different types of Portland cement were used (Numata et al., 1990b did not specify the exact type) and that different cement-to-water ratios were used for the samples.

Hochel and Clark (2000) used hammer drilling to collect concrete samples from two facilities at the Savannah River Site that had been exposed to tritium. Analysis of the concrete revealed a relatively constant tritium concentration with depth, a finding not previously reported in the literature. The authors suggested that this profile was the result of relatively rapid transport of tritiated liquid through the water-filled pores of the concrete. They argued that their results indicate that tritium concentration depth profiles in concrete produced from liquid exposure are fundamentally different from those produced by vapor exposure. Diffusion theory was unable to describe the constant concentration profile, whereas a hydraulic flow model could explain the tritium distribution.

The penetration of tritiated liquid water through concrete was studied from a waste management perspective by Eichholz et al. (1989). Tests were performed on concrete cylinders. Dry, uncoated concrete absorbed water rapidly and conducted the tritiated water at a nearly constant rate once it was wetted. For specimens over 10 cm thick, tritium movement was controlled exclusively by only the porosity and permeability of the concrete.

Chen et al. (2003) measured diffusion of tritium in stainless steel vessels that stored tritium at high pressures at room temperature for 4-6 years. The concentration distribution of tritium at different depths from the surface was measured by gradually etching the surface with acid and then analyzing the released gases. The concentrations of elemental tritium gas (T_2) were found to be nearly the same with depth and were lower than the HTO concentrations. High concentrations of HTO were measured on the surface, indicating that tritium had adsorbed onto the thin surface oxide layer. Sorption of HT on stainless steel has been analyzed in several earlier studies (e.g., Hirabayashi et al., 1984, 1985; Surette et al., 1988). Hirabayashi et al. (1985) found that surface tritium constitutes around 90% of the tritium contamination from a 7-day exposure to HT. In the

study by Chen et al. (2002), the HTO concentration decreased quickly with depth, and a "valley" in the profile was observed followed by an increase in HTO concentration. The decrease and subsequent increase in HTO concentration with depth was explained by tritium escaping through microcracks. Maienschein et al. (1985; 1988) studied tritium permeation through low-permeability metals and found that tritium diffusion is generally controlled by diffusion along grain boundaries and other defects rather than diffusion through the crystalline metal structure.

5.3 Diffusion Tests in Concrete and Host Rock Samples

Diffusion tests through concrete and host rock have been conducted at LBNL to quantify the tritium diffusion and retardation by exchange with hydrogen in less mobile water throughout the concrete or rock. As a simplification, we used deuterium as an analogue for tritium in these tests. Based on the ratio of the reduced masses of HDO and HTO, the difference in the measured diffusion rates is small, just over 1% larger for HDO compared to HTO. Through-diffusion tests were performed on fabricated Decay Pipe concrete, the Target Hall concrete, and the dolomite rock from the Decay Pipe walkway. Two back-diffusion tests were conducted on powdered concrete from the Target Hall.

The governing equation for one-dimensional diffusion along the x-axis is given by

$$D_m \frac{\partial^2 C}{\partial x^2} + D_i \frac{\partial^2 C_i}{\partial x^2} + \phi D_F \frac{\partial^2 F}{\partial x^2} = \phi_c \frac{\partial C}{\partial t} + (\phi - \phi_c) \frac{\partial C_i}{\partial t} + (1-\phi)\rho \frac{\partial F}{\partial t} \qquad (1)$$

where

C	species concentration in the mobile pore water
D_m	intrinsic diffusion coefficient for the mobile pore water
C_i	species concentration in the immobile pore water
D_i	intrinsic diffusion coefficient in the immobile pore water
F	$= K_d K_i C$, relative concentration of the adsorbed mass
K_d	distribution coefficient
K_i	mass transfer coefficient
D_F	apparent surface diffusion coefficient
ρ	grain density
ϕ	total porosity
ϕ_c	$= \phi (1 - S_r)$, kinematic porosity
S_r	irreducible water saturation
X	length coordinate in the diffusion equation
t	time

The three terms on the left-hand side of (1) describe diffusion in the mobile pore water, diffusion through the immobile thin film adjacent to the porous medium grains, and surface diffusion, respectively. Surface diffusion is the phenomenon of increased diffusive flux caused by the sorbed species being partly mobile. The three terms on the right-hand side of (1) describe the dissolved species accumulation in the pore water, in the immobile fraction, and on the porous

medium grains due to sorption, respectively. The kinematic porosity ϕ_c is the portion of the porosity corresponding to the mobile fraction of the fluid phase.

Moridis (1999) derived a semianalytical (SA) solution to the diffusion problem under the conditions of diffusion cell experiments using Equation 1, subject to mass conservation of the dissolved species and the appropriate initial and boundary conditions. The SA solution is used to analyze the results of the through-diffusion experiments presented in Section 5.3.2.

5.3.1 Through-Diffusion Tests: Methods

Two through-diffusion tests were conducted on fabricated Decay Pipe concrete using the recipe provided by Fermilab, which consisted of Portland Type III cement, aggregate, water, and cement admixture. A sample of FA-5 aggregate from Vulcan Material's McCook Quarry in McCook, Illinois was sent to LBNL. This aggregate was sieved using a #6 sieve (3.35 mm openings) to remove the largest pieces of aggregate. Portland Type III cement was obtained locally from Alta Building Materials in Oakland, California. Darecem ML 330 cement admixture was purchased from GRACE Construction.

Through-diffusion tests were also conducted on the Target Hall concrete (LEDGE-MID sample) and dolomite rock from grate #1 along the Decay Pipe walkway that were sent to LBNL by Fermilab. Two tests were conducted on the Target Hall concrete and two were conducted on the dolomite. The density and porosity of the three different materials used in the through-diffusion tests were measured in the laboratory and their properties are summarized in Table 5.3-1.

Table 5.3-1. Summary of material properties

Material	Density (g/cm^3)	Porosity	K_d (m^3/kg)
Decay Pipe concrete	2.1	0.23	1.2×10^{-5}
Target Hall concrete	2.2	0.15	6.9×10^{-5}
Dolomite	2.6	0.06	6.2×10^{-6}

The measured Decay Pipe concrete density is used in the numerical simulations in Section 5.6. The porosities of the Decay Pipe concrete and dolomite, and the dolomite density used in the simulations are literature values. The Target Hall is not simulated in this study.

Batch sorption tests were conducted to obtain the sorption coefficient, K_d, of deuterium on the concrete and the rock. For the Decay Pipe concrete, a mixture of mm-sized FA-5 aggregate (92% by weight) and Portland Type III Cement was prepared for these tests. The powdered Target Hall concrete sent by Fermilab (NuMI TH East Pit Ledge, L-MIDHR-46) was used to estimate the sorption coefficient. The dolomite was crushed to powder for these tests. For each material, five vials containing 300 ppm HDO solution and solid mixture were prepared with a solid to water ratio (g solids/ml water) of 0.167. The vials containing the mixture were placed on a shaker table and analyzed after 7, 14, and 21 days. The sorption coefficients (volume of HDO per kg of solid) at ambient temperature and pressure obtained from these tests are summarized in Table 5.3-1 for the three materials used in the through-diffusion experiments.

For the through-diffusion tests, a 5 mm thick slice of concrete or dolomite with a diameter of 4.4 cm was placed between two acrylic boxes with dimensions of 9.7 cm × 9.7 cm × 11.8 cm (L × W × H). The sample was epoxied into a plastic ring to seal the outside edges. A hole was cut in the boxes with the same diameter as the sample, and the plastic ring holding the sample was glued between the two boxes. A schematic of the through-diffusion cell is shown in Figure 5.3-1.

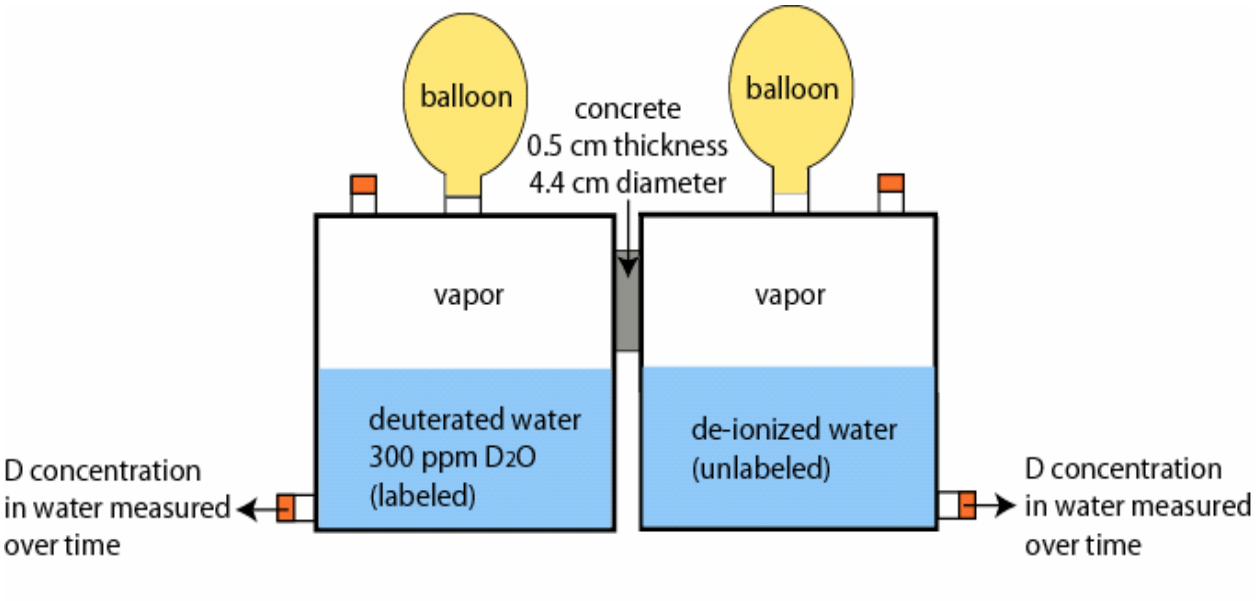

Figure 5.3-1. Schematic of through-diffusion cell

In the tests, 500 mL of water tagged with deuterium at a concentration of 300 ppm was added to one cell, and 500 mL of unlabeled water (no deuterium added) was placed into the other cell. The water level in the cells remained below the sample, since we are interested in obtaining the diffusion coefficient when the sample is in contact with vapor. A small tube with a septum stopper was placed near the bottom of both cells to extract the water over time using a syringe. Another tube with a septum stopper was placed at the top of the cell to initially equilibrate both sides of the cell to atmospheric pressure, using a syringe that was open to the atmosphere. Because water is extracted from the cells for sampling, the volume and pressure of the vapor phase will change as water is removed if the cell volume is fixed. Therefore, we designed a cell with a flexible top such that the volume and pressure of the vapor remained constant as the water is extracted. A tube was glued to the top of the cell and a balloon was placed over it to provide the flexible top. The diffusion cell was placed inside an incubator at a temperature of 22°C and the experiments were run for a period of 30 days. Water samples were extracted from the cell more frequently during the first half of the experiment (up to twice a day during the first three days in some experiments, then once a day for a week or two), and then less frequently during the latter half (every other day).

In Experiment DK-1, an experiment conducted on the Decay Pipe concrete, the cells were placed over magnetic stirrers to continually mix the water. A temperature gradient in the cells developed from the heat generated by the stirrers and resulted in condensation in the diffusion cells.

Measurement of the water saturation in the concrete after the completion of the experiment demonstrated that the condensed water had completely saturated the concrete. Therefore, diffusion of deuterium through the liquid water is measured in this experiment. Because the relative humidity in much of the Decay Pipe walkway is near or at 100% humidity and the concrete is wet, the conditions from this through-diffusion experiment are representative of the conditions in portions of the walkway.

In the remaining through-diffusion experiments conducted on another piece of the Decay Pipe concrete, the Target Hall concrete, and the dolomite, the magnetic stirrers were not used to eliminate the temperature gradient that resulted in condensation in the cells. After the completion of the experiments, the sample was removed from the cell and its water saturation was measured gravimetrically. Some of the samples were unsaturated; therefore, a combination of diffusion of deuterium through both the air and water was measured in those experiments.

5.3.2 Through-Diffusion Test Results

Results of the through-diffusion tests on the Decay Pipe concrete, Target Hall concrete, and the dolomite are presented in this section. Analyses of the data to obtain estimates of the diffusion coefficient were performed using the semianalytical (SA) solution derived by Moridis (1999) for diffusion cell experiments. In deriving this solution, Equation 1 was subject to mass conservation of the dissolved species, and the upstream and downstream volumes of the diffusion cell and the area and thickness of the sample became part of the calculations because of this condition. The parameter values used in the semianalytical solution are provided in Table 5.3-1 and in Table 5.3-2. V_L and V_U are the volumes of the vapor phase in the labeled and unlabeled cells, A is the area of the concrete sample, L is the thickness of the sample, S_r is the residual saturation, D_F is the apparent surface diffusion coefficient, ϕ_c is the kinematic porosity, and K_i is the mass transfer coefficient. We assume that all the pore water is mobile when analyzing the data.

Table 5.3-2. Parameters used in the semianalytical solution

Parameter	Value
V_L, m^3	5×10^{-4}
V_U, m^3	5×10^{-4}
A, m^2	1.55×10^{-3}
K_i	1
L, m	5×10^{-3}
S_r	0
D_F	0
ϕ_c	0

5.3.2.1 Decay Pipe Concrete

The deuterium concentrations measured over time in the through-diffusion experiments conducted on the Decay Pipe concrete are shown in Figures 5.3-2a and 5.3-2b for Experiments DK-1 and DK-2, respectively. The fluctuations in the deuterium concentrations on the labeled (upstream) side are primarily because of carryover from previous samples that were analyzed in the mass spectrometer. However, the concentrations on that side have an overall decreasing trend over time, and mass balance between the labeled and unlabeled sides is achieved in both experiments. The deuterium concentration on the unlabeled side in Experiment 2 (partially saturated concrete sample) increases with time at approximately half the rate of Experiment 1, indicating that the diffusion rate increases as the concrete saturation increases. The higher temperatures in the diffusion cell when the stirrers were used could have also contributed to the larger diffusion rate. However, the air temperature in the diffusion cells was only around 2°C higher with the stirrers. This temperature difference is unlikely to account for the twofold increase in the diffusion rate.

The semianalytical solution derived by Moridis (1999) was used to analyze the results of the data from Experiment DK-1. The results from Experiment DK-2 cannot be analyzed with the SA solution because the concrete was partially saturated in that experiment, and the SA solution was formulated only for liquid diffusion. A saturation of 0.6 was measured in the sample from Experiment DK-2. The diffusion coefficient, D_m, was adjusted to obtain the best fit of the SA solution to the data, which is shown in Figure 5.3-2a. The estimated diffusion coefficient of 2.4×10^{-10} m^2/s (used in the flow and transport simulations presented in Section 5.6) is 2.4 times larger than the diffusion coefficient Fermilab obtained (1×10^{-10} m^2/s) by adjusting this value to obtain a best fit of the diffusion equation to the measured tritium concentrations in the Decay Pipe concrete (Lundberg, 2006). The differences in the values may result from our experiments being conducted using fabricated Decay Pipe concrete, which probably has a different porosity and aggregate grain size distribution compared to the actual concrete. The value of the Decay Pipe concrete porosity used in the simulations presented in Section 5.6 was obtained from the literature.

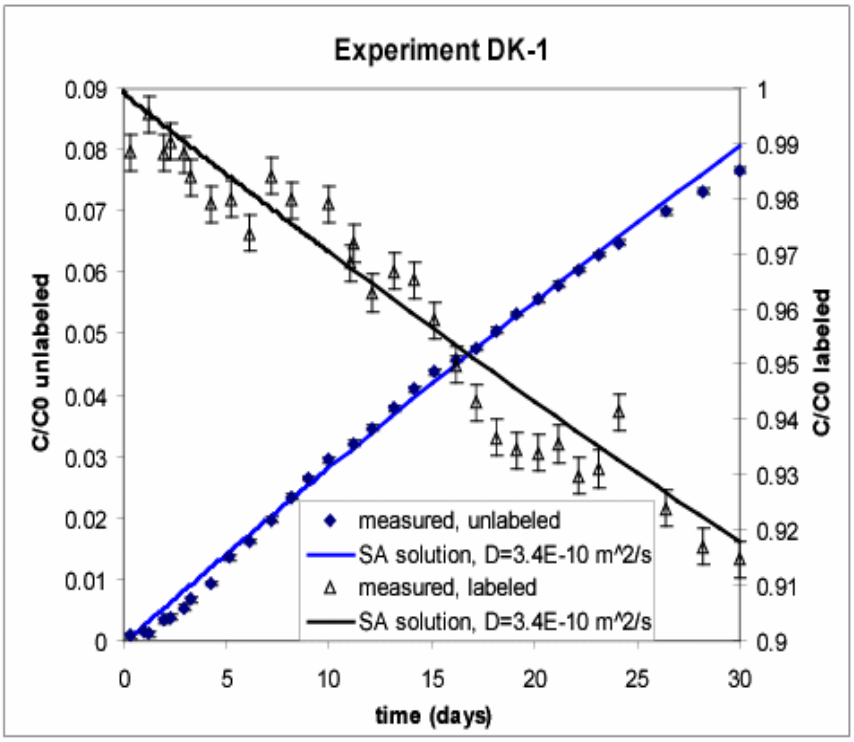

(a)

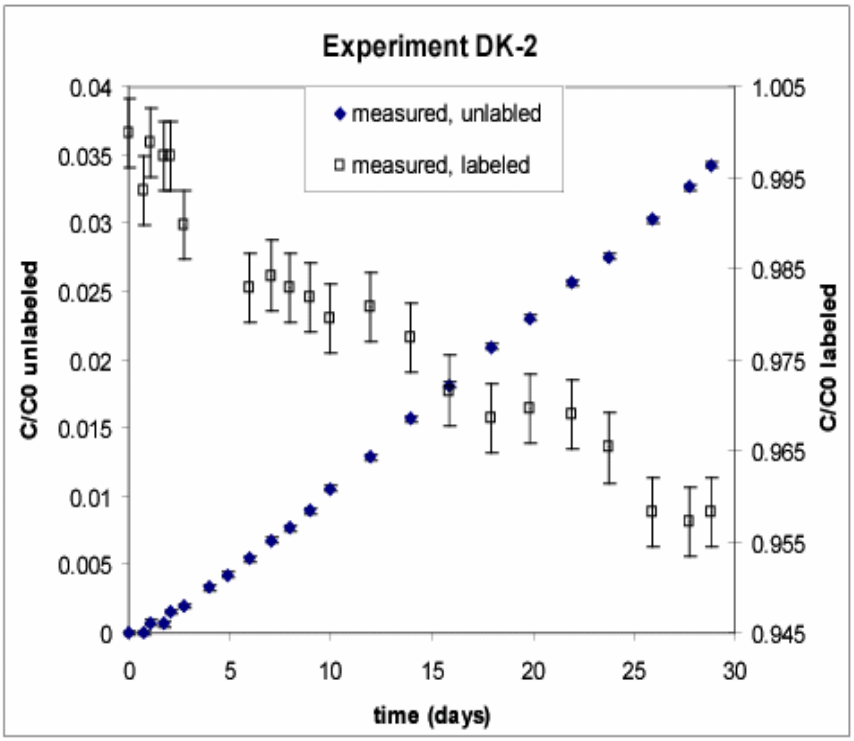

(b)

Figure 5.3-2. Through-diffusion test results on fabricated Decay Pipe concrete from (a) Experiment DK-1 and (b) Experiment DK-2

5.3.2.2 Target Hall Concrete

The deuterium concentrations measured over time in the unlabeled and labeled sides are shown in Figure 5.3-3 below for the through-diffusion experiment conducted on the Target Hall concrete, Experiment THD-1. Measurement of the water saturation of the sample at the completion of the experiment indicated that it was saturated. Fluctuations in the deuterium concentrations on the labeled side are once again observed in the experiment. The labeled deuterium concentrations alternate between a higher and lower value in each successive measurement suggesting that there may have been a systematic error when the water samples were analyzed in the laboratory. The concentrations on the labeled side have an overall decreasing trend over time, and mass balance between the labeled and unlabeled sides is achieved. An estimated diffusion coefficient of 2.1×10^{-11} m^2/s was obtained from the best fit of the semianalytical solution to data. The diffusion coefficient of the Target Hall concrete is about an order of magnitude smaller than the Decay Pipe concrete. A second test was performed on another sample of the Target Hall concrete, but the results indicated that there was a leak in the system. We therefore did not use the data from the second test to estimate the diffusion coefficient.

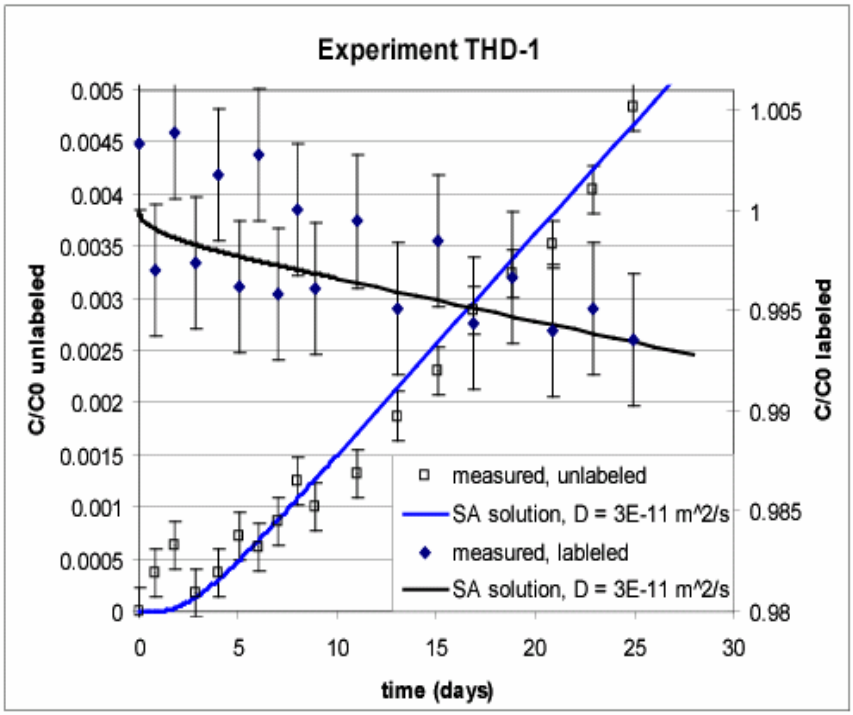

Figure 5.3-3. Through-diffusion test results on fabricated Target Hall concrete.

5.3.2.3 Dolomite

The results from the through-diffusion tests conducted on two dolomite samples, Experiments DD-1 and DD-2, are shown in the Figures 5.3-4. The rate of increase in the deuterium concentration on the unlabeled side is greater in Experiment DD-1 compared to DD-2. Estimated diffusion coefficients of 2.1×10^{-10} m^2/s and 9.3×10^{-11} m^2/s were obtained for DD-1 and DD-2, respectively, using the SA solution. A summary of the diffusion coefficients obtained from all the experiments is provided in Table 5.3-3. The two experiments were set-up identically; therefore, the differences in the diffusion coefficients are probably because of heterogeneities in the samples, and in particular, the presence of microfractures in the samples. The diffusion coefficient would vary depending on the length, aperture, and density of the microfractures in the samples. The porosity of the dolomite was lower than the Target Hall concrete (6% versus 15%); however, the diffusion coefficient of deuterium in the dolomite is nearly an order of magnitude greater than the Target Hall concrete and nearly the same magnitude as the Decay Pipe concrete. (Note that the saturation in both samples was approximately 0.8; the resulting diffusion coefficients obtained using the semi-analytical solution therefore represent effective values.) The smaller sorption coefficient of deuterium on the dolomite compared to the Target Hall concrete combined with diffusion through microfractures in the dolomite matrix are the likely reasons for the higher diffusion coefficients in the dolomite.

Table 5.3-3. Summary of best-fit diffusion coefficients obtained from the SA solution

Experiment	Diffusion coefficient (m^2/s)
DK-1[a]	2.4×10^{-10}
THD-1[b]	2.1×10^{-11}
DD-1[c]	2.1×10^{-10}
DD-2[c]	9.3×10^{-11}

[a] The estimated diffusion coefficient for the Decay Pipe concrete is used in the simulations presented in Section 5.6, 3.4×10^{-10} m^2/s, was from an earlier calculation that used an upstream and downstream cell volume of 7×10^{-4} m instead of 5×10^{-4} m.

[b] The Target Hall is not simulated in this study.

[c] The estimated diffusion coefficients for the dolomite were not used in the simulations since they were not available at the time the simulations were performed.

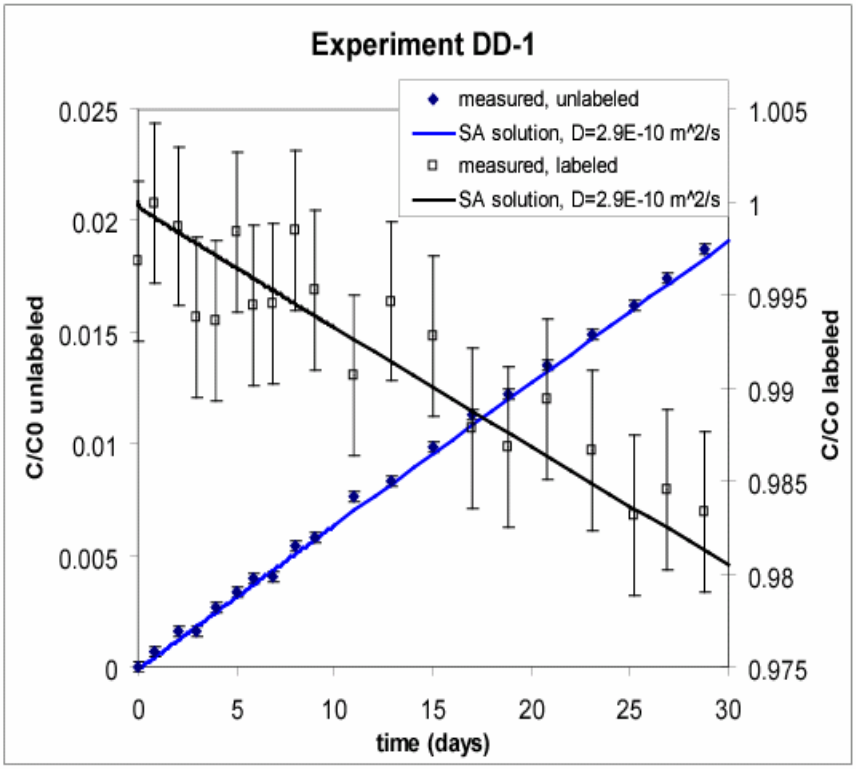

(a)

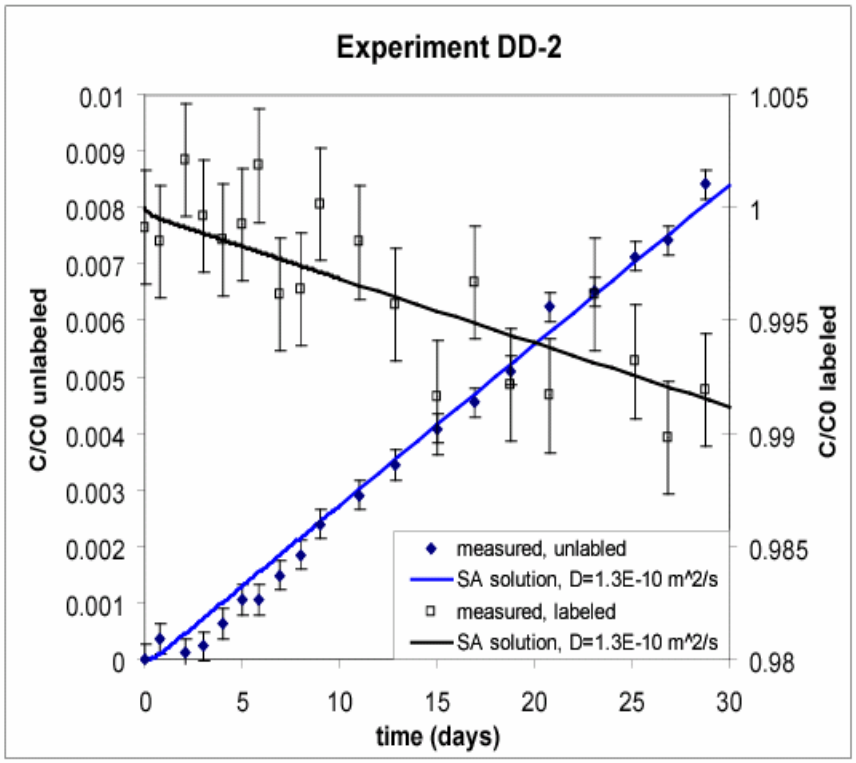

(b)

Figure 5.3-4. Through-diffusion test results on dolomite from (a) Experiment DD-1 and (b) Experiment DD-2

5.3.3 Back-Diffusion Tests

Back-diffusion tests were conducted to investigate the hypothesis that the tritium source when the beamline is shut down is a fairly thin superficial layer in the outer concrete surfaces from the Target Hall, Target Chase and Decay Pipe, in which tritium accumulates by vapor deposition during beam operation. The surfaces of the iron shielding blocks are another source of tritium during beamline shut down, but they are not being considered in this study. Experiments were conducted by placing powdered concrete from the Target Hall in a chamber and exposing it for eight days to moist air containing deuterated water vapor. The deuterium-enriched air was then purged and replaced by moist air without deuterium enrichment. Powdered samples were used so that the experiment could be performed in a relatively short time-frame. Because the powdered concrete has a larger porosity compared to the solid concrete, the diffusion rate of deuterium is greater through powdered samples versus solid concrete.

The chamber used in the experiments was an acrylic box with dimensions of 9.7 cm × 9.7 cm × 11.8 cm. A plastic ring with a thickness of 0.5 cm and an inside diameter of 4.4 cm was glued inside of the box and then filled with powdered concrete from the NuMI facility. A plastic mesh was placed over the concrete to keep it inside the ring. (A schematic of the cell is shown in Figure 5.3-5.) Two cells were assembled, one containing powdered concrete from the Target Hall pit and the other containing powdered concrete from the ledge. In both cells, 500 mL of 300 ppm deuterated water was added to enrich the concrete samples with deuterated water vapor for a period of 8 days. Water was sampled several times over that time period to measure the change in deuterium concentration with time. After the 8-day period, the deuterated water was drained from the cell and replaced with 500 mL of unlabeled de-ionized water. A small tube with a septum stopper near the bottom of the cell was used to obtain periodic water samples that were analyzed for the change in deuterium concentration, using a mass spectrometer.

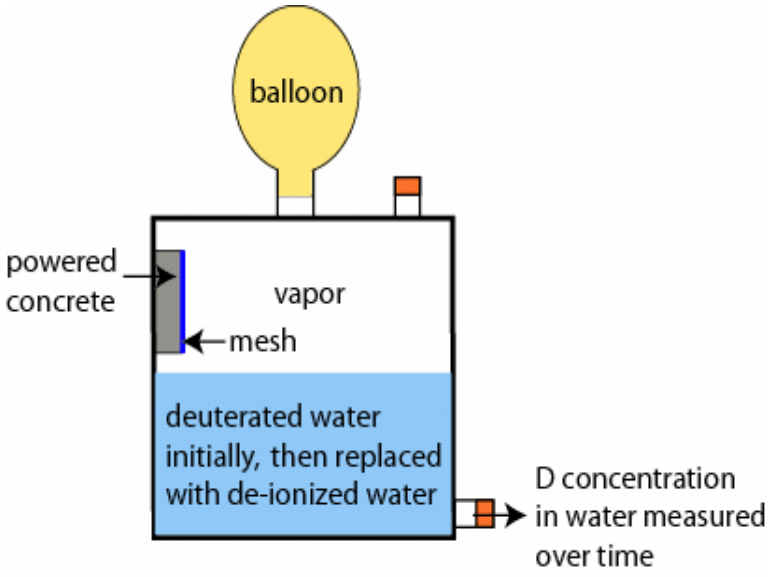

Figure 5.3-5. Schematic of back-diffusion cell

The results in Figure 5.3-6 show an increase in the deuterium concentrations over time, where a constant concentration is reached after approximately 3 days. A first-order estimate of the back-diffusion coefficient can be obtained from L^2/t, where L is the thickness of the sample (0.5 cm) and t is the time it takes for the deuterium to back diffuse out of the sample (3 days). A diffusion coefficient of 9.6×10^{-11} m^2/s is calculated using these values. The actual time constant for back diffusion from the Target Hall concrete would be larger than the results from these experiments since the powdered concrete has a larger porosity than the solid concrete. When these experiments were performed, only the powdered Target Hall concrete had been sent to LBNL. Nevertheless, the increase in deuterium concentration over time in our back diffusion experiments demonstrates that back-diffusion could be a transport process contributing to the tritium concentrations observed after the beamline is shutdown.

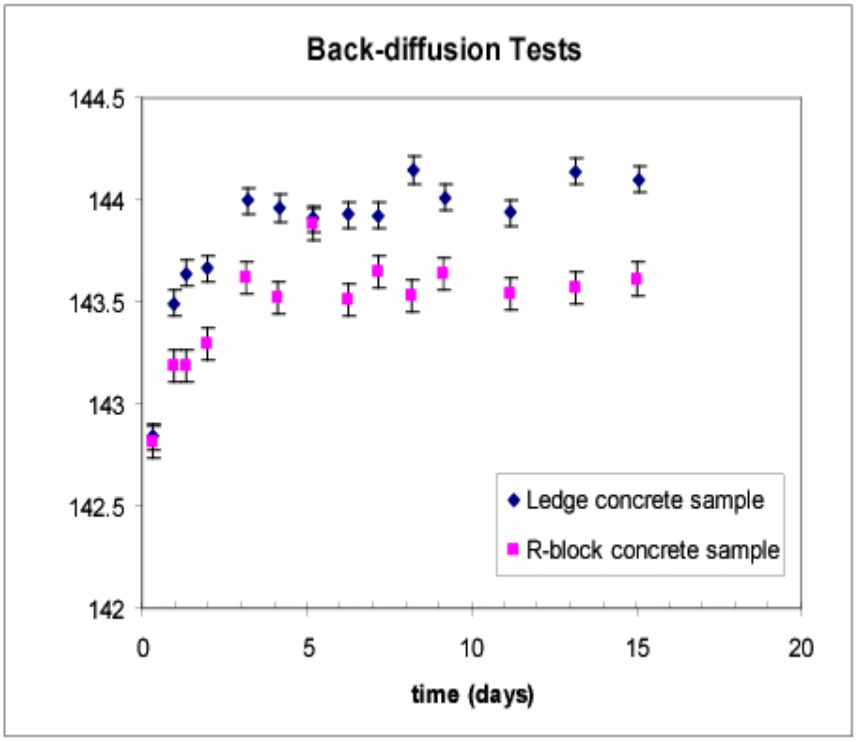

Figure 5.3-6. Results from back-diffusion experiments

5.4 Identification of Tritium Location in Concrete and Rock, and Evaluation of Tritium Mobility

5.4.1 Introduction

The focus of this task is to determine the concentrations and distribution of tritium in the concrete shielding around the beam-line in the Target Hall. This work builds on preliminary studies done at FNAL of tritium concentrations in concrete cores from in the Target Hall. These analyses were performed on powders produced by a coring process using a hammer drill technique. The powders were leached with de-ionized waters and the tritium measured in the leachate. The results of those studies identified tritium concentration depth profiles (1) increasing towards the beam line—consistent with *in situ* production—and (2) increasing towards concrete surfaces in contact with ambient air—consistent with adsorption and inward diffusion of vapor-transported tritium. However, these concentrations appeared to be too low to account for the persistent tritium levels observed when the beam is off. It was thought that this technique might inadvertently under-represent the concentration of tritium in the concrete because of the potential loss of concrete pore-water during and subsequent to the coring process, as any pore-water would readily evaporate and be lost from the powdered samples.

To test whether or not the pore water loss from the samples did affect the tritium concentrations in the cores, 12 sections of intact core from the Target Hall cores were shipped to LBNL in early September 2006 (the cores were originally drilled during May 2006 and had been stored in plastic bags at FNAL until they were sent to LBNL). The pore waters contained in samples of concrete from 4 of these sections of core were extracted for tritium analyses. To extract the pore water, the samples were placed under vacuum and heated to ~100 °C. Water evolved during the heating was collected using two traps in series held at the temperature of liquid nitrogen. Following extraction of the pore water from the samples, additional tests (de-ionized water leaches, heating) were conducted to determine the amount of additional water and tritium contained in the concrete. The results of these studies are given in Table 1 and discussed below.

5.4.2 Moisture Contents of Target Hall Concrete Shielding

In addition to the water contained within pore spaces in the concrete, water can be bound as H_2O as interlayer water (e.g., between layers in phyllosilicate minerals such as clays) or as molecular water contained in the mineral structure (e.g., gypsum, zeolites). It can also occur as hydroxyl groups, $(OH)^-$, within minerals (e.g., micas, amphiboles). These waters will be released from the different sites at different temperatures. To determine how much water this represents in the concrete, we sequentially heated the 3 of the samples after extraction of the pore water to 200°C (primarily representing interlayer water), 350°C (representing molecular water), 500°C (representing hydroxyl water) and 800°C (complete dehydration plus de-carboxylation of carbonate minerals). For each temperature, the samples were weighed, heated in a muffle furnace for 18 hours, and then weighed again. The results of these measurements are given in Table 5.4-1 and plotted on Figure 5.4-1.

The measured pore water concentrations in the concrete were much lower in the two core samples from near the exposed surface of the concrete blocks (Core #2 = 3.0 wt.%, Core #4 =3.5

wt.%) than in the two samples from deeper in the cores (Core #1.1 = 5.1 wt.%, Core #5 = 5.3 Wt.%). This could be an indication that the near-surface samples underwent more drying than the inner samples. It could also mean that the cement in the surface samples set (reacted) more. However, the cumulative mineral water released from the samples during the heating to 500°C following extraction of the pore water (average = 1.23 wt.%) was essentially identical to the amount of water released from the deeper sample (1.27 wt.%), suggesting that there was no difference in the degree of setting for the surface concrete versus the deeper concrete. The amount of weight loss for the samples heated to 800°C was large, but was likely primarily due to de-carboxylation of carbonate minerals. Although only a minor amount of carbonates probably formed as the concrete set, the aggregate used to make the concrete was largely dolomite, which contains a high concentration of CO_2.

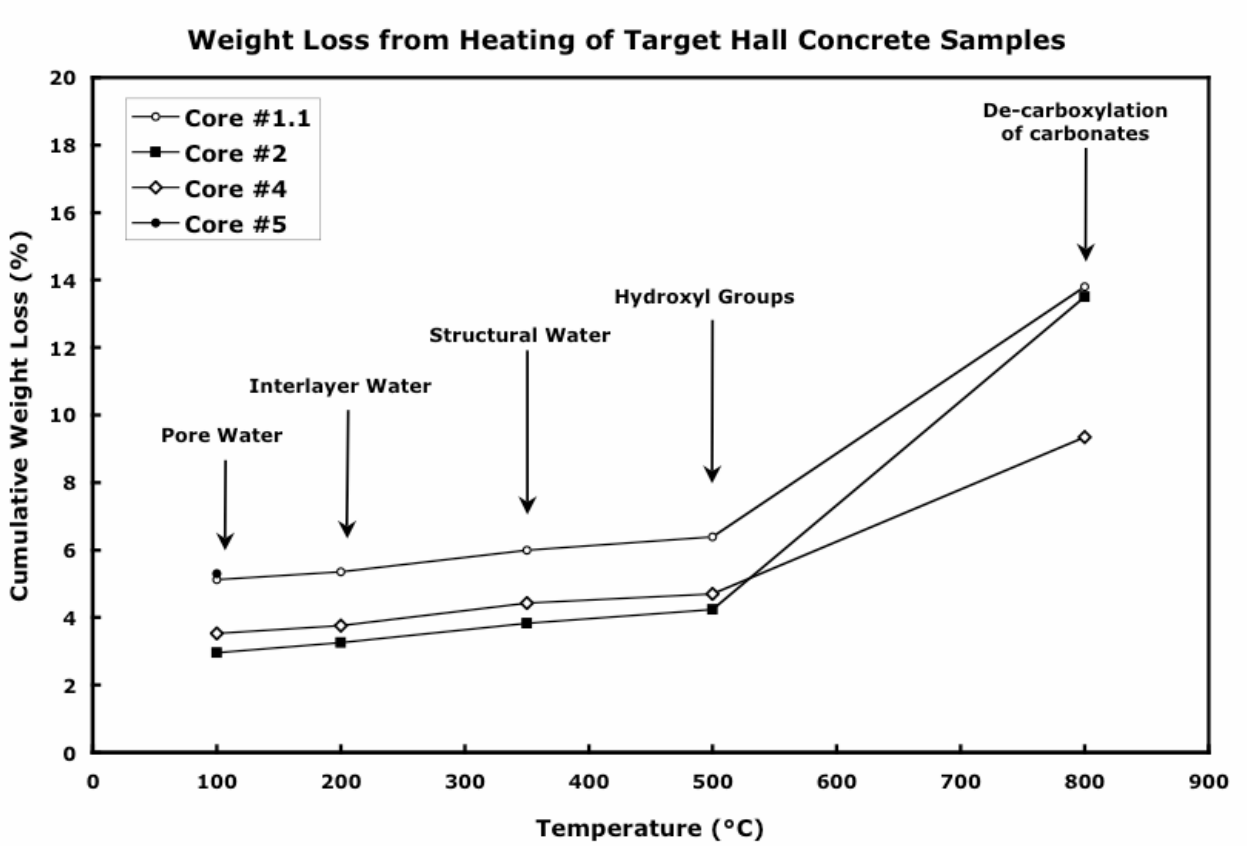

Figure 5.4-1. Cumulative weight loss for concrete samples during step heating to 800°C. Pore water extracted from the samples by heating to ~100°C under vacuum ranged from 3.0 to 5.3 wt.%. The lower concentrations were for core samples from the surface of the blocks, suggesting that evaporation from the surface of the blocks may be a factor. The total weight loss by heating from 100 to 500°C was very constant for all three samples, ranging from 1.2 to 1.3 wt.%. This weight loss presumably represents water in the mineral structure (as interlayer water or hydroxyl groups) of the concrete. At 800°C, carbonate minerals will breakdown and it is believed that most of the weight loss at this temperature represent loss of CO_2 and not water.

Table 5.4-1. Data for experiments conducted on core samples collected from the concrete shielding blocks in the NuMI facility Target Hall

Sample	Location	Depth (in)	Treatment	Wt. Loss (g)	% loss[1]	Tritium (pCi/ml PW)	Tritium (pCi/g concrete)[2]
Core #1.1	Ledg-Mid	42.5 to 54.5	Fermi Lab DI Leach	N/A			36.5
			LBNL Porewater Extraction	13.0	5.1	245.5	12.6
			LBNL Heat to 200°C	0.6	0.2		N/A
			LBNL Heat to 350°C	1.6	0.6		N/A
			LBNL Heat to 500°C	1.0	0.4		N/A
			LBNL Heat to 800°C	18.9	7.4		N/A
			LBNL DI Leach (post-800)	N/A			3.2
Core #2	Ledg-US	0 to 13.5	Fermi Lab DI Leach	N/A			750
			LBNL Porewater Extraction	6.1	3.0	1665	49.2
			LBNL DI Leach (w/o Porewater)				14.6
			duplicate T measurement				18.8
			LBNL DI Leach 2				27.2
			LBNL Heat to 200°C	0.6	0.3		N/A
			LBNL Heat to 350°C	1.2	0.6		N/A
			LBNL Heat to 500°C	0.8	0.4		N/A
			LBNL Heat to 800°C	19.1	9.3		N/A
			LBNL DI Leach (post-800)	N/A			10.6
Core #4	Ledg-Mid	0 to 13.75	Fermi Lab DI Leach	N/A			420
			LBNL Porewater Extraction	7.6	3.5	2611	92.1
			LBNL DI Leach (w/o Porewater)				70.2
			duplicate T measurement				69.1
			LBNL DI Leach 2				51.0
			LBNL Heat to 200°C	0.5	0.2		N/A
			LBNL Heat to 350°C	1.4	0.7		N/A
			LBNL Heat to 500°C	0.6	0.3		N/A
			LBNL Heat to 800°C	10.0	4.6		N/A
			LBNL DI Leach (post-800)	N/A			2.1
Core #5	Ledg-US	21 to 29	Fermi Lab DI Leach	N/A			42.0
			LBNL Porewater Extraction	11.7	5.3	500.0	26.5
			LBNL DI Leach (w/ Porewater)				36.2

[1] % loss calculated = 100 x Wt. Loss/Initial Wet Wt.

[2] Tritium concentrations are given per gram of concrete. For pore water samples, the weight of concrete is taken as the weight prior to pore water extraction.

5.4.3 Tritium Activities in Target Hall Concrete

Tritium activities in the extracted pore water and in de-ionized (DI) water leach samples was measured at LBNL's Heavy Element Research Laboratory (HERL), directed by Prof. Heino Nitsche (Table 5.4-1). For these analyses, 1 ml of water from the dehydration and leach experiments was added to ~10 ml of a scintillation cocktail. The data were then calibrated against tritium standards obtained from FNAL.

The DI water leaches were done by mixing equal weights of DI water with samples of core that had been crushed with a mortar and pestle. The samples were placed on a shaker for 20 to 24 hours and then centrifuged at 1000 rpm for 30 minutes. The free water (only approximately half of the water added was recovered) was then decanted from the sample, filtered and analyzed for tritium activity. DI water leaches were done on samples Core #2 and Core #4 (the two surface samples) after the pore water was extracted, a separate split of sample Core #5 still containing the pore water, and on samples Core #1.1, Core #2, and Core #5 after they had been heated to 800°C. In addition, the samples from Core #2 and Core #4 with the pore water extracted were leached a second time after sitting for almost 3 months. In this case, only enough DI water was added to the sample in order to bring the mass of water back to a 1:1 mixture (a significant amount of water from the first leach was trapped in the sample). The measured tritium activities measured for the DI Water leaches and the pore waters are plotted on Figure 5.4-2.

The purpose of the DI water leaches done at LBNL was to attempt to duplicate the DI leaches that were done at FNAL. However, there were still some significant differences in the way the samples were prepared. The drill used to sub-sample the cores powdered the FNAL samples, whereas the samples used for the DI leaches performed at LBNL were ground by hand. This resulted in less finely powdered samples for the LBNL DI leaches. In addition, for all but the DI leach of Sample #5, the pore water was extracted from the sample prior to the experiment. The amount of material used for the DI leaches for those samples was also smaller (50 g of concrete mixed with 50 g of DI water, versus 75 g of concrete with 75 g of DI water for the FNAL samples and Sample #5 at LBNL). These differences may have led to some of the differences in tritium concentrations measured for the DI leach samples.

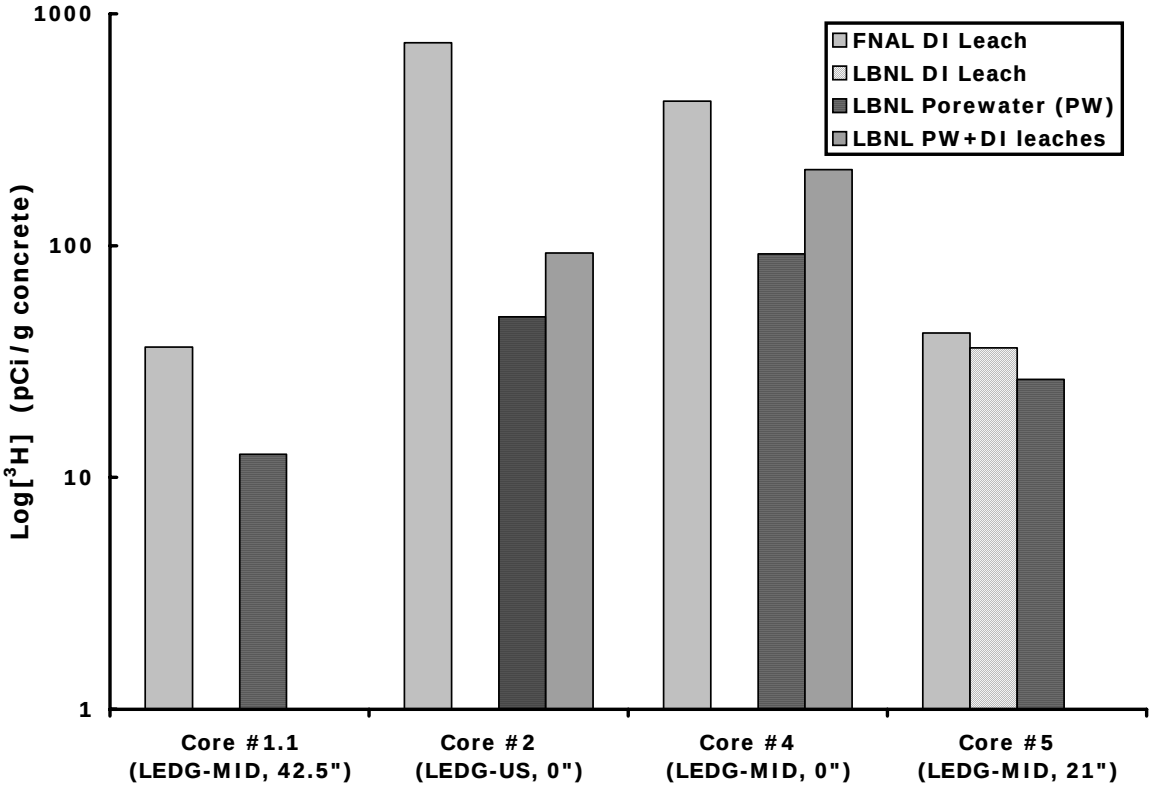

Figure 5.3-6. Measured tritium activities for samples of pore water and DI water leaches of NuMI target hall concrete shielding. In all cases, the tritium activities are normalized to the initial wet weight of the samples (with pore water). The FNAL samples were DI water leaches of powdered sub-samples of the concrete collected immediately after the cores were drilled. For all four samples, the pore water in the samples was extracted from the core samples by vacuum distillation at approximately 100°C at LBNL. After the pore water was extracted, the samples from Core #2 and Core #4 were powdered and leached with DI water twice. A separate sample of Core #5 still containing the pore water was powdered and leached with DI water (following the protocol used at FNAL).

5.4.4 Discussion

The tritium activities measured for all of the pore water and DI water leach samples at LBNL were lower than the tritium activities originally measured at FNAL (even when the pore water and all of the DI leach samples for a given sample were added together). The largest difference was for the one sample from the LEDG-US core, for which the FNAL analysis almost an order of magnitude higher. There are two possible explanations for these differences (aside from analytical errors, which seem unlikely). The first possibility is that there was significant loss of tritium from the core samples before they were shipped to LBNL. After the cores were sampled by FNAL, they were stored in un-sealed plastic bags (the samples were double-wrapped in sealed plastic and then wrapped in shrink wrap when they packaged for shipment to LBNL). Exchange between atmospheric vapor and the pore water in the concrete (which was probably

actively exchanging with tritium in the rest of the sample) could lead to a significant decrease in the tritium activity. This could be tested if DI water leaches of freshly drilled cores were conducted at both FNAL and LBNL at the same time.

The other possibility is that a large proportion of the tritium was contained in the solid concrete (e.g., in hydroxyl groups or from primary production in the matrix). For this case, the finer grain size of the leach samples prepared at FNAL could have resulted in more rapid rate of exchange with the DI water. This is supported by the fact that secondary DI water leaches of both the FNAL and LBNL still contained significant tritium. In fact, the tritium activity measured in the second leach of the LEDG-US sample at LBNL was approximately 50% higher than for the first leach (Table 5.4-1). To determine how much of an effect this could have had, would require heating the sample to 800°C under vacuum, collecting all of the water generated (including converting any H_2 gas produced to water) and measuring the tritium activity in the water. It should also be noted that de-ionized water leaches of the samples after heating to 800°C still produced measurable tritium activity, implying that there was still some tritium trapped in the matrix of the concrete (Table 5.4-1).

5.4.5 Conclusion

The original goal of these experiments was to determine whether or not loss of pore water during sub-sampling of the cores at FNAL led to loss of pore water resulting in lower measured tritium activities. While the pore water tritium activities were higher than the tritium activities measured for the DI water leaches, they were not high enough to account for the tritium activities measured in the water vapor collected from the target hall when the beam is shut off.

5.5 Plan to Develop Field Investigations of Tritium at the NuMI Facility

The initial proposal from LBNL to Fermilab on May 2006 included a task to develop a program to investigate the movement of tritium at the NuMI facility after LBNL scientists had familiarized themselves with the layout of the facility and its relationship to the surrounding geologic and hydrologic features. In July and August 2006, LBNL scientists made two visits to the NuMI facility at Fermilab. These visits included tours of the tunnel and extensive dialogues with Fermilab scientists and engineers who work directly with the NuMI facility. In addition, we reviewed information collected by Fermilab scientists on various aspects of tritium movement at NuMI, which is summarized in Section 5.1. From these communications, we developed a conceptual model (presented in Section 3) and have concluded that:

1. Water-vapor flow is a major mechanism of tritium transport in the facility.
2. Water flows into the facility from the surrounding dolomite formation.

These conclusions form the basis for the proposed set of field activities that we have recommended to understand the movement of tritium at the NuMI facility (see Section 7).

5.6 Numerical Modeling and Systematic Flow and Transport Analysis

In a preliminary effort to simulate water and gas flow as well as tritium transport through the NuMI facility, we considered a highly simplified system with the goal to obtain initial estimates and sensitivities of the system behavior. The preliminary modeling was conducted for a two-dimensional, vertical cross section perpendicular to the Decay Pipe, with a one-dimensional subsystem attached that represents the passageway running parallel to the Decay Pipe. Tritium transport from different sources (e.g., fractured rock, concrete, and passageway) was simulated separately to analyze the specific transport mechanisms and demonstrate the contributions of the respective sources to the tritium concentrations in the holding tank. Tritium is assumed to be present at certain concentrations in each of the source zones considered, and the simulations start at the time the beam was turned off. Note that this model is a first-order, approximate model without deliberate calibration against the data in Section 5.1. The purpose of this modeling effort is to demonstrate the modeling capabilities and roughly predict the integrated system response of a 60-meter segment of the Decay Pipe after the beamline is shut off.

Numerical modeling of all processes relevant to the understanding of tritium transport in the NuMI facility is challenging mainly because different transport processes occur on vastly different spatial and temporal scales: Gas transport within the ventilation system and mass transfer between phases in the tunnel occur on the order of hours and over the entire length of the facility, whereas the diffusive transport in the concrete and fractured rock occurs slowly (on the order of days and years) and over small distances. This challenge is partly addressed using a refined mesh in the vicinity of the tunnel, and a relatively coarse mesh for the concrete and fractured rock.

The model is briefly described in Section 5.6.1. Section 5.6.2 discusses the calculation of the steady-state field of water flowing towards the drainage system of the NuMI facility. Two different sets of simulations were performed to study the transient migration of tritium generated in the fractured rock and concrete (Section 5.6.3), and carried by ventilation through the passageway (Section 5.6.4). The results are integrated and discussed in Section 5.6.5.

5.6.1 Representative Cross Section of the Decay Pipe

A vertical cross section was selected for numerical analysis, representing the 60 m (200 feet) long region from the upstream beginning of the Decay Pipe to Grate 1. Figure 5.6-1 shows the cross-section geometry of the system components, including fractured rock, dimple mat, concrete with the inner vacuum pipe, passageway, and the drainage system (main drain and grates). The elements representing the passageway were connected to a one-dimensional subsystem perpendicular to the cross-section (i.e., parallel to the Decay Pipe) to allow the simulation of gas flow along the passageway. Since the main water flow direction is expected to be towards the dimple mat, resulting in a quasi radial geometry, a cylindrical model domain with a radial grid design extending to a distance of 15 m from the vacuum pipe center was used. All other geometric values were taken from STA 8+48.52 to STA 9+93.00.

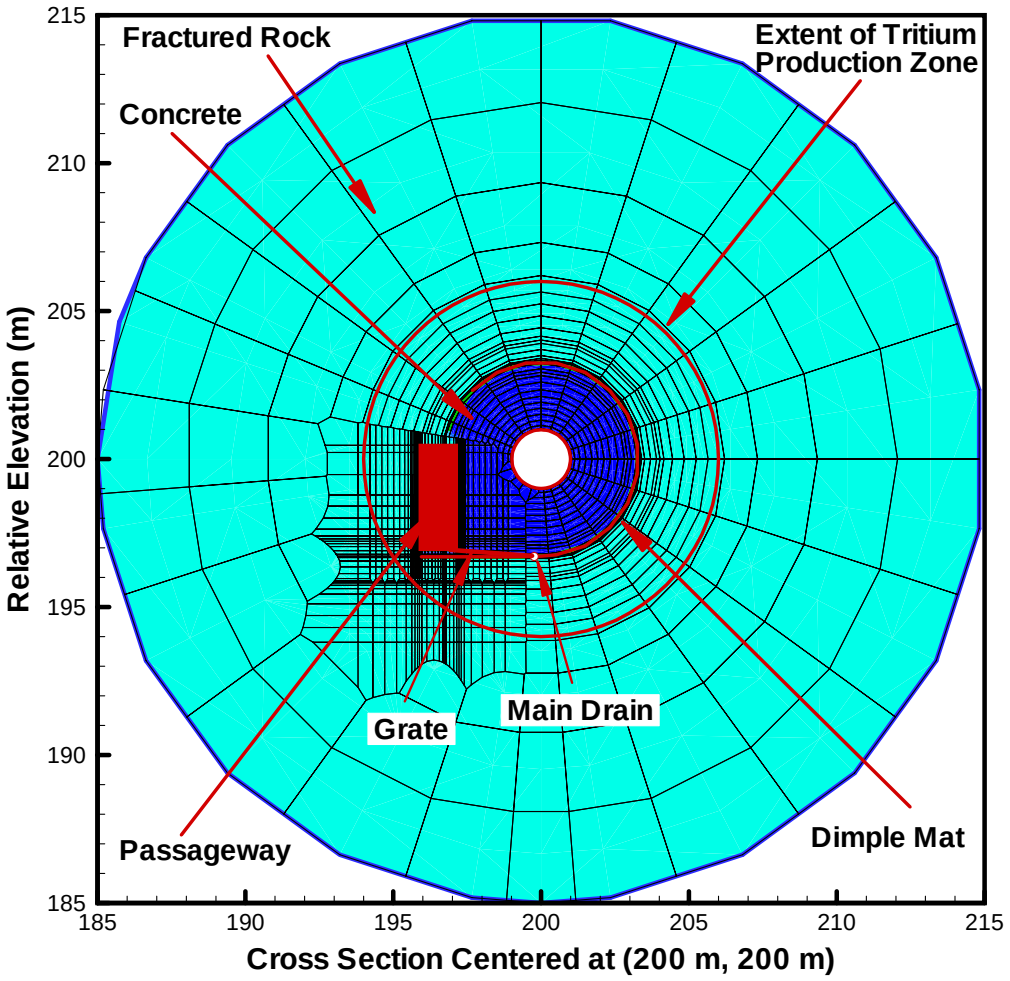

Figure 5.6-1. Model domain, numerical mesh, and material property distribution for a representative vertical cross section of the Decay Pipe

The model domain was non-uniformly discretized into 1,858 gridblocks with 3,692 connections between them. The numerical mesh was composed of two parts: the radial part in the first, second, and fourth quadrants, and the rectangular gridblocks in the third quadrant. The radial part consists of four concentric zones: (1) the vacuum tube (r < 1 m), (2) the Decay Pipe concrete (1 m < r < 3.3 m), (3) the tritium-producing zone of the fractured rock (3.3 m < r < 6 m), and (4) an outer, tritium-free region (6 m < r < 15 m). No discretization is needed for the vacuum tube. The Decay Pipe concrete around the vacuum tube has a gridblock size of 0.2 m in radial direction and sectors of 0.1π radians. The Decay Pipe concrete is embedded in fractured rock. As indicated by the star-density distribution calculated by the MARS model, no significant amounts of tritium were produced in the rock at distances greater than 6 m from the center of the vacuum tube (Lundberg, 2006). The tritium-production zone in fractured rock (3.3 m < r < 6 m) was discretized into gridblocks of size 0.4 m by 0.1π radians. The mesh is even coarser in the outer, tritium-free zone of the fractured rock (6 m < 15 m). A thin (0.05 m) ring of high-permeability elements at r = 3.3 m represents the dimple mat. At its lowest point, the dimple mat

is connected to an element representing the main drain, which is held at atmospheric pressure. This boundary condition—combined with the high permeability of the dimple mat—makes the dimple mat act as a cylindrical drainage system to which water converges radially from surrounding fractured rock. The rectangular part of the mesh (representing the passageway and its immediate surroundings) is refined in the vicinity of the concrete and rock walls to be able to appropriately resolve the diffusive transport of tritium into the concrete and rock from the passageway. The multiple interacting continua (MINC) approach (Pruess and Narasimhan, 1985) was used for accurate modeling of diffusive mass transport between fractures and the rock matrix in the fractured rock, i.e., each gridblock of the fractured rock was further discretized into one fracture subgridblock and five matrix subgridblocks.

5.6.2 Steady-State Water Flow to the Drainage System

For this preliminary modeling study, no regional groundwater flow over a large scale was considered. Only the local water flow converging towards the NuMI drainage system (i.e., dimple mat, grates in passageway, and main drain) was simulated. The convergent water flow in the representative cross section of the NuMI facility was assumed to be at steady state. The water pressure at the outer radial boundary was specified assuming hydrostatic conditions with a water level of 210.30 m (690 feet). The passageway is connected to EAV 2, which is at atmospheric pressure. The main drain is also at atmospheric pressure. The hydraulic properties of the concrete, fractured rock, and dimple mat were specified using the site-specific values (if available) provided in NuMI facility reports, or (if unavailable) are taken from the literature (see Table 5.6-1). For example, the concrete permeability was taken from Selih et al. (1996) and assigned a value of 10^{-16} m^2.

Figure 5.6-2 shows the distribution of the simulated liquid saturation and hydraulic head. The dimple mat is mostly unsaturated, with liquid saturations ranging from 0.50 at the main drain to 0.25 at the apex of the mat. There are two sections of the dimple mat that are fully saturated. On the top-left side, the dimple mat is saturated because water cannot drain around the left side of the Decay Pipe through the dimple mat, which is discontinued before it reaches the passageway (see Figure 5.6-1). A short section of the dimple mat under the passageway is also fully saturated, because the mat terminates there and is horizontal. The flow regime changes to unsaturated conditions as water in this section of the dimple mat approaches the main drain. Although most of the dimple mat is unsaturated, the velocity of water collected within the dimple mat is relatively high, as the dimple mat captures most of the water that flows from the fractured rock towards the low-pressure region caused by the drainage system, resulting in negligible flow into the concrete. This can be seen from the water mass flux shown as arrows in Figure 5.6-2d, which indicates the dimple mat (and the space between the fractured rock and concrete) acts as a channel of fast flow for water collected from the fractured rock.

The passageway is essentially gas filled, with some small amount of immobile water provided in the model to ensure 100% relative humidity (a result of the assumption that thermodynamic equilibrium exists locally). Water entering the passageway flows along the rock wall (represented by a thin layer) of the passageway in the form of film flow. The water seeping into the passageway is collected by the grate (one gridblock on the passageway floor), which is connected to the main-drain gridblock.

The concrete on the right-hand side and top of the passageway is not fully saturated, but the water saturation exceeds 90%. All other portions of the concrete are fully saturated. The water flow in concrete is very small because of its low permeability; nevertheless, this water flow may affect the long-term, downward tritium transport (see Sections 5.6.3.3 and 5.6.3.4).

Since the water collected in the drainage system (i.e., dimple mat, grate, and main drain) predominantly originates from the fractured rock (with only minor contributions from the low-permeability concrete), the calculated rate in the main drain is calibrated to the measured rate at the sump to estimate fracture permeability. Assuming that flow of collected water to the sump is proportional to the length of a cross-sectional segment along the main drain, we calculated the total flow rate to the main drain from the 60 m long cross section to be 10.6 gallons per minute (gpm). (Note that the total flow rate at the sump is 177 gpm, and the length of the main drain is approximately 1000 m; a uniform distribution of flow rate to the main drain was assumed in this preliminary study, regardless of the effect of geological layering on flow rate distribution.) Based on this value, we obtained a fracture permeability of 1.44×10^{-14} m^2, which is approximately two orders of magnitude lower than the value in a NuMI report (Grossman, 2004). The permeability estimated by calibration against the main drain outflow rate may be smaller than that used in the regional groundwater flow model of Grossman (2004) because (1) a reduction of effective permeability by grouting of the tunnel walls, (2) the difference between the observation scale (in meters) in this study and the large regional scale for groundwater flow, and (3) the relatively lower mass fluxes in the downstream portion of the Decay Pipe, which are included in the average value used for calibration. The preliminary fracture-permeability calibration can be improved by using more data on water flow rates in the drainage system. The simulated flow rate of collected water through the grate is 2.4 gpm, which is 23% of the total mass flow rate (10.6 gpm) of the water collected in the main drain for the representative cross-sectional segment. This flow rate is close to that for Grate 1 (2.2 gpm) as estimated by Fermilab staff in their calculation of tritium mass contribution at different grates (Hylen, 2006e, water flow data table).

Hydraulic and transport parameters used in the flow and transport model are summarized in Table 5.6-1.

Table 5.6-1. Hydraulic and transport parameters used in the flow and transport model

Property	**Fracture***	**Matrix***	**Concrete**
Permeability[@]	$1.44 \times 10^{-14}\ \mathrm{m}^2$	$1.00 \times 10^{-17}\ \mathrm{m}^2$	$1.00 \times 10^{-16}\ \mathrm{m}^2$
Porosity[#]	0.01	0.15	0.12
van Genuchten[%] α	$1.0 \times 10^{-3}\ \mathrm{Pa}^{-1}$	$1.0 \times 10^{-6}\ \mathrm{Pa}^{-1}$	$1.0 \times 10^{-4}\ \mathrm{Pa}^{-1}$
van Genuchten[%] m	0.6	0.6	0.6
Tortuosity[&]	0.25	0.15	0.17
Diffusion coefficient[^] D_m	$5.0 \times 10^{-10}\ \mathrm{m}^2/\mathrm{s}$	$3.0 \times 10^{-10}\ \mathrm{m}^2/\mathrm{s}$	$3.4 \times 10^{-10}\ \mathrm{m}^2/\mathrm{s}$
Tortuosity[&]	0.25	0.15	0.17
Fracture spacing[$]	4 m		
Free-water diffusivity, D_0	$2.0 \times 10^{-9}\ \mathrm{m}^2/\mathrm{s}$		
Gas diffusivity	$1.0 \times 10^{-5}\ \mathrm{m}^2/\mathrm{s}$		
Inverse Henry's constant[+]	$3.2 \times 10^{3}\ \mathrm{Pa}$		
Tritium half-life	12.3 years		

* In this study, the fractured rock is conceptualized as a dual-permeability medium. All fractures are lumped into a domain with effective continuum properties; the rock mass between the fractures is represented by the matrix continuum; both the fracture and matrix continua occupy the same computational space. Flow occurs within each of the continua as well as between the fracture and matrix continua.

[@] The absolute (or intrinsic) permeability k [m^2] is a measure of the ability of a material to transmit fluid. It is related to the hydraulic conductivity K [m/s] (which is a lumped parameter that includes both material and fluid properties) by $K = k \cdot (\rho g / \mu) \approx k \cdot 10^7$. The fracture permeability is calibrated using the flow rate in the main drain; the matrix permeability is taken from Grossman (2004, Table 2); the concrete permeability is taken from Selih et al. (1996) .

[#] Porosity is defined as the ratio of the pore volume to total volume. Values for matrix and concrete porosities are taken from Grossman (2004, p. 6) and Selih et al. (1996), respectively Fracture porosity is defined as the volume associated with fractures per cubic meter; 1% is a typical value

[%] The van Genuchten model describes the capillary pressure and relative permeability as a function of liquid saturation (van Genuchten, 1980). The capillary pressure P_c [Pa] is the difference in pressure across the interface of two immiscible fluids; it can be expressed as a macroscopic quantity and related to the average saturation within a continuum element. Relative permeability k_{rl} [-] captures phase interference processes, i.e., the reduction in permeability of a given phase due to the presence of another phase. Both quantities depend on fluid properties as well as the pore size distribution and pore connectivity. The parameter α is related to the air-entry pressure (the threshold pressure that has to be overcome for gas to be able to displace liquid—it is determined by the largest pore); the parameter m is related to the pore-size distribution. At the NuMI facility, two-phase conditions may arise due to drainage and ventilation effects.

[^] Defined as $D_m = \tau \cdot D_0$. The concrete value was determined experimentally (see Section 5.3)

[&] Tortuosity is defined as the ratio of the distance between the two end points of a pore segment and the actual length of the tortuous pore. The tortuosity of the straight pore is 1; the tortuosity of a twisted pore approaches zero. Under two-phase conditions, the tortuosity is saturation-dependent. Tortuosity is used here to calculate diffusive fluxes in a porous medium given the diffusivity in free water. The concrete tortuosity is estimated from the diffusion-cell experiments described in Section 5.3; fracture and matrix tortuosities represent typical values.

[$] Based on Grossman (2004, Table 5)

[+] Partitioning of tritium between the liquid and vapor phase is approximated here using an inverse Henry's constant, which can be thought of as an aqueous phase solubility of the radionuclide.

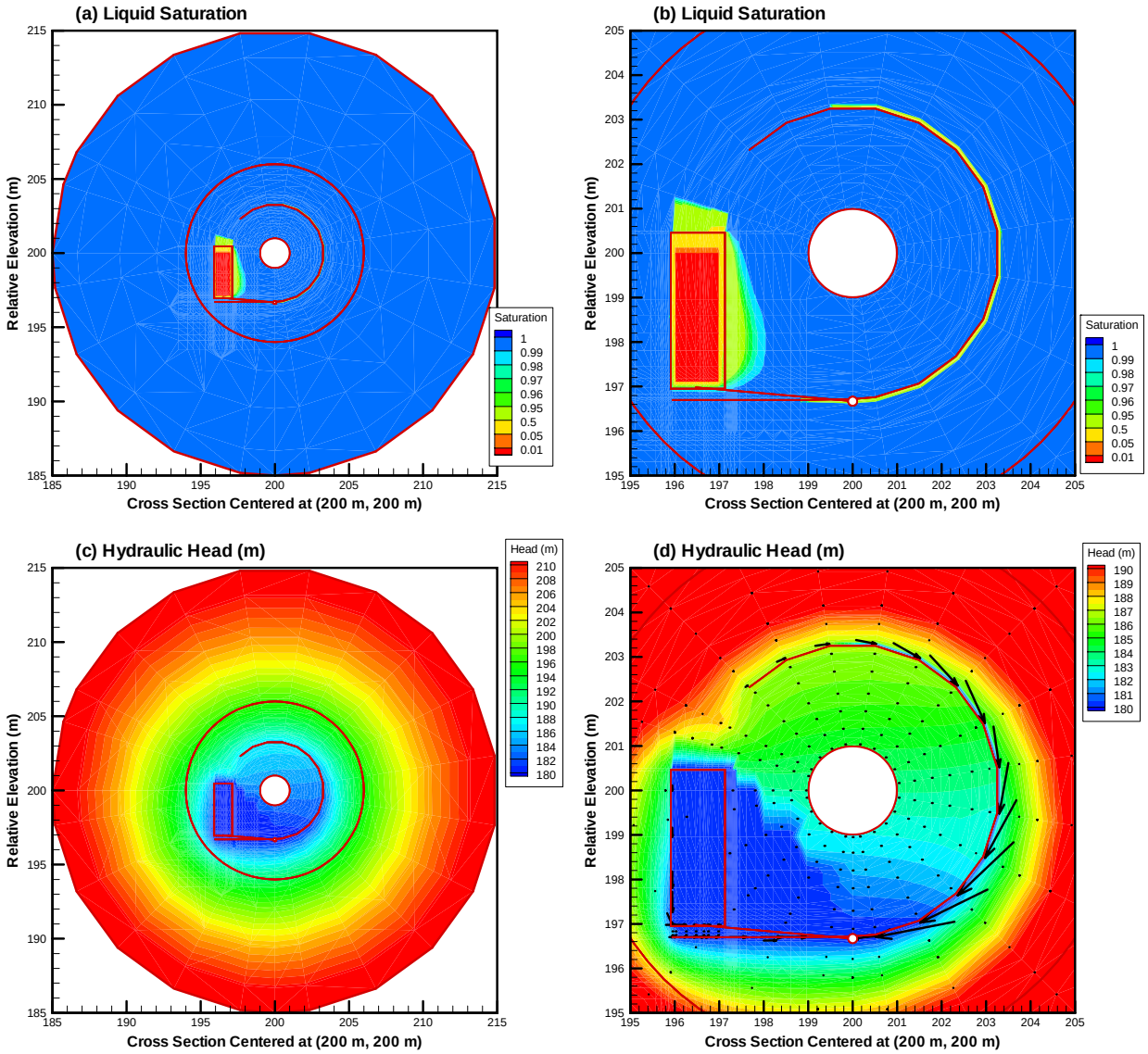

Figure 5.6-2. Simulated fields of (a) liquid saturation; (b) enlargement of (a), (c) hydraulic head, and (d) hydraulic head and mass flux in the vertical cross section

5.6.3 Transport of Tritium Produced in Concrete and Fractured Rock

In this first set of transport simulations, we track the transient migration of tritium that was generated in the concrete and fractured rock during beamline operation from May 1, 2005 to February 25, 2006. A non-uniform tritium concentration is introduced into the steady-state water flow field in the concrete (i.e., 1 m < r < 3.3 m) and in the fractured rock within the tritium-production zone (i.e., 3.3 m < r < 6 m); in all other areas, initial conditions are specified as tritium-free. The spatially varying initial tritium concentration is specified based on the star density distribution obtained from the MARS model (Lundberg, 2006). We are interested in the time-dependent contribution of tritium generated in the concrete and fractured rock to the tritium concentration in the sump holding tank after the beamline is turned off. The transient transport of tritium by diffusion and advection is simulated up to 20 years. To understand the mechanisms of tritium transport in the fractured rock and concrete and the contribution of tritium in the two materials to the total NuMI system, we simulated the transient transport for three cases: (1) tritium produced in the fractured rock, (2) tritium produced in the concrete, and (3) tritium produced in both the fractured rock and concrete. In all three cases, the initial tritium concentration is determined as described in Section 5.6.3.1.

5.6.3.1 Initial Tritium Concentration

In this preliminary modeling, the initial tritium concentration in the model domain is calculated based on the cumulative tritium mass generated in the concrete and fractured rock during 301 days of beam beamline operation from May 1, 2005 to February 25, 2006. More specifically, the non-uniform distribution of initial tritium concentration is calculated using (1) the star density-distribution in the concrete and fractured rock predicted by the MARS model (Lundberg, 2006), and (2) the cumulative total number of protons on target (pot) during this period. The tritium activity (M) generated within a given volume is calculated as

$$M = N_S \times K_p \times W_m \times M_n \times SA \times N_P \tag{2}$$

where N_S (star/pot) is the number of stars, K_p (^{3}H/star) is the tritium production rate per star, W_m ($= 20$ mole/atom) is the molar weight of the tritiated water (HTO), M_n (1.67×10^{-24} g/mole) is the mass of HTO per nuclei, SA (1520 Ci/g) is the specific activity of HTO, and N_P (pot) is the total number of protons on target for a given time period. Based on the parameter values provided above (Lundberg, 2006), the tritium activity in the concrete is calculated to be:

$$M_C = 3.72\times10^{-21} N_S N_P \,(Ci) \tag{3}$$

where a value of $K_p = 0.0732$ ^{3}H/star is used for the concrete, and M_C is the tritium activity in the concrete. During the 301 days of beamline operation, the total number of protons on target is $N_P = 1.391\times10^{20}$ pot (Hylen, 2006c).

The star density of the concrete is fitted by Lundberg (2006) using the simulated results from the MARS model as follows:

$$S_C = A_0 \exp(Az)\left[A_1 \exp(B_1 r + D_1) + \exp(B_2 r + D_2)\right] \tag{4}$$

where S_C (star/cm^3 pot) is the star density (defined as a hadronic interaction vertex with at least one secondary particle that has a kinetic energy higher than a cut-off value (e.g., 30 MeV)) per unit volume of concrete per proton on target, r (cm) is the radius from the center of the vacuum pipe, z (cm) is the longitudinal distance from the start of the Target Pile, and the fitting parameters are $A_0 = 2.73\times10^{-7}$, $A_1 = 0.14$, $A = -4.49\times10^{-5}$, $B_1 = -0.032$, $D_1 = 2.91$, $B_2 = -0.082$, and $D_2 = 7.462$. Based on the reference point for the coordinate z ($z = 9{,}300$ cm for STA 9+84) the Decay Pipe starts at approximately $z = 5{,}100$ cm, and ends at $z = 72{,}000$ cm. The number of stars (N_S) generated per pot within a given concrete element of volume ($r_{\min}$, $r_{\max}$) by ($z_{\min}$, $z_{\max}$) in the two-dimensional radial system can be calculated as

$$\begin{aligned} N_S &= 2\pi r \int_{r_{\min}}^{r_{\max}} \int_{z_{\min}}^{z_{\max}} S_C \, dr dz \\ &= \left(2\pi A_0\right)\left(\frac{1}{A}\exp(Az)\Big|_{z_{\min}}^{z_{maz}}\right)\left\{\left(A_1\left(\frac{r}{B_1}-\frac{1}{B_1^{\,2}}\right)\exp(B_1 r + D_1) + \left(\frac{r}{B_2}-\frac{1}{B_2^{\,2}}\right)\exp(B_2 r + D_2)\right)\Big|_{r_{\min}}^{r_{\max}}\right\} \end{aligned} \tag{5}$$

The average tritium concentration (C_C) in the concrete pore water for a given volume of concrete V during the 301-day beamline operation is calculated by

$$C_C = \frac{\phi_C M_C}{\phi_C V} = \frac{0.5175 N_S}{V} \tag{6}$$

where V is the volume of the concrete of interest, ϕ_C is the concrete porosity, and C is tritium concentration [Ci/cm^3]. In this approximation, the difference in the solid and liquid densities and their impact on tritium generation is not accounted for. The tritium concentration in the concrete pore water at any point is calculated by

$$C_C(r,z) = 0.5175 S_C \tag{7}$$

For the representative cross section from the start of the Decay Pipe ($z = 5{,}100$ cm) to Grate 1 ($z = 11{,}100$ cm), and from the inner wall of the vacuum pipe ($r = 99$ cm) to the outer radius of the concrete ($r = 328$ cm), the radial distribution of tritium concentration (averaged in the longitudinal direction), is given by:

$$\begin{aligned} C_C(r) &= \frac{\phi_C M_C}{\phi_C V} = \frac{\int C_C(r,z)dz}{\int dz} = \frac{\int 0.5175 S_C(r,z)dz}{L} \\ &= 9.85\times10^{-8}\left[A_1 \exp(B_1 r + D_1) + \exp(B_2 r + D_2)\right] \end{aligned} \tag{8}$$

where L = 6,000 cm is the longitudinal length of the representative cross section. Note that Eqs. (6)–(8) assume that tritium is produced in both concrete aggregates (i.e., the solid phase) and water in the pore space, and that the production rates for solid and liquid are the same. Since the physics of transport of the tritium directly produced in solid to the pore water is not well established, we assume that the tritium in the solid phase is immobile, and only the tritium in the pore water is considered in our current model.

Considering the difference in grain density and production rate between the concrete and dolomite (i.e., fractured rock), the tritium concentration for the fractured rock in the representative cross section can be obtained by

$$C_R(r) = \frac{\phi_R M_R}{\phi_R V} = \frac{(K_{PR}/K_{PC})(\rho_R/\rho_C)M_C}{V} = 0.8343\frac{M_C}{V} \\ = 8.218\times10^{-8}\left[A_1\exp(B_1 r + D_1) + \exp(B_2 r + D_2)\right] \quad (9)$$

where the subscripts *R* and *C* are for the fractured rock and concrete, respectively, and ρ is the grain density.

The geometric parameters and material properties for determining tritium production and initial concentration are listed in Table 5.6-2. The resulting initial tritium concentration is shown in Figure 5.6-3. The tritium concentration varies from 6.2×10^4 pCi/mL at the vacuum pipe wall to 7.0 pCi/mL at the outer radius of the Decay Pipe concrete. The tritium concentration varies from 5.8 pCi/mL at the fractured rock close to the dimple mat to 1.0×10^{-3} pCi/mL at a radius of 6.0 m, which is taken as the outer radius of the tritium production zone. Note that the tritium possibly produced directly in the passageway air and dimple mat is not considered here, because the tritium will be transported quickly to the drainage system or to the atmosphere via EAV 2.

Table 5.6-2. Geometric parameters and material properties for the calculation of the initial tritium concentration

Parameter/Property Name	Value	Reference
z value at start of the Decay Pipe: STA 8+48.52	5,100 cm	Lundberg (December, 2006)
z value at the end of Decay Pipe: STA 28+08.12 + A8+48.52	72,000 cm	-
z value at Grate 1	11,100 cm	-
Radius of the inner wall of Decay Pipe concrete	99 cm	-
Radius of the outer wall of Decay Pipe concrete	328 cm	-
Decay Pipe concrete density	2,100 kg/m^3	-
Dolomite density	2,850 kg/m^3	-
Concrete production rate	0.0732 ^{3}H/star	Lundberg (December, 2006)
Dolomite production rate	0.045 ^{3}H/star	-
Total number of protons on target	1.391×10^{20} pot	Hylen (2006c)

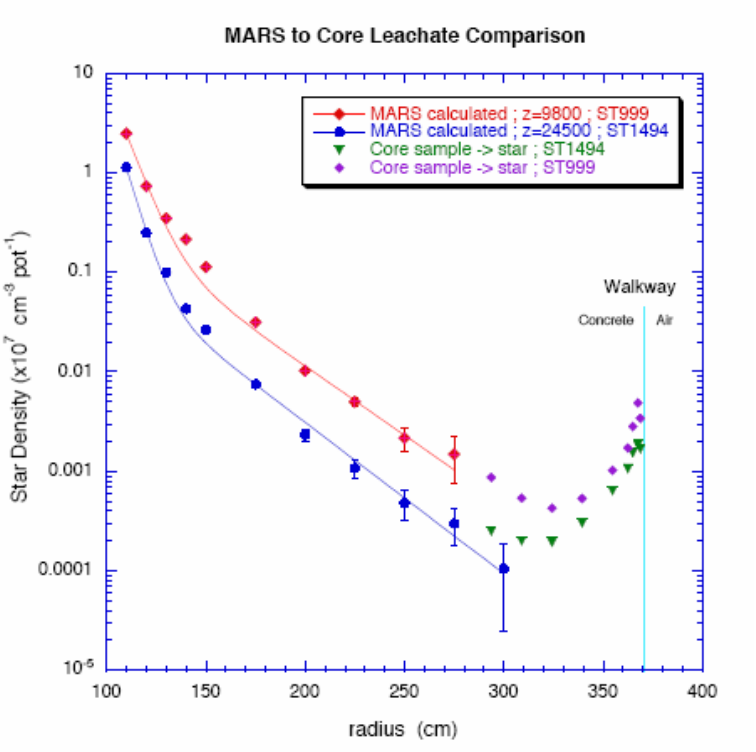

(a)

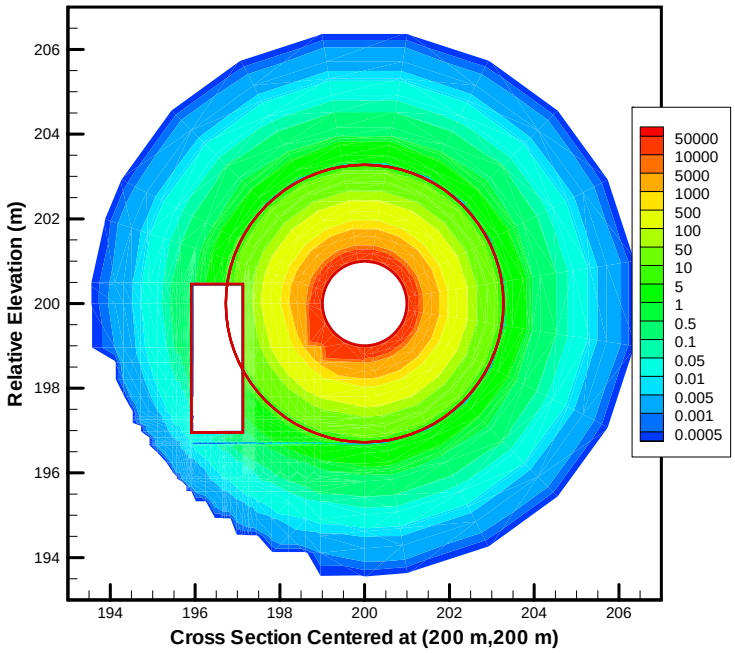

(b)

Figure 5.6-3. (a) Fitting of star density values (symbols) calculated using the MARS model by exponential functions(solid line), with converted star density values (symbols) from tritium concentration measured in concrete cores (Lundberg, 2006); (b) Initial tritium concentration (pCi/mL) in the fractured rock and concrete (averaged in the longitudinal direction), calculated based on the star-density distribution and the number of protons on target during 301 days of beamline operation for the representative vertical cross section

5.6.3.2 Transport of Tritium Produced in Fractured Rock

The transient transport of tritium produced in the fractured rock is simulated to obtain an initial understanding of the transport mechanism and to estimate the contribution of this source zone to the total amount of tritium released to the NuMI drainage system. Figure 5.6-4 shows the absolute tritium concentrations in the pore water 1, 5, 10, and 20 years after the beamline is turned off. The concentration pattern (higher concentrations in the region close to the dimple mat and lower concentrations at the outer edges of the tririum production zone) changes only slowly, because water flow in the rock matrix is very small, with the dominant transport process being diffusion from the rock matrix to the fractures. The tritium mass diffusing to the fractures is transported advectively through the fracture network to the dimple mat and further to the main drain. The advective transport in fractures to the main drain is fast, resulting in quick depletion of the (small) tritium mass initially specified in the fractures. The tritium mass generated in the rock matrix is depleted slowly, limited by the matrix diffusion process. For example, the total tritium mass in the rock matrix is 70, 37, 18, and 5% of the initial tritium mass at 1, 5, 10, and 20 years after the beamline is turned off (see Figure 5.6-5). Radioactive decay of tritium with a half-life of 12.3 years also helps reduce the tritium concentration in the rock matrix. Note that the tritium concentrations shown in Figure 5.6-4 are the volume-weighted average values from all matrix subgridblocks for each gridblock. The diffusion into the concrete and passageway is negligible.

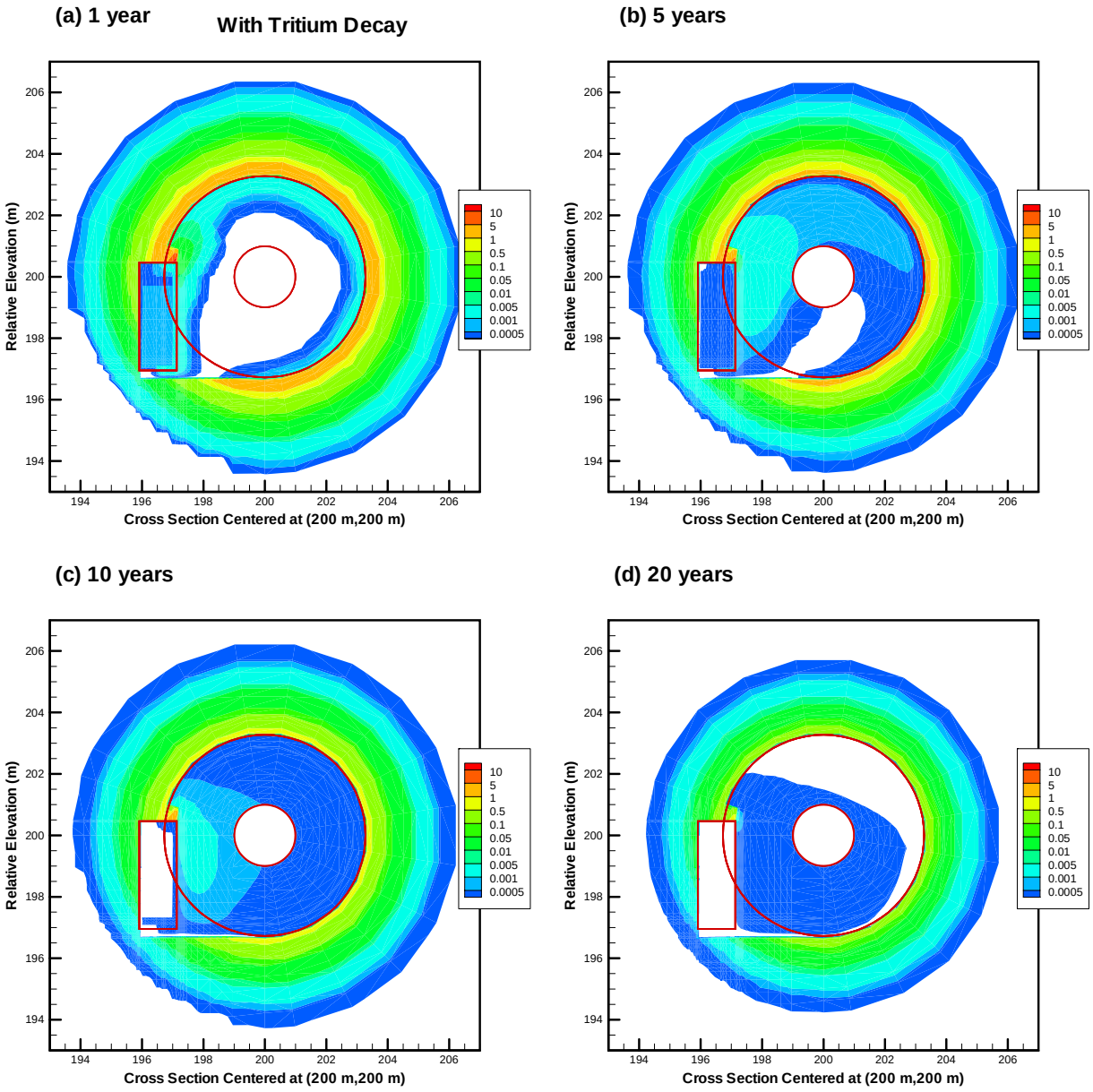

Figure 5.6-4. Distribution of simulated tritium concentration (pCi/mL) in the rock matrix and concrete as a function of time (1, 5, 10, and 20 years after the beamline is turned off). White areas denote tritium concentrations below the cut-off value of 0.0001 pCi/mL.

Figure 5.6-5 shows the calculated tritium concentration in the main drain and the mass storage in the fractured rock as a function of time. The concentration in the main drain (resulting from the transport of tritium generated in the fractured rock) decreases quickly with time from 0.04 pCi/mL after 1 day to 0.001 pCi/mL after 200 days, and further decreases to 0.0001 pCi/mL after11 years. The tritium concentration in the main drain decreases relatively quickly. The reason for this behavior is that the concentration in the main drain depends on the diffusive transport between the rock matrix and fractures. The concentration gradient at the fracture-matrix interface is high at very early times, i.e., immediately after the tritium mass produced in fractures is depleted by advection. With time, the tritium mass in the rock matrix close to the interface is

depleted, and the gradient decreases, leading to decreases in the diffusive mass flux from the rock matrix to the fractures. However, the majority of the rock matrix between the fractures is still close to the initial tritium concentration at early time. This decrease in diffusive mass release is also evident in Figure 5.6-5, which shows the total tritium mass stored in the fractured rock decreases quickly at early time, and then more gradually decreases at a reduced rate. The diffusive transport between the matrix and the fractures is accurately captured in our numerical model by the MINC method, which employs a decreasing thickness of matrix layers away from the fracture-matrix interface. In addition to the local concentration gradient from the rock matrix to the fractures, there is also a radial concentration gradient in the rock matrix resulting from the non-uniform tritium production. This initial concentration gradient is slowly reduced by diffusive transport away from the vacuum tube. However, this Figure 5.6-4 shows that this transport process may be negligible as the concentration pattern does not change significantly with time. Note that the simulation results are sensitive to fracture spacing, which is assumed to be 4.0 m. Decreasing fracture spacing will increase fracture-matrix interface area and reduce diffusive transport distances, resulting in higher diffusive releases to the fractures. This will lead to a higher concentration in the main drain and quicker depletion of tritium mass in the rock matrix.

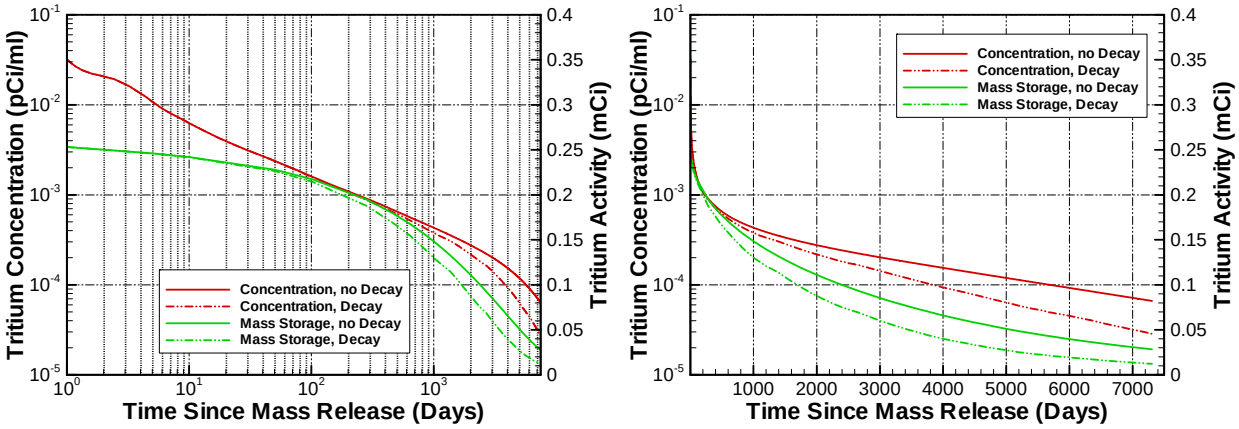

Figure 5.6-5. Tritium concentration in the main drain and tritium activity stored in pore water of the fractured rock (of the 60-m long representative cross section) as a function of time since the beamline was turned off

5.6.3.3 Transport of Tritium Produced in Concrete

To simulate the transport of tritium directly produced in the concrete to the drainage system, we specified a non-uniform tritium concentration in the area of the Decay Pipe concrete (i.e., for 1 m < r < 3.3 m; see Section 5.6.3.1). Tritium transport over a period of 20 years after the beamline is turned off is simulated. Figure 5.6-6 shows the distribution of tritium concentration in the concrete and its vicinity after 1, 5, 10, and 20 years. The tritium mass diffuses into the water collected by and flowing through the dimple mat, as well as into the water flowing down the concrete wall of the passageway. (Note that the diffusion of tritium from the concrete into the passageway is overestimated as a result of simulating the three source areas—fractured rock, concrete, and passageway—in separate models. Tritium concentrations in the passageway wall may be higher than assumed here, reducing or even reverting the concentration gradient—see

Section 5.6.4.) Water collected by the dimple mat and passageway carries the tritium away into the main drain, slowly depleting tritium in the concrete. Within the concrete, tritium mass migrates by diffusion from high-concentration regions close to the vacuum pipe to low-concentration regions close to the outer boundary of the concrete, reducing the initial, radial concentration gradient. Since there are no fast-flow paths in the concrete (as there are in the fractured rock), the diffusive transport resulting from the non-uniform initial condition drives tritium mass slowly outwards to the drainage system. In addition, the asymmetric concentration distribution shows that the advective transport within the concrete from the top to the bottom also contributes to long-term transport, in spite of the very small water velocity in the concrete. The magnitude of advective transport in the concrete depends mainly on the concrete permeability, which is assumed to be 10^{-16} m^2.

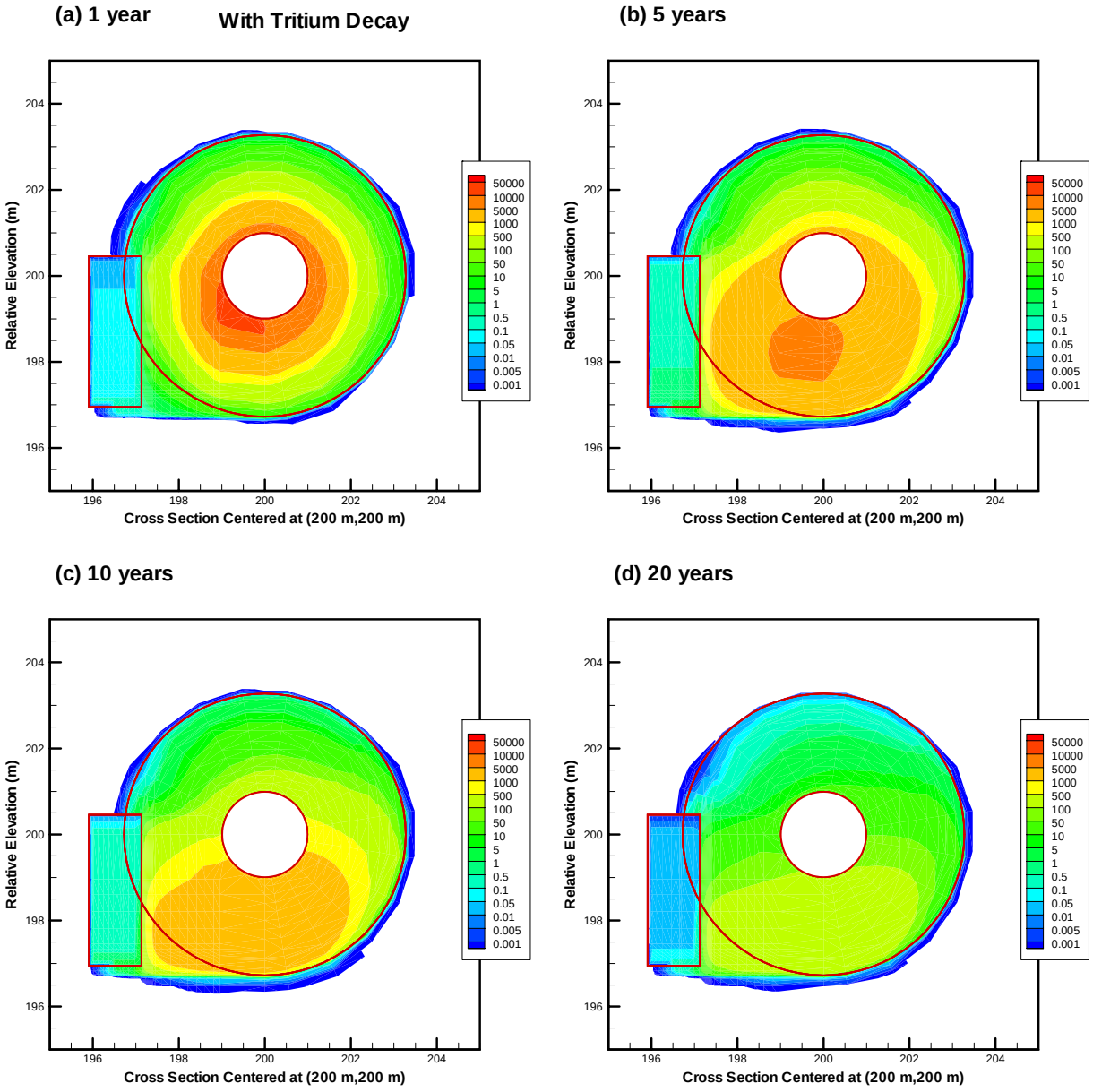

Figure 5.6-6. Distribution of tritium concentration (pCi/mL) in the Decay Pipe concrete as a function of time (1, 5, 10, and 20 years after the beamline is turned off). White areas denote tritium concentrations below the cut-off value of 0.0001 pCi/mL.

Figure 5.6-7 shows the contribution of tritium produced in the concrete to the tritium concentration in the main drain as a function of time after the beamline is turned off. At early times (up to 100 days), the tritium concentration in the main drain is less than 0.06 pCi/mL due to the slow, mainly diffusive release from the concrete and the relatively large dilution in the drainage water. During this time period, the tritium mass released from the concrete to the drainage system mainly originates from the region close to the outer boundary of the concrete, where low initial concentrations (on the order of 10 pCi/mL) prevail. After 100 days, the tritium concentration in the main drain increase significantly, because of (1) downward advective transport of high-concentration water from the region close to the vacuum pipe to the drainage system, and (2) diffusive transport from the region with considerable tritium mass near the vacuum pipe to the low-concentration region close to the dimple mat. The concentration in the main drain reaches a maximum value of 1.0 pCi/mL at 6.8 years. After that time, the concentration decreases slowly to 0.1 pCi/mL at 20 years. The transport mechanisms can also be understood from the tritium mass remaining in the concrete as a function of time. At 100 days, approximately 3% of the initial tritium mass is transported to the drainage system, while about 8% has decayed; after 1000 days, the tritium released to the drainage system increases in comparison with the first 1000 days. The effect of radioactive decay can be seen from the separation between the cases with and without decay.

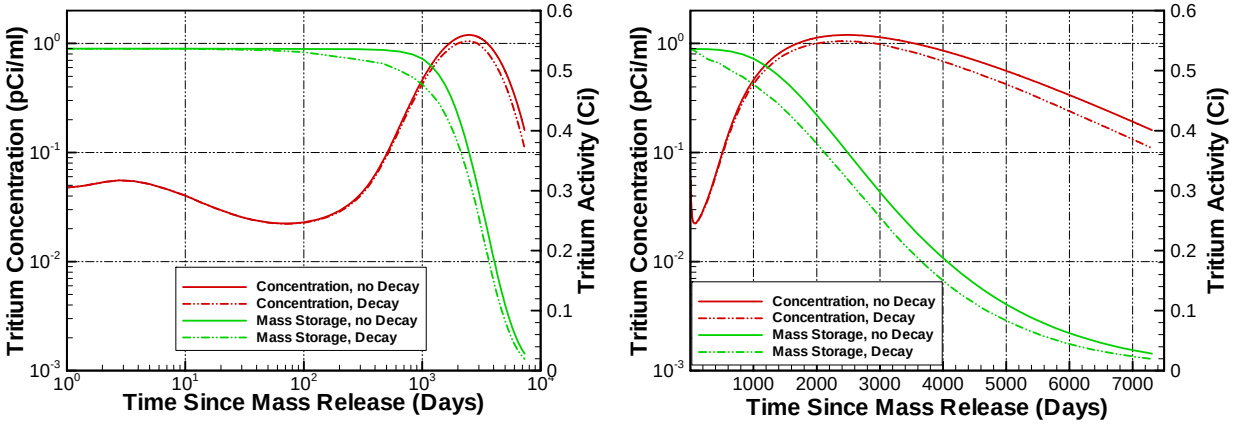

Figure 5.6-7. Tritium concentration in the main drain and tritium activity in the concrete pore water of the 60-m long representative cross section, as a function of time since the beamline is turned off

5.6.3.4 Transport of Tritium Produced in Concrete and Fractured Rock

In addition to the simulations of tritium produced in the fractured rock and concrete in separate cases, we also simulate the transport of tritium in the fractured rock and concrete simultaneously. Tritium transport over a period of 20 years after the beamline is turned off is simulated. Figure

5.6-8 shows the resulting distribution of tritium concentration at 1, 5, 10, and 20 years. This distribution can be understood by combining the distributions in Figures 6.5-4 and 6.5-6. Note that in Figures 5.6-8c and d, there is a region of relatively low concentrations near the apex of the Decay Pipe concrete close to the dimple mat. The water flowing through the dimple mat has generally a lower concentration than the water in the rock matrix (shown in Figure 5.6-8), because it is diluted by the water entering through the fracture network. Moreover, the mass transfer between the fractured rock and concrete (while limited by the drainage effect of the dimple mat) results in a region of relatively low concentrations near the dimple mat in the upper half of the Decay Pipe.

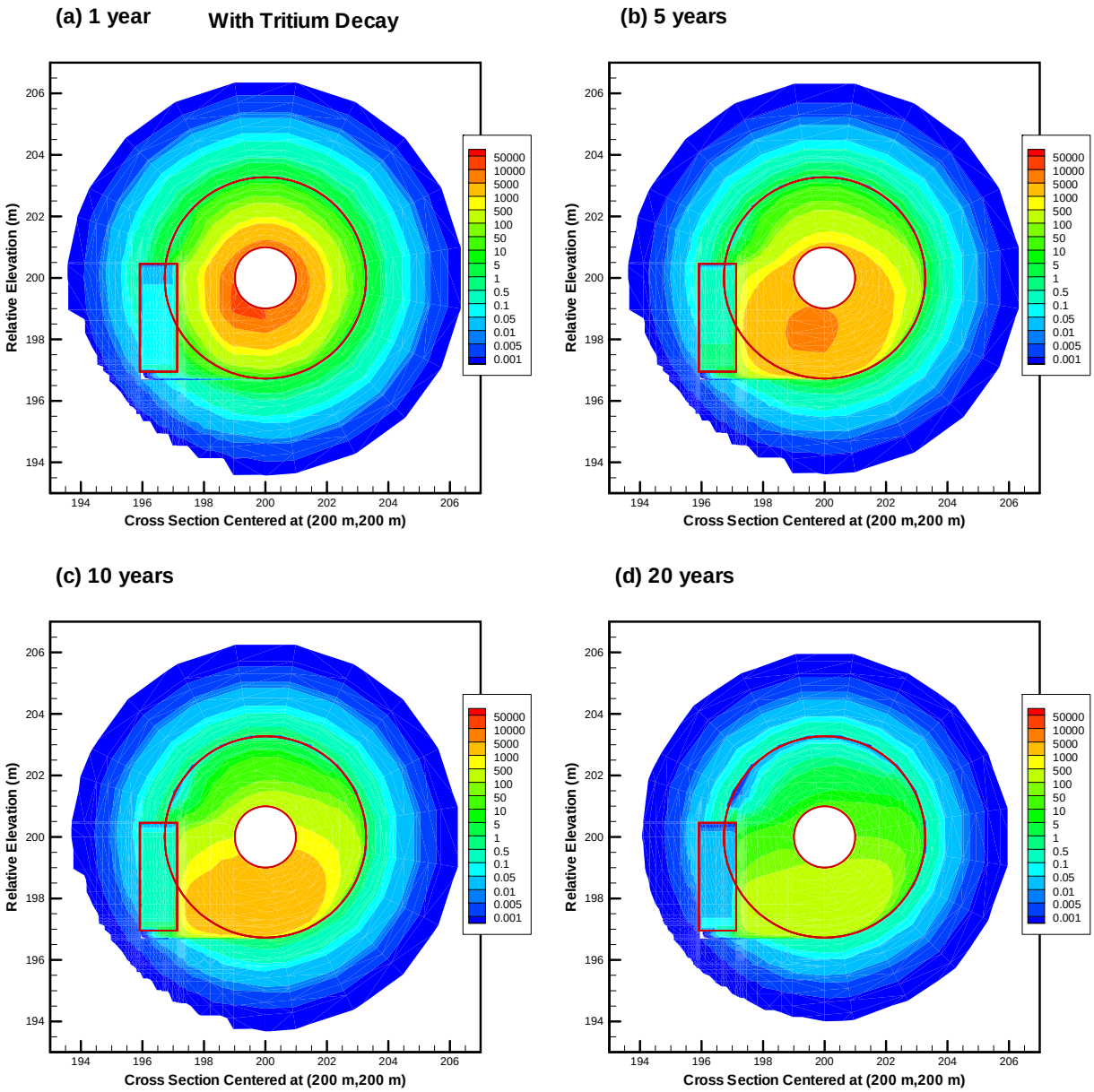

Figure 5.6-8. Distribution of simulated tritium concentration (pCi/mL) as a function of time (1, 5, 10, and 20 years after the beamline is turned off). Tritium is initialized in both the fractured rock and Decay Pipe concrete. White areas denote tritium concentrations below the cut-off value of 0.0001 pCi/mL.

As shown in Figure 5.6-9, the contribution of the tritium produced in the concrete dominates the tritium mass transported to the drainage system, while the contribution from the fractured rock is insignificant under the current modeling assumptions and preliminary parameter set. This is manily because the initial tritium inventory in the concrete is orders of magnitude higher than that in the fractured rock.

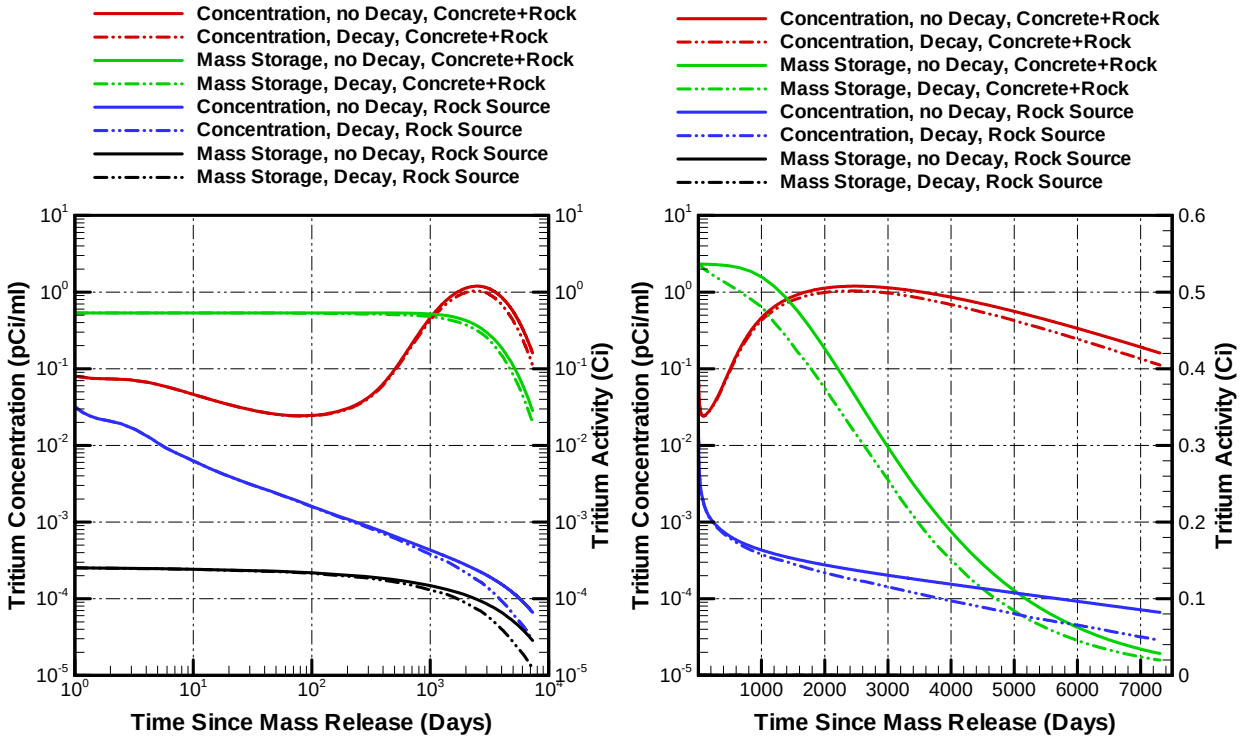

Figure 5.6-9. Tritium concentration in the main drain and tritium activity stored in the pore water of the fractured rock and concrete (of the 60-m long representative cross section) as a function of time since the beamline is turned off, in comparison with those obtained for the tritium produced in pore water of the fractured rock only.

5.6.4 Transport of Tritium Carried by Air through the Passageway

Flow of air and vapor (containing tritium) in the passageway occurs from the upstream end (near the Target Hall) along the Decay Pipe to EAV 2. The airflow rate used in the simulations is 400 cubic feet per minute (design value). The key transport processes are (1) advective flow of tritiated water vapor in the gas phase through the ventilated passageway, (2) mass transfer between the tritiated water vapor and water seeping into the passageway, (3) vertical liquid flow of seepage water along the passageway walls, (4) collection of seepage water at the tunnel floor and drainage through the grates to the main drain, and (5) diffusive transport of tritium into the

concrete/rock wall. Based on the assumed equilibrium partitioning of tritium between the gaseous and aqueous phases, we specify a tritium concentration in the gaseous phase of 0.32 pCi/mL, which is equivalent to 14,000 pCi/mL measured in the Target Hall dehumidifier (see Section 5.1). Note that these conditions reflect the situation before effective mitigation measures have been implemented.

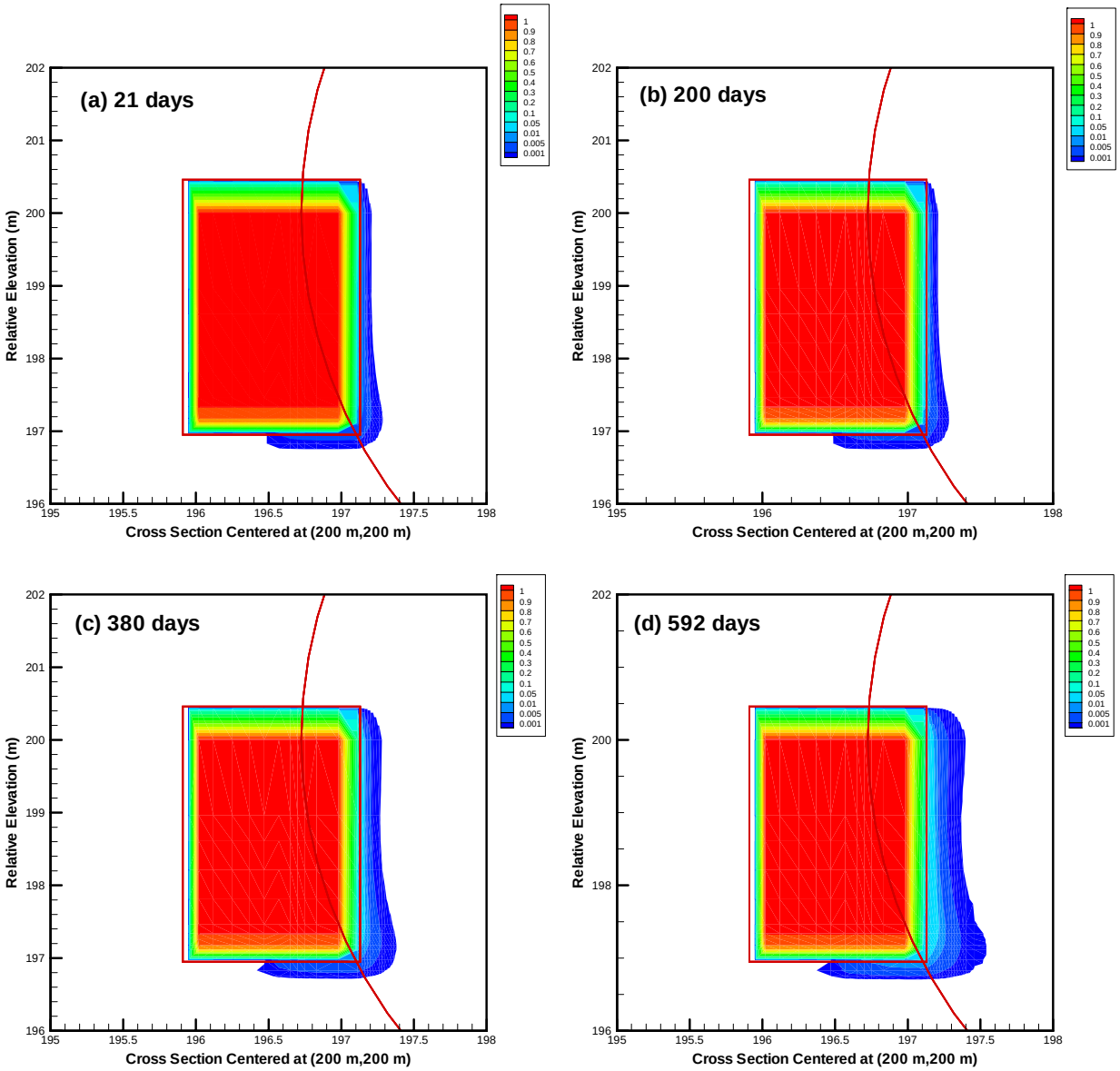

Figure 5.6-10. Tritium concentration distribution in the vicinity of the passageway as a function of time (21, 200, 380, and 592 days) when the passageway is continuously ventilated. White areas denote tritium concentrations below the cut-off value of 0.0001 pCi/mL.

Figure 5.6-10 shows the transient penetration of tritium into the concrete by diffusion through the concrete wall. The simulated penetration depth at 592 days is less than 0.4 m, which is close to the values from the core samples extracted in the upstream section of the Decay Pipe (see Figure 5.1-8). Diffusion into the concrete is a slow transport process. Note that tritium is not

found in the vicinity of the rock wall of the passageway tunnel, because (1) tritium transferred from the gaseous phase into the water film flowing along the rock wall is flushed with the collected water to the grate, and (2) the diffusive transport is counteracted by advective water flow from the fractured rock into the passageway, a process not occurring on the side of the passageway in contact with the Decay Pipe concrete.

Eighty-five percent of the tritium mass introduced into the cross-sectional segment at the upstream boundary of the Decay Pipe leaves the 60-m long segment with the ventilated air. The bulk of the tritium stripped from the air ends up in the main drain, leading to a concentration in the water collected in the sump of 3.9 pCi/mL at 592 days. The remaining tritium mass is stored in the concrete by diffusion.

To analyze the sensitivity of the tritium concentration in the main drain to the operation of the ventilation system, we stop ventilation at 592 days (an arbitrary time not related to the real operation of the ventilation system, but selected to ensure quasi-steady state conditions). After ventilation is stopped, the stripping of tritium from the humid air in the passageway is simulated for 138 days. Figure 5.6-11 shows the aqueous tritium concentration in the main drain for the total simulation time of two years with and without ventilation. The concentration steadily increases with time, from 3.6 to 3.9 pCi/mL when the ventilation system is continuously operated. The steady increase in the main-drain concentration is caused by the decrease in the diffusive loss into the concrete from the passageway. The concentration in the main drain sharply decreases to 1.1 pCi/mL within one day after ventilation stops, as diffusion of tritium into the water running down the passageway walls effectively removes the tritium from the tunnel air. The tritium contained in the stagnant air in the passageway is eventually depleted, since no additional tritium is provided through by the ventilation system. The concentration in the main drain steadily decreases with time to less than 0.8 pCi/mL at two years.

Note that the hydraulic properties of fractured rock and concrete near the walls and above the ceiling of the passageway are critical to the rate and location of seepage, which affects the efficiency with which tritium is stripped from the passageway air. The seepage pattern also significantly affects the diffusive tritium transport into the concrete and back-diffusion to the passageway after the ventilation is turned off, as shown in Figures 5.6-2 and 5.6-10. As a result, the contribution of the tritium vapor ventilated through the passageway to the tritium collected in the drainage system depends on how accurately seepage into and passageway and along its walls is reproduced in the model. The location-specific geometry of the passageway ceiling and the hydraulic properties (varying along the Decay Pipe and other underground openings) would need to be accurately implemented in the model to reduce prediction uncertainty.

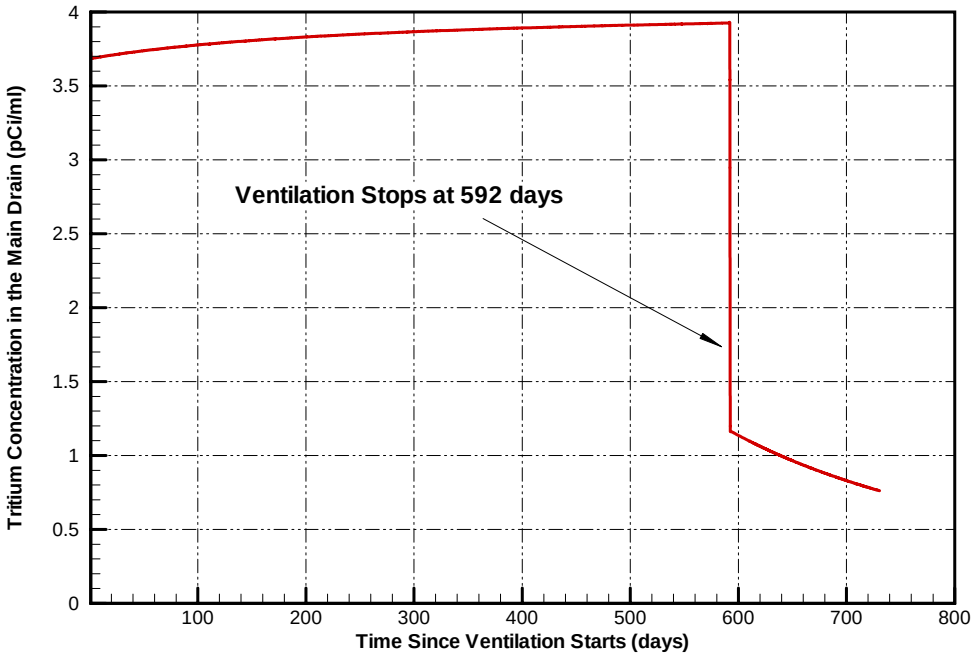

Figure 5.6-11. Breakthrough curve of tritium concentration in the main drain with and without ventilation

5.6.5 Integrated Tritium Transport Analysis

To answer the question of why the tritium concentration in the holding tank did not significantly decrease after the beamline was turned off, we combined the simulation results based on the concentrations (predicted by the MARS model) in the concrete and fractured rock (see Section 5.6.3.4) and the measured concentration in the air flowing through the passageway (see Section 5.1). We used the concentration of 0.32 pCi/mL in the humid air ventilated from the Target Hall into the passageway (equivalent to 14,000 pCi/mL in the aqueous phase) as input to our model (see Section 5.6.4). Note that the tritium mass in concrete and fractured rock was specified as initial conditions after the beamline was turned off; the passageway was continuously ventilated up to 592 days, when the ventilation was turned off, and the ventilation was turned on again at 730 days. Since the concentration in the main drain resulting from the ventilation is relatively stable, a constant concentration of 3.9 pCi/mL is assumed after 730 days for this integrated transport analysis.

Figure 5.6-12 shows the tritium breakthrough curve in the main drain in response to tritium sources in the fractured rock, concrete, and air flowing through the passageway. This breakthrough curve is obtained by combining the simulation results shown in Sections 5.6.3–5.6.4, by assuming that the transport equation in the system is linear and superposition can be

used. The dominant contribution is from the airflow through the passageway, which contains high concentrations of tritium (provided that the assumption of equilibrium with the measured aqueous-phase concentrations is valid). When the ventilation system is turned off, tritium mass flux into the modeled cross-sectional segment through the tunnel ceases, reducing the concentration in the main drain by a factor of approximately three. Nevertheless, tritium continues to be released to the main drain from the fractured rock, the concrete, and as a result of back-diffusion of tritium to the passageway, which is expected to be a long-term process. The simulated transient pattern of the tritium concentration in the main drain is similar to the observed concentration time series (shown in Figure 5.1-2b), when ventilation through EAVs 2 and 3 was turned off and on again in May 2006. With time, the tritium transported from the concrete into the main drain accounts for up to 20% of the total tritium mass collected in the main drain, whereas the tritium transported from the fractured rock is negligible.

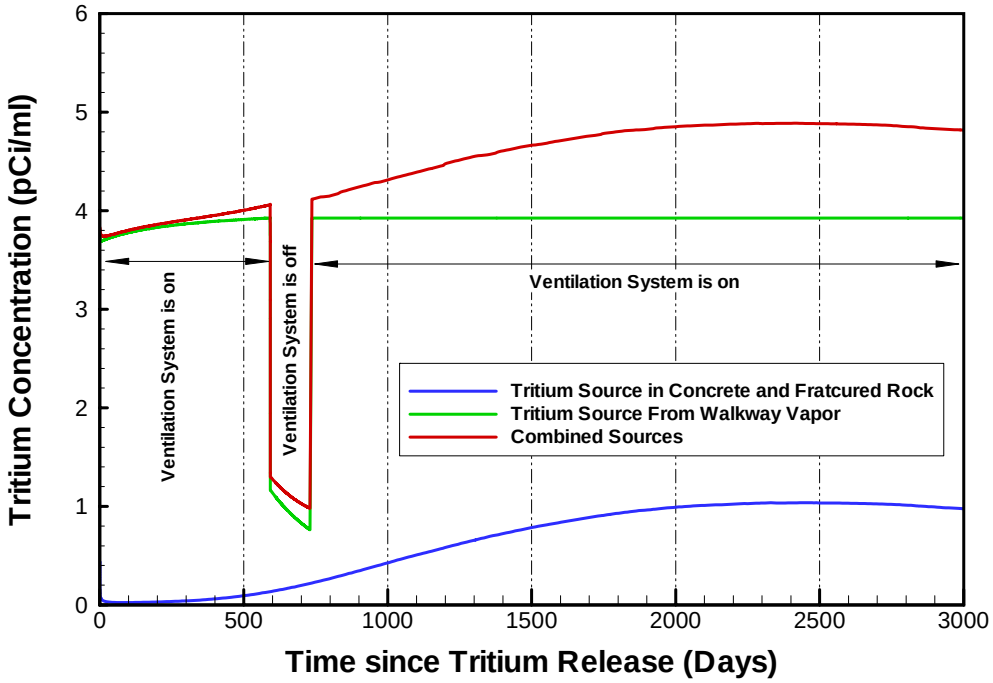

Figure 5.6-12. Simulated tritium breakthrough curves in the main drain. Sources consider include tritium produced in fractured rock and concrete, and tritium mass entering the passageway (walkway) from the Target Hall during ventilation periods. The effect of temporarily shutting down the ventilation system is also shown. The cumulative breakthrough curve is obtained by superposition of the results discussed in Sections 5.6.3 and 5.6.4.

Note that the preliminary modeling results may be subject to uncertainties in the model parameters, physical properties, geometric representation of the system, and the operation of the NuMI facility. Some model parameters used in this modeling effort are taken from the NuMI facility reports and derived from the ongoing laboratory diffusion-cell experiments (e.g., the diffusion coefficient in the concrete was measured to be approximately 3.4×10^{-10} m^2/s).

However, many other parameters need to be updated based on further data collection and analysis, refinement of the model, and more accurate incorporation of facility operation modes. The preliminary results are for one cross section only, and non-uniform water flow rates and geologic layering has been observed along the Decay Pipe. Consequently, these results should be used only as a first-order approximation. A full-scale, three-dimensional model is needed to represent the system, with more accurate tritium sources generated and accumulated in concrete, fractured rock, the Target Pile, and the Absorber Hall.

6. CONCLUSIONS

Between June and September 2006, LBNL developed a conceptual model of tritium fate and transport in the NuMI facility, compiled and analyzed datasets from Fermilab on tritium concentrations, performed a literature review on tritium transport through concrete and steel, conducted diffusion tests and chemical analyses on concrete, developed a field investigation plan, and simulated water flow and tritium transport in a vertical cross section of the Decay Pipe.

To develop a conceptual understanding of tritium production and transport, data collected by Fermilab on tritium concentrations in the Decay Pipe concrete, the drainage system, and the ventilation system at multiple locations were evaluated. High tritium concentrations were observed in condensate in the Target Hall and in dehumidifiers in the Target and Absorber Halls, with a gradual decline of the vapor concentration away from these two halls to other parts of the NuMI facility. Sharp and significant changes in the tritium concentration in the holding tank in response to the operation status of five engineering controls (recirculation fan, EAVs 2 and 3, chase, chiller, and dehumidifier) were observed, with a strong correlation of tritium levels observed in the main drain to the tritium vapor transported with ventilated air. Tritium concentrations in the grates of the Decay Pipe are higher than those observed in the holding tank, indicating that the seepage water collected in the passageway is diluted by the water entering the main drain from the dimple mat. Different transient patterns of tritium concentration are observed in the upstream and downstream sections of the Decay Pipe in response to the operation of the beamline and the five engineering components. Tritium vapor concentrations in open pails and trays along the passageway in the Decay Pipe are higher than those observed in grates, with a concentration gradient from the Target and Absorber Halls to EAVs 2 and 3. Depth profiles of tritium concentration measured from leached concrete samples extracted from the Decay Pipe passageway show (1) a decrease in concentration away from the concrete surfaces that are exposed to ambient air, and (2) an increase in concentration towards the central beamline, indicating primary tritium production.

Based on the analysis of the tritium data collected by Fermilab, the main tritium transport processes in our conceptual model (which are also included in our numerical model) are:

1. Advective transport with airflow and mass transfer between gaseous and aqueous phases in the passageway and other underground openings
2. Advective and diffusive transport in concrete and fractured rock
3. Mass transfer between tritium vapor in the openings and concrete/rock

To estimate tritium mobility through concrete and rock, we have designed and manufactured a diffusion cell for conducting through-diffusion experiments on samples exposed to vapor, and we have completed two experiments on fabricated Decay Pipe concrete exposed to deuterated water vapor. The concrete was fully saturated in Experiment 1 and had a saturation of 0.6 in Experiment 2. The deuterium concentration in Experiment 2 increased with time at approximately half the rate of Experiment 1, indicating that the diffusion rate decreases as the concrete saturation decreases. The semianalytical solution developed by Moridis (1999) was used to analyze the results from Experiment 1, giving a diffusion coefficient of 3.4×10^{-10} m^2/s. A semianalytical solution for vapor and liquid diffusion will be developed to analyze the results

from Experiment 2, where the concrete was partially saturated; inverse modeling using iTOUGH2 (Finsterle, 2004) may also be used to analyze the results from this experiment. The estimated diffusion coefficient from the first experiment was used in the numerical model of the Decay Pipe region. Back-diffusion experiments were also performed and an increase in deuterium concentration over time was measured after powdered concrete from the Target Hall had been enriched with deuterated water vapor. This result demonstrates that back-diffusion of tritium from the concrete could be contributing to the tritium concentrations observed after the beamline is shut down.

Tritium concentrations in the Decay Pipe concrete and the surrounding rock in the NuMI facility are being measured to determine whether or not the concrete and/or rock walls contain enough tritium to act as a long-term source. We have extracted pore water from three Target Hall concrete samples. The tritium concentrations in the water samples extracted using a dehydration technique are significantly lower (~5 to 30 times) than the concentration of the leached concrete sample measured by Fermilab. There are several potential possibilities for the discrepancy between the leach and de-hydration samples: the concrete samples may have experienced drying out and exchange with non-tritiated water vapor during storage, the pore water sample may have been diluted (contaminated) by nontritium-bearing drilling fluid during the coring process, or the two measurement techniques are measuring tritium from different reservoirs in the concrete. To test these hypotheses, we will analyze fresh core by both methods, run a series of leach experiments on both vacuum dehydrated and un-processed, powdered concrete samples, and recommend that future cores be drilled with drilling fluid spiked with a tracer.

Our preliminary modeling effort was focused on water flow and tritium transport in a vertical cross section of the Decay Pipe. Tritium transport from three different sources (fractured rock, concrete, and passageway) was simulated separately to analyze the transport mechanisms and demonstrate their relative contributions to the tritium concentrations in the holding tank as a function of time after the beam was turned off. For this preliminary modeling study, water flow in the cross section of the NuMI facility was assumed to be at steady state. The simulated breakthrough curves from the three source zones were then compared to determine their relative contributions to tritium in drainage water. Contributions from the tritium generated in fractured rock and concrete were not significant. The dominant contribution is from the airflow through the passageway. Provided the equilibrium assumption between measured aqueous-phase tritium concentrations and tritiated vapor concentrations is valid, the ventilated air contains relatively high levels of tritium since it was in contact with high-concentration tritiated water in the main source zones, i.e., the Target Hall and Absorber Hall. When the ventilation system is turned off, tritium mass flux into the modeled cross-sectional segment ceases, drastically reducing the concentration in the main drain. Nevertheless, tritium continues to be released to the main drain from the fractured rock, the concrete, and back-diffusion to the passageway from concrete walls.

Based on the discussions with Fermilab staff and the evaluation of the data collected from the NuMI facility, it appears that the movement of tritium through the facility is dominated by vapor transport. The preliminary numerical model also indicates that the primary source of tritium in the holding tank is from tritium transported through the vapor phase. In addition to the tritium directly produced in the humid air during beamline operation, tritium is expected to enter the airstream by diffusion of tritium produced in the shielding materials close to the Target Pile and

absorber. Production of tritium in the concrete and fractured rock along the Decay Pipe may provide another source of tritium that is slowly released by diffusive processes. Once in the air phase, tritiated vapor is transported by the ventilation system to other parts of the facility, where it may condense, diffuse into the concrete and rock, and—if conditions change—diffuse back from these materials. These transport, exchange, and phase partitioning processes explain why high tritium concentrations persist even when the beam is shut off.

A number of issues deserve further consideration. The total tritium inventory (from production, diffusion, and adsorption) and the release rate of tritium in the Target Hall region remain uncertain, as no direct measurements of tritium are available from the immediate vicinity of the Target Pile. The movement of tritium through the water and in the air pathways created by the ventilation system and other engineering controls are not yet well understood. Monitoring vapor and water movement will help determine the source and transport pathways of tritium in different parts of the NuMI facility. For instance, efforts to seal the Pre-Target region from the Target Hall did not eliminate tritium in the Pre-Target Tunnel, suggesting that tritiated vapor leaks from the Target Hall and/or that tritium is transported through the water from another location into the facility. Increased concentrations of other radionuclides produced at the NuMI facility, such as Na-22, could also have a significant environmental impact; therefore, in addition to tritium, transport of these radionuclides should be investigated.

7. RECOMMENDATIONS

Our understanding of tritium transport in the entire NuMI facility system has improved through systematic analysis of the site-specific data (Section 5.1), literature data (Section 5.2), laboratory studies (Sections 5.3 and 5.4), and preliminary numerical modeling (Section 5.6). Based on the results from the investigations conducted between June and September 2006, five key questions have been identified that must be addressed to understand the movement of tritium at the NuMI facility:

1. What are the main sources and mechanisms for tritium release when the beamline is off?
2. What is the total tritium inventory (from production, diffusion, and sorption) and what are the tritium exchange and release rates between different elements in the Target Pile/Hall region?
3. What are the main pathways for tritium movement through the air and water at the NuMI facility?
4. What are potential long-term environmental impacts of tritium and other radionuclides of concern to Fermilab (e.g., Na-22)?
5. What are the projected absolute tritium concentrations expected for future beamline operation scenarios, and what mitigation measures for tritium release could be developed?

To address these questions, we recommend a series of laboratory, field, and modeling investigations, using the systematic and integrated approach presented in Section 4:

1. Conduct additional measurements (by vacuum dehydration and leach techniques) of concrete tritium concentrations and pore-water saturation to accurately capture the tritium inventory in the source zones, and to provide a basis for calibrating and validating the MARS and tritium flow and transport models.
2. Conduct additional laboratory experiments on transport properties through earth and engineered materials under varying liquid/vapor conditions for tritium and for Na-22.
3. Conduct gas tracer tests to track the major airflow pathways.
4. Place boxes containing multiple blocks of engineered and natural materials throughout the facility to capture tritium production rates and the dynamic depth profiles of tritium concentrations in these materials
5. Develop a water and water vapor monitoring program to provide details of moisture dynamics in the immediate vicinity of the facility.
6. Develop a three-dimensional fluid flow and tritium transport model to integrate all observations from the laboratory and field; reproduce the observed system behavior and predict system responses to future operational scenarios (e.g., increase in beam intensity and implementation of mitigation measures).

Each investigation is briefly described below.

7.1 Laboratory Experiments

- It is essential to obtain an accurate tritium inventory and to estimate spatial distribution with respect to key facility components. Moreover, tritium concentration data may be used to provide confidence in the MARS model predictions of tritium production in zones were no measurements are available. Finally, these data can be used as initial conditions as well as calibration and validation data for the tritium transport model. Experiments to identify the tritium concentration in concrete and rock should continue with the following tests:

  1. Resolve differences in tritium concentration as measured at Fermilab and LBNL by (1) performing a cross calibration of the Fermilab and LBNL analytical laboratories using a documented tritium standard, (2) reproducing the leach technique for measuring tritium concentrations used at Fermilab by powdering aliquots of dehydrated concrete and leaching with de-ionized water; and (3) analyzing extracted pore water and water from the leaching experiments at both laboratories.
  2. Measure pore-water tritium concentration using both the vacuum dehydration and leach techniques. These tests should include concrete and wall rock core samples from representative locations throughout the NuMI facility.
  3. For direct comparison with results obtained using the dehydration method for extracting pore-water, aliquots of dehydrated concrete should be powdered and leached with de-ionized water, reproducing the leachate technique for measuring tritium concentrations used at Fermilab.
  4. Powdered and un-powdered aliquots of dehydrated concrete should be exposed to de-ionized water in time-series experiments to set limits on exchange rates.
  5. Samples of dehydrated concrete should be heated to higher temperatures under controlled conditions to further evaluate tritium sites and their relative importance to the overall tritium budget.
  6. Conduct a cross calibration of the Fermilab and LBNL analytical laboratories using a documented tritium standard.
  7. Initiate study of tritium concentrations and mobility in the steel shielding in the Target Hall.

- The impact of operational and engineering changes on the tritium concentrations in the different materials at the NuMI facility needs to be understood. For instance, Fermilab plans to increase the beam intensity, which will increase the tritium production in the facility. Dehumidifiers have been used in the Target Hall for the past several months as a mitigation measure for the tritium. These humidifiers may have decreased the water saturation in the outer surfaces of the concrete. The diffusion tests described in Section 5.3 indicate that the tritium diffusion rate decreases with decreasing water saturation. We propose to conduct laboratory experiments to systematically understand how the tritium concentrations in concrete and rock vary as the water saturation and the tritiated vapor concentration changes.

- The time constant for free-water and pore-water samples to equilibrate with the tritiated vapor will be measured to understand the kinetics of phase partitioning processes.
- In addition to tritium, transport of Na-22 in rock should be quantified because of the potential that Na-22 levels increase above the regulatory limits for groundwater in the Decay Pipe rock after the beam intensity increases. We recommend performing batch and column experiments to obtain transport parameters for Na-22 in rock.

7.2 Field Experiments

- **Air-Flow along the NuMI facility**

  1. Conduct air tracer tests under different operation and ventilation conditions to determine airflow magnitude and pathways through the facility from the two primary tritium source zones (Target Pile and Absorber Hall) and the residence time in each area for the different operating conditions.
  2. Develop an airflow model of the facility to predict the impact of proposed mitigation measures involving manipulation or modification of existing equipment and/or operation.

- **Liquid-vapor exchange and water movement in the NuMI facility**

  Perform tracer tests using deuterated water to differentiate between tritium exchange between liquid water and water vapor in the facility, and tritium exchange between collected groundwater. Deuterated water will be added to different potential sources of tritiated water (e.g., Gollum's Cave, Pre-Target drain) found at the NuMI facility.

- **Dynamic depth profiles of tritium concentration in component materials of the NuMI facility**

  Determine the dynamic tritium-concentration depth profiles in engineered and natural materials along the NuMI facility during and between periods when the beam is running. This experiment will be conducted using a portable box (containing multiple material specimens) placed at different locations along the major airflow pathways. For each specimen, we will use multiple blocks to track the dynamic depth profiles of tritium concentrations. Specimens sealed from the surrounding environment and emplaced during beam operation will provide tritium production data useful for the calibration and/or validation of Fermilab’s MARS model.

7.3 Long-Term Monitoring Program

- Developing a water and water-vapor monitoring plan will provide details of moisture dynamics in the immediate vicinity of the facility and serve as a basis for environmental assessment and monitoring.

  Components:

  – Monitoring flow and seepage below shaft in Pre-Target Hall.

  – Monitoring flow rates in drainage pipes.

  – Monitoring condensation rates and tritium concentration in chillers.

  – Extension and optimization of the existing groundwater sampling program.

7.4 Numerical Modeling of Fluid Flow and Tritium Transport

- Step-wise development of a full-scale, three-dimensional numerical model of liquid, vapor, air, and tritium transport in porous materials (concrete, rock) and underground openings (Pre-Target Tunnel, Target Hall, passageway, Absorber Hall, air vents) in an integrated and systematic way is recommended. This model needs to be calibrated and validated against all available data. The overall objectives of the forward and inverse modeling studies are:

  – To further improve our understanding of full-scale system behavior under the current operational conditions, and to identify key parameters and properties affecting tritium migration.

  – To help design measures for mitigating the release of tritium and other radionuclides to the surrounding environment by changing the current operation of the engineering components in the framework of the numerical model. Mitigation strategies may be optimized using numerical models, complementing the on-site, field testing by Fermilab.

  – To predict the system response (tritium concentrations at multiple locations within the facility and in the surrounding environment) under the condition of increased beamline intensity.

  – To provide actionable control and management strategies to meet the environmental standard under increased beam-intensity conditions.

This full-scale numerical model will honor:

1. The site-specific geological layering and geometry of the engineered components (Pre-Target Tunnel, Target Hall, Decay Pipe, and Absorber Hall) in three dimensions

2. The site-specific and transient hydrology, including spatially varying water flow rates measured in the drainage system
3. The spatially varying airflow
4. The tritium sources predicted by the Fermilab MARS model, which has been updated and verified by the measured tritium concentration profiles in concrete
5. The measured system behavior (e.g., tritium concentration at multiple locations) in response to changing operation of engineering components by calibrating the model against measured data
6. The transport properties (e.g., concrete diffusion coefficient and retardation factor) estimated by our laboratory experiments and other hydraulic and transport properties available

These general recommendations can be implemented in a staged manner, allowing for modifications in proposed testing, analysis, and modeling techniques as the conceptual model is revised.

8. ACKNOWLEDGMENT

We would like to thank Fermilab staff for providing data and for most useful discussions. Curt Oldenburg and Eric Sonnenthal (Earth Sciences Division, LBNL) reviews of the manuscript are gratefully acknowledged. Richard Sextro, Doug Black, and Woody Delp (Environmental Energy Technologies Division, LBNL) contributed to Section 7.2 regarding air-flow monitoring. This work was supported by the Fermi National Accelerator Laboratory (Fermilab). The support is provided to Berkeley Lab through the U.S. Department of Energy Contract No. DE-AC02-05CH11231.

9. REFERENCES

Chen, C-A., Y. Sun, Z. Huang, C. Liu, and S. Wu, The diffusion of tritium and helium-3 in 21-6-9 stainless steel during the storage of tritium at high pressure and room temperature, *Physica Scripta*, T103, 97-100, 2003.

Department of Energy, Environmental assessment, proposed Neutrino Beams at the Main Injector Project, DOE/EA-1198, December 1997.

Dickson, R.S, Tritium interactions with steel and construction materials in fusion devices – A literature review, Report AECL-10208, CFFTP-G-9039, Chalk River Laboratories, 1990.

Eichholz, G.G., W.J. Park, and C.A. Hazin, Tritium penetration through concrete, *Waste Management*, 9, 27–36, 1989.

Finsterle, S., Multiphase inverse modeling: Review and iTOUGH2 applications, *Vado*se Zone *J.*, 3: 747–762, 2004.

Furuichi, K., H. Takata, T. Motoshima, S. Satake, and M. Nishikawa, Study on behavior of tritium on concrete wall, *J. of Nuclear Materials*, 350, 246–253, 2006.

Grossman, N., NuMI primary beamline groundwater protection radiation safety, Fermilab report, July 2001.

Grossman, N., Radionuclide concentrations in groundwater in the vicinity of NuMI beamline enclosures, NuMI-Note-BEAM-1020, Fermi National Accelerator Laboratory, Batavia, IL, 2004.

Grossman, N., Summary of Tritium Measurments to Date , Projects Document 14-v1, , March 10, 2006a.

Grossman, N., NuMI Shielding Assessment Groundwater Review, Projects Document 13-v1, , April 18, 2006b.

Hirabayashi, T. and M. Saeki, Sorption of gaseous tritium on the surface of type 316 skinless steel, *J. of Nuclear Materials*, 120,309–315, 1984.

Hirabayashi, T., M. Saeki and E. Tachikawa, Effect of surface treatments on the sorption of tritium on type-316 stainless steel, *J. of Nuclear Materials*, 127, 187–192, 1985.

Hochel, R.C., and E.A. Clark, Tritium characterization in cement and concrete, Report WSRC-TR-99-00081, Westinghouse Savannah River Company, 1999.

Hochel, R.C., and E.A. Clark, Corroborative studies of tritium characterization and depth profiles in concrete, Report WSRC-TR-2000-00021, Westinghouse Savannah River Company, 2000.

Hylen, J., NuMI tritium sources, models, Powerpoint presentation, April 18, 2006a.

Hylen, J., Projects Document 144-v1 CHAFT tritium humidity transport model, Fermi National Accelerator Laboratory, October 2006b.

Hylen, J., Projects Document 102-v3, Tritium-time-ordered-spreadsheet, Fermi National Accelerator Laboratory, December 2006c.

Hylen, J., Projects Document 152-v1,core samples spreadsheet, Fermi National Accelerator Laboratory, December 2006d.

Hylen, J., Chaft Model Spreadsheet , Projects Document 8-v1, Fermi National Accelerator Laboratory, December 2006e

Lundberg, B., Tritiated water in the decay region: model comparisons to data, Projects Document 136-v3, , Fermilab Report, December 2006.

Maienschein, J., V. DuVal, F. McMurphy and F. Uribe, A novel technique for measurement of tritium permeation through resistant materials near room temperature: Demonstration of method with copper at 50- 170ºC, *Fusion Technology*, 8, 2360–2365, 1985.

Maienschein, J.L, F.E. McMurphy and V.L. DuVal, Increase of tritium permeation through resistant metals at 323K by lattice defects, *Fusion Technology*, 14, 701–706, 1988.

Mokhov, N.V., and C.C. James, The MARS code system user's guide, Fermi National Accelerator Laboratory, May 2006.

Moridis, G., Semianalytical solutions for parameter estimation in diffusion cell experiments, *Water Resources Research*, 35(6), 1729–1749, 1999.

Numata, S., H. Amano, M. Okamoto, Tritium inventory in Portland cement exposed to tritiated water vapor, *J. of Nuclear Materials*, 171, 350–359, 1990a.

Numata, S., H. Amano, and K. Minami, Diffusion of tritiated water in cement materials, *J. of Nuclear Materials*, 171, 373–380, 1990b.

Numata, S., Y. Fujii, and M. Okamoto, Diffusion of tritiated water vapor into concrete, *Fusion Technology*, 19, 140–145, 1991.

Pruess, K., and T.N. Narasimhan, A practical method for modeling fluid and heat flow in fractured porous media, *Soc. Pet. Eng. J.*, 25 (1), 14–26, February 1985.

Pruess, K, The TOUGH Codes—A family of simulation tools for multiphase flow and transport processes in permeable media, *Vadose Zone J.*, 3, 738–746, 2004.

Selih, J., A.C.M. Sousa, and T. W. Bremner, Moisture transport in initially fully saturated concrete during drying, *Trans. Porous Media*, 24, 82–106, 1996.

Surette, R.A and R.G.C. McElroy, Regrowth, retention and evolution of tritium from stainless steel, *Fusion Technology*, 14, 1141–1146, 1988.

Tits, J., A. Jakob, E. Wieland, and P. Spieler, Diffusion of tritiated water and $^{22}Na^{+}$ through non-degraded hardened cement pastes, *J. of Contaminant Hydrology*, 61, 45–62, 2003.

van Genuchten, M.T., A closed-form equation for predicting the hydraulic conductivity of unsaturated soils, *Soil Sci. Soc. Am. J.*, *44*, 892–898, 1980.

Wehmann, A., W. Smart, S. Menary, J. Hylen, and S. Childress, Groundwater protection for the NuMI project, FERMILAB-TM-2009 and NuMI-B-279, Fermi National Accelerator Laboratory, October 1997.

Wehmann, A., and S. Childress, Tritium production in the Dolomitic rock adjacent to NuMI beam tunnels, FERMILAB-TM-2083, Fermi National Accelerator Laboratory, May 1999.